Aqua notes 2026:1

A population assessment model for the European perch along the Swedish Baltic Sea coast

Torbjörn Säterberg and Jens Olsson

Sveriges lantbruksuniversitet, SLU
Institutionen för akvatiska resurser

A population assessment model for the European perch along the Swedish Baltic Sea coast

En populationsanalysmodell för lokala abborrpopulationer längs Östersjöns kust

Torbjörn Säterberg, https://orcid.org/0000-0002-5881-7983, Sveriges lantbruksuniversitet, Institutionen för akvatiska resurser,

Jens Olsson, https://orcid.org/0000-0002-8075-419X, Sveriges lantbruksuniversitet, Institutionen för akvatiska resurser,

Rapportens innehåll har granskats av:

Mikko Olin, Natural Resource Institute Finland (Luke)

Szymon Smoliński, National Marine Fisheries Institute, Poland

Finansiär: SLUs miljöanalysprogram Kust och Hav (SLU-ID: SLU.aqua.2023.5.1-387)
Havs- och vattenmyndigheten, Dnr. 2025-001661 (SLU-ID: SLU.aqua.2025.5.1-199)

Rekommenderad citering:	Säterberg, T., Olsson, J. (2026). A population assessment model for the European perch along the Swedish Baltic Sea coast. Aqua notes 2026:1. Uppsala: Institutionen för akvatiska resurser. https://doi.org/10.54612/a.7bs7klrgkg
Publikationsansvarig:	Sara Bergek, Sveriges lantbruksuniversitet (SLU), Institutionen för akvatiska resurser
Redaktör:	Stefan Larsson, Sveriges lantbruksuniversitet (SLU), Institutionen för akvatiska resurser
Utgivare:	Sveriges lantbruksuniversitet, Institutionen för akvatiska resurser
Utgivningsår:	2026
Utgivningsort:	Uppsala
Illustration framsida:	-
Upphovsrätt:	Alla bilder används med upphovspersonens tillstånd.
Serietitel:	Aqua notes
Delnummer i serien:	2026:1
ISBN (elektronisk version):	978-91-8124-157-0
DOI:	https://doi.org/10.54612/a.7bs7klrgkg
Nyckelord:	European perch, age-base model, population indicator

Summary

The status of nationally managed fish stocks in Sweden is assessed following the temporal development of three indicators reflecting their abundance, size structure and mortality. The assessments are conducted by either comparing the indicator values in relation to reference points set by management, or if reference points do not exist, by investigating indicator values' trends over time. In practice, time trends are the most used approach.

For the European perch (*Perca fluviatilis*) populations along the Swedish coast of the Baltic Sea, assessments have mainly been based on the two indicators representing abundance and size structure. Although an indicator reflecting total mortality has also been included as part of the assessment in more recent years, the temporal variability of this indicator is currently not assessed. Moreover, despite that a rigorous length-stratified sampling program, which includes data collection of age, sex, and many other biological variables of perch individuals, is conducted along the Swedish coast of the Baltic Sea, this valuable data set is currently not used to a larger extent in the assessment of local perch populations.

In this report we develop a population assessment model to be used for female part of perch populations along the Swedish Baltic Sea coast. The model is age-based and it can be used to track variability in mortality, recruitment and abundance of females in the populations. Moreover, temporal changes in indicators can be assessed per age-class, enabling a more detailed description of population status than done previously, where mortality was estimated at the whole population scale. Furthermore, uncertainty in population indicators naturally follow as an output from the model.

Implementations of the model on multi-mesh gillnet data from eleven local perch populations along the Baltic Sea coast revealed some general patterns. For example, the model suggests that total mortality has increased over time in several local perch populations along the southern Swedish Baltic Sea coast and that age-class specific mortality in the populations increase with age.

Four explanations are specifically laid out as potential reasons behind the observed pattern of increasing mortality with age for local perch populations. First, size selectivity in the multi-mesh gillnets may cause smaller and younger individuals to be under-represented as compared to larger and older individuals in gillnet catches, inferring that higher mortality of younger individuals and hence a less pronounced age-mortality pattern would be observed if size selectivity was accounted for compared to when it is not. Second, fishing mortality that mainly affects large individuals in the populations may increase the mortality of older individuals as compared to young individuals. Third, size selective predation mortality may cause a general age-specific pattern in total mortality. Fourth, changes in habitat utilisation of perch individuals may change during ontogenetic development, causing older individuals not to be caught representatively in the multi-mesh gillnets. The relative importance of the proposed explanations cannot at present be disentangled, and we hence conclude that the observed age-mortality relationship observed here likely results from multiple reasons, both described and to date unknown. More studies are therefore needed to address the relative importance of the reasons proposed here.

Overall, the population dynamic model developed here is a tool that can be used to study variability in indicators, both at the population level and on a more detailed age-class specific level. Hence, it can be used to assess the status of local European perch populations, results of which may be used to pinpoint actions needed for strengthening and conserving local perch populations. Such results are of importance both for Fisheries and Marine Environmental Management.

Content

1. Background

1.1 Population definition

Previous studies have found that the European perch tend to exhibit a rather fine scaled local population structure, with tagged individuals seldom migrating further than 10 kilometres from the point of release (Böhling & Lehtonen 1984). Similarly, it has been found that perch individuals within 100 kilometres are genetically more similar than individuals that reside at further spatial distance from one another (Olsson et al. 2011). Genetical differences between perch individuals have even been found in relatively small lakes (Bergek & Björklund 2007), suggesting that spatially distinct populations are to be expected. Hence, population dynamics and management measures should be assessed at local scales. Therefore, the model developed here focuses on estimating total mortality for local populations, for which standardized multi-mesh gillnet data is available, along the Baltic Sea coast.

1.2 Population drivers

In the Baltic Sea, European perch is caught commercially using various gears such as gillnets, fyke-nets and fish traps, out of which gillnets is the most used gear. Total commercial landings along the Swedish Baltic Sea coast were somewhat higher in 1980-1999 (~140 tons yr^{-1}) compared to the landings in 2023 (~81 tons), and the total landings are relatively even distributed across the three main basins in the Baltic Sea, i.e. the Bothinian Sea, the Bothnian Bay and the Baltic proper (Fiskbarometern 2024).

Recreational fishing for the European perch is very popular in Sweden, and recreational catches are likely much higher than commercial catches, which is also the situation on the Finnish Baltic Sea coast (Kokkonen et al. 2019), although the accessible statistics is very uncertain (Statistics Sweden). Existing data though suggests that the outtake from recreational fishing on local perch populations in the Baltic proper could very well be ten times higher than the outtake from the commercial fishery (Fiskbarometern 2024). Moreover, as many of the perch individuals caught through sportfishing are released again in a fishery often called catch-and-release, the total impact from recreational fishing on local populations could be even higher than estimated from landings alone (Fiskbarometern 2024). As for the other two sub-basins, the Bothinian Sea and the Bothnian Bay, recreational fishery catch is likely also higher than the commercial catch, although the difference is likely not as large as it is for the more by humans densely populated area in the Baltic proper.

The European perch is a warm water adapted species. It has been found that its recruitment success relates to temperature during spring and the first summer experienced as juveniles (Kjellman et al. 2003, Linløkken 2023). The primary reason to this is likely that juveniles experience increased growth at high temperatures (Huss et al. 2019). However, for older perch it has been suggested that the positive effect of increasing temperature decreases or vanishes (Huss et al. 2019). In general, climate warming is hence likely beneficial for body growth in local perch populations (Lindmark et al. 2025), which may in turn lead to an increased reproductive output of local populations. However, an increased growth of perch, which has been observed over the last two decades for local perch populations along the Swedish coast (Fig. 20, Fig. 21 and Fig. 22 in Fiskbarometern 2024) and over a latitudinal gradient from North to South (Heibo et al. 2005), may potentially be counteracted by a simultaneous increase in total mortality (Heibo et al. 2005, Ning et al. 2025). For example, Lindmark et al. (2023) found using catch-curve analyses that the total mortality was higher in a heated ecosystem as compared to in a non-heated reference area in the Forsmark region on the Swedish Baltic Sea coast. Meanwhile the growth rate was higher in the heated ecosystem, leading to a generally higher mean length, with a fish population composed of younger individuals, in the heated ecosystem as compared to the non-heated ecosystem (Lindmark et al. 2023). However, the extent to which temperature driven increases in growth and mortality simultaneously affects the abundance and biomass of perch populations has not been investigated thoroughly.

There are several important food-web interactions that may affect local perch populations. It has for example been found that the extensive increase in abundance of three-spined stickleback (*Gasterosteus aculeatus*) in the Baltic Sea (Bergström et al. 2015), that although being a common prey in the diet of perch (Jacobson et al. 2019), affects the recruitment of large predatory fish such as perch and pike possibly through egg and juvenile predation (Eklöf et al. 2020). Such effects are particularly pronounced in the outer open archipelago, from which local perch populations appears to have been retracted (Eklöf et al. 2020). Moreover, perch is also being predated upon by large predators such as cormorants and seals. For example, very course estimates suggest that the combined fish extraction by cormorants is higher than the total extraction by the fishery (commercial and recreational), whereas the impact of seals is smaller (Hanson et al. 2018, Bolund et al. 2025).

2. Data

As neither commercial or recreational catch statistics nor predator consumption estimates are available at the spatio-temporal resolution required for modelling the development of local perch populations, the model presented here only uses data from Nordic coastal multi-mesh gillnets (See 2.1), and as it is only female perch that are age-read in the sampling program only females are considered in the model. The model is age-based and it tracks cohorts of female perch, hence it requires information on annual catches of female perch of age *a*, for the age-classes represented by the model. Input data, that is, number of female perch of age *a* caught per multi-mesh gillnet and night, is acquired by the following data processing steps:

(i) Data on the number of perch caught per cm-class and night is collected, and subsets of individuals are aged and sexed (See 2.1)
(ii) Lengths from the full sample are transformed to age using age-length keys (ALK´s) based on the subsample of age-read female individuals (See 2.2).
(iii) Individuals in the full sample are assigned sex based on the proportion females per cm-class in the subsample of sexed individuals (See 2.2).
(iv) Number of females of age *a* caught per net-night are summarized based on age and sex information acquired through data processing steps ii-iii.

Data collection and data processing is described in detail in the following sections (2.1-2.2).

2.1 Biological data

Scientific monitoring performed using multi-mesh gillnets is conducted on an annual basis as part of regional and national assessment of Swedish coastal fish communities. Collection of the monitoring data used here started in the early 2000s and is performed using so called Nordic coastal multi-mesh gillnets (Havs- och vattenmyndigheten 2020, Söderberg 2006). Nordic coastal multi-mesh gillnets are 1.8 m deep, they have a length of 45 m and consist of 5 m sections with mesh sizes 30, 15, 38, 10, 48, 12, 24, 60 och 19 mm. The gillnetting follows a depth stratified sampling scheme where 30-45 multi-mesh gillnets (dependending on monitoring area) are randomly deployed on the bottom, in four depth strata (0-3 m, 3-6 m, 6-10 m and 10-20 m) (Havs- och vattenmyndigheten 2020), a depth stratification which is ought to give a representative picture of the local fish community (Blomqvist et al. 2003). The overarching aim with the gillnet surveys is to representatively sample local fish communities, allowing for an assessment of the temporal variability of biodiversity, size structure and abundances of fish communities (Havs- och vattenmyndigheten 2020). As gillnet surveys are conducted along the whole Swedish Baltic Sea coast, it allows for an assessment of regional as well as a national status of fish communities, although geographical gaps in monitoring do exist (Bolund 2024; Bolund 2024 et al.; See Fig. 1 for the areas considered in this report and Tab. 1 for the data used). For warm water fish, such as perch, Nordic coastal multi-mesh gillnets are deployed in August, a period during which perch tend to distribute relatively widely across costal habitats (Mustamäki et al. 2014). Perch spawn during spring where they aggregate in shallow coastal habitats (Mustamäki et al. 2014), or in freshwater habitats (Hall et al. 2022), as water temperatures get favourable approximately above 10 ºC (Linløkken 2023). In summer, after spawning, perch tend to distribute more widely across costal habitats (Mustamäki et al. 2014), and in the autumn they tend to go to deeper zones for overwintering (Järv 2000). All perch are length measured to the nearest centimeter, making it possible to assess the development of its size structure (Havs- och vattenmyndigheten 2020).

Apart from sampling individual lengths, a subset of perch individuals is more rigoursly investigated. Following a length-stratified sampling scheme, approximately 10-20 perch individuals per cm-class are age-read, sexed, weighted and length-measured.

As information on gonad status is not collected in the sampling program the extent to which perch individuals are mature cannot be assessed. Hence, it is not possible to estimate the spawning population of perch based on these data.

There is some juvenile survey data available that could be used to follow recruitment of the European perch on the Swedish Baltic coast. However, it is only in a few of the locations considered in this report that such data is available at a sufficiently high temporal resolution to allow for modelling of recruitment dynamics. Hence, juvenile survey data is not used as input data to the perch model developed here. However, by back-calculations it is possible to derive a recruitment index, that in hindcast can be used to assess year-class strength (See Eq. 16).

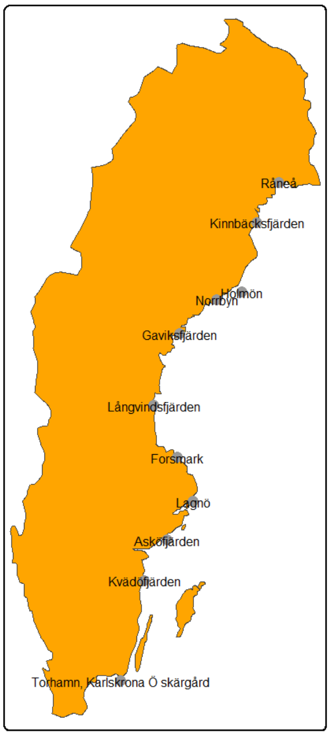

Figure 1. Map showing gillnet survey locations. Age-based models representing the population dynamics in each of these areas are fitted to standardized Nordic coastal multi-mesh gillnet data from each of these areas.

Table 1. Years with total gillnet catches, age-reading and sex subsample data available. The rightmost column shows the average number of gillnets deployed annually in each survey area. The number of gillnets deployed are not the same every year due to disturbances caused by for example predators and weather conditions. Hence, the average number of gillnet nights are presented as non-integer values.

Survey area	Years included in the model	Average number of gillnet nights per year
Råneå (Rå)	2006-2024	41.9
Kinnbäcksfjärden (Ki)	2007-2021	31.9
Holmön (Ho)	2002-2024	29.0
Norrbyn (No)	2002-2018,2021	31.3
Gaviksfjärden (Ga)	2007-2021	32.4
Långvindsfjärden (Lå)	2002-2021	36.8
Forsmark (Fo)	2007-2024	43.1
Lagnö (La)	2004-2021	36.7
Asköfjärden (As)	2005-2024	31.4
Kvädöfjärden (Kv)	2002-2024	34.2
Torhamn (To)	2002-2024	37.0

2.2 Data processing

First, before any data processing, data from multi-mesh gillnets disturbed by factors such as predators or severe weather conditions affecting the catches was filtered out from the full data set. Also, data from the 10-20 m depth interval was filtered out, as this depth strata only gives a qualitative and not a quantitative representation of the fish communities (Havs- och vattenmyndigheten 2020). Second, total catches per length-class and net-night were converted to number of females caught per age-class and net-night following the description below.

The model presented in this report is age-based, that is, it follows cohorts of female individuals as they age. Hence, it requires data on number of individuals caught per age-class. Similar to many fishery sampling programs, we here made use of length-stratified samples of dissected individuals, approximately 10-20 individuals per cm-class (Havs- och vattenmyndigheten 2020), to develop so called forward age-length-keys (ALKs) (Ailloud & Hoenig 2019), defining the probability that a fish of length l is of age a. Multiple ALKs were derived, one per area and year as the growth might differ between areas and years, to assign age to length measured fish caught in the Nordic coastal multi-mesh gillnets. Individual ages were assigned using the “alkIndivAge”-function from the FSA r-package (Ogle et al. 2025). Next, as perch display sexual size dimorphism where females grow faster and larger than males (Estlander et al. 2017), and since it is only females that are aged in the monitoring program, the model only considers the female part of the populations. Perch individuals were assigned sex based on the proportion females in random subsamples of individuals per cm-class and area. This was done assuming that the proportion of females observed per cm-class represents the proportion of females per cm-class in the whole population, that is:

$$X_{ikl} \sim Bern(\hat{p}_{kl}) \quad (1)$$

where *Bern* represents the Bernoulli distribution, X_{ikl} is an indicator giving information as to whether the individual i in area k of length l is a female (coded as 1) or male (coded as 0), and $\hat{p}_{kl}$ is the observed proportion of females in subsamples of individuals of length l from area k.

Using the individual information above, data was summarized, counting the number of females of age a caught per net and night. Catch-curves, with number of females caught per age-class and net-night, were thereafter created for each area independently. Age-classes below the peak age in the catch-curves were assumed to be non-representatively sampled (e.g. Appelberg et al. 1995), and hence not included as data input in the models. Moreover, in each area, individuals at certain age or older were aggregated into plus-groups. In order to avoid issues with modelling data with many zeros, a threshold age of the plus-group in each areas was defined using a prespecified catch-per-unit-effort value (CPUE < 0.2). If the mean number of individuals caught per net-night for a given age-class was below this value, it was assumed to belong to the plus-group. Moreover, the plus-group also included the age-class just above this threshold. Age-classes included in the models for each area are displayed in Table 2.

Table 2. Age-classes used in models. A_{plus} represents the lowest age considered in the plus-group, i.e. the plus-group consists of individuals of age ≥ A_{plus}, and A_{min} shows the smallest age-class (the peak in the catch-curve) used in the model (See Appendix 1).

Area	A_{plus}	A_{min}
Råneå	8	2
Kinnbäcksfjärden	5	3
Holmön	6	1
Norrbyn	5	2
Gaviksfjärden	5	2
Långvindsfjärden	7	2
Forsmark	6	1
Lagnö	5	1
Asköfjärden	5	2
Kvädöfjärden	6	1
Torhamn	3	1

3. Population assessment model

3.1 General description

The model considered is an age-based population dynamic model, i.e. a model where the temporal development of fish cohorts can be followed, fitted in a Bayesian framework. The model only estimates total mortality rate per year (yr^{-1}) and hence does not distinguish different mortality sources, such as fishing, predation or other natural induced mortality rates. Further, as no catch statistics neither any estimates of total consumption by predators are used in the estimation process, the model can only produce estimates of population dynamics in a relative sense, that is, it cannot be used to estimate variability in total population size within areas but instead reflects the scale of the survey data. Here, we use multi-mesh gillnet data, and hence, the unit considered is the number of female perch caught per age-class, net and night, that is, catch-per-unit-effort (CPUE).

3.1.1 Detailed model description

The population dynamics follow a standard age-based model:

$$N_{a,t} = \begin{cases} N_{a,t} & \text{if } a = A_{min} \\ N_{a-1,t-1} \cdot \mathrm{e}^{-Z_{a-1,t-1}} & \text{if } a > 1 \text{ and } a \neq A \\ N_{a-1,t-1} \cdot \mathrm{e}^{-Z_{a-1,t-1}} + N_{a,t-1} \cdot \mathrm{e}^{-Z_{a,t-1}} & \text{if } a = A_{plus} \end{cases} \qquad (2)$$

where $N_{a,t}$ is the number of perch female individuals of age a year t, $Z_{a-1,t-1}$ is the total mortality experienced by female individuals of age *a-1* during year *t-1*, that is, from the census at time *t-1* to the census at time *t*, A_{min} refers to the minimum age-class (the peak age-class in the catch-curve analysis) considered in an area and A_{plus} is the plus-group, i.e. female individuals of age A_{plus} or above.

The model could include size or age selectivity in the fishing gear. However, indirect (Appelberg et al. 1995) and direct measures (Prchalova et al. 2009) of catchability in multi-mesh gillnets similar to the Nordic coastal multi-mesh gillnets used here suggest that selectivity is relatively constant over the age-classes used in this analysis and hence we do not correct for selectivity.

Recruitment of perch is likely temperature dependent (Kjellman et al. 2003, Linlökken 2023) and such information could be used to model abundance of the first age-class in the model, i.e. $N_{A_{min},t}$. For simplicity, however, recruitment to the fishing gear was model as a lognormal process, following:

$$\ln\left(N_{A_{min},t}\right) \sim \text{normal}\left(\mu_{\ln\,(N_{A_{min}})}, \sigma_{\ln\,(N_{A_{min}})}\right) \tag{3}$$

where $\mu_{\ln\,(N_{A_{min}})}$ is mean recruitment on the ln-scale and $\sigma_{\ln\,(N_{A_{min}})}$ is the standard deviation of annual of recruitment on the ln-scale.

Age-class specific mortality rate (i.e. $Z_{a,t}$) was modelled following Nielsen & Berg (2014), where age-class specific fishing mortality rates are modelled as a random-walk process with innovations, that is, the random noise in the random walk process, correlated across age-classes. The rationale behind this model choice is that mortality is likely evolving more similarly for adjacent age-classes as compared to more distant age-classes. The random walk process was modelled on the ln-scale to avoid the implausible outcome of negative mortality, that is, population growth instead of mortality. The random walk process is defined as:

$$\begin{aligned}&\ln\left(\mathrm{Z}_{a,t}\right) = \ln\left(\mathrm{Z}_{a,t-1}\right) + \epsilon_{a,t},\\&\boldsymbol{\epsilon}_t \sim \mathcal{N}(\mathbf{0}, \boldsymbol{\Sigma}),\\&a = A_{min}, \dots, A_{plus} - 1,\end{aligned} \tag{4}$$

where $\mathrm{Z}_{a,t}$ is the mortality rate at time *t* for age class *a*, and $\boldsymbol{\epsilon}_t$ is a multivariate normal process error vector with covariance matrix

$$\boldsymbol{\Sigma}_{a,\tilde{a}} = \rho^{|a-\tilde{a}|}\sigma_a\sigma_{\tilde{a}}, \qquad a, \tilde{a} = A_{min}, \dots, A_{plus} - 1, \tag{5}$$

where $\tilde{a}$ and a define two age-classes, σ_a and $\sigma_{\tilde{a}}$ their respective age-class specific standard deviations, and ρ the correlation parameter.
For the plus group age-class A_{plus}, mortality is defined as equal to the previous age-class:

$$Z_{A_{plus},t} = Z_{A_{plus}-1,t} \tag{6}$$

The model is coupled to multi-mesh gillnet data using a negative binomial likelihood parameterized in terms of its mean, and a dispersion parameter:

$$y_{i,a,t} \sim \text{NegBin}\left(N_{a,t}, \phi\right) \tag{7}$$

where $N_{a,t}$ is the expected number of perch in age-class a caught at time t, and ϕ is a dispersion parameter. $y_{i,a,t}$ defines data, that is, the number of perch individuals of age-class a caught during one night year t, where i is an index of the observation.

The specific parameterization of the negative binomial distribution used in this model infers an assumed variance of observations following:

$$\mathrm{Var}[y_{i,a,t}] = N_{a,t} + \frac{{N_{a,t}}^2}{\phi} \quad (8)$$

where the dispersion parameter, ϕ, scales how variance is related to the expected value of the process.

3.1.2 Priors

As the model is fitted in a Bayesian framework, priors were assigned to the different parameters considered in the model, and the same priors were assigned for each area, i.e. each local perch population, except initial abundances which were assigned area specific priors (Eqs. 13-14). The rationale behind choosing the same priors in each area is that model results, such as mortality rates, are comparable across local populations if the same priors are used across areas.

The dispersion parameter used in the negative binomial likelihood was assigned a relatively uninformative prior as no prior information on this parameter was available:

$$\phi \sim \mathrm{Gamma}(2,1) \quad (9)$$

Age-class specific mortality rates were initialized at the same value for all age-classes, with a relatively broad prior centred at 0.2, a standard value often assigned for natural mortality rates in different stock assessment models (Jörgensen & Holt 2013):

$$\ln{(Z_{a,t_{min}})} \sim \mathcal{N}(\ln(0.2), 1) \quad (10)$$

where $Z_{a,t}$ refers to the total mortality for age-class a at the initial time step t_{min}, i.e. the first year of data for a specific area.

Standard deviations for the random walk mortality process were assigned unique positive priors:

$$\sigma_a \sim \mathrm{half} - \mathcal{N}(0,1) \quad (11)$$

where half- $\mathcal{N}$ is a normal distribution restricted to positive values.

The correlation of the innovations used in the random walk mortality process was assigned a prior scaled such that the correlation parameter ρ is constrained within its feasibile range. Specifically, let

$w \sim Beta(2,2),\ w \in (0,1),$
and
$$\rho = 2 \cdot w - 1, \quad (12)$$
then
$\rho \in (-1,1),$

where $Beta$ denotes the beta distribution.

Population dynamics in each area was initialized assuming that initial age-class abundance, i.e. abundance of the first age-class considered in the model, should be centred close to the mean abundance across the whole time series. Hence, initial abundances at age were given the following lognormal priors:

$$\ln\left(N_{a,t_{min}}\right) \sim \mathcal{N}\left(\ln\left(\frac{1}{n}\sum_{i=1}^{n} y_{i,a,t_{min}}\right), 1\right) \text{ for } a > A_{min} \quad (13)$$

The mean recruitment to the initial age-class, A_{min}, in the areas was given lognormal priors centred on the mean abundance over the time series for this age-class, that is:

$$\mu_{\ln\,(N_{A_{min}})} \sim \mathcal{N}\left(\frac{1}{t_{max}}\sum_{t=1}^{t_{max}} l\,n\left(\frac{1}{n_t}\sum_{i=1}^{n_t} y_{i,1,t}\right), 1\right) \quad (14)$$

Annual variability in recruitment was informed by a hyperparameter constrained to positive values:

$$\sigma_{\ln\,(N_{A_{min}})} \sim \text{Half} - \text{Cauchy}(0,1) \quad (15)$$

where half-Cauchy is a Cauchy distribution restricted to positive values.

3.1.3 Population indicators

Apart from generating predictions of abundance and total mortality per age-class (Eq. 1), a couple of population indicators can readily be derived as generated quantities from the model. These indicators are detailed in the subsections below.

Annual mortality

An index of annual mortality generally experienced by perch individuals in the population was derived using an abundance weighted mortality given by:

$$\bar{Z}_t = \frac{\sum_i \hat{Z}_{a,t}\hat{N}_{a,t}}{\sum_i \hat{N}_{a,t}} \tag{16}$$

where $\hat{Z}_{a,t}$ and $\hat{N}_{a,t}$, are estimates of total mortality rate and abundance of females of age-class *a* at time point *t*, respectively.

CPUE

An abundance index for perch populations was derived simply by summing age-class specific female abundance estimates:

$$\bar{N}_t = \sum_a \hat{N}_{a,t} \tag{17}$$

where $\hat{N}_{a,t}$ is an estimate of female abundance of age-class *a* at time point *t*.

Recruitment index

A recruitment index was derived by back-calculating the number of female individuals at age 0+, that is, an estimate of the number of 0-year-olds at census in August:

$$\hat{R}_t = \hat{N}_{A_{min},t} \cdot e^{\sum_{k=t-A_{min}}^{t-1} \bar{Z}_k} \tag{18}$$

where $\hat{R}_t$ is the recruitment index at time *t*, $\hat{N}_{A_{min},t}$ is the estimate of abundance of age-class A_{min} (Eq. 1) at time point *t*, and $\bar{Z}_k$ is the annual mortality (Eq. 16) at time *k*.

Mean age-class mortality

Mortality rates were compared across areas using an indicator of area and age-class specific mortality rate. These were calculated as the mean of age-class specific mortality rates for the whole time series, that is:

$$\bar{Z}_a = \frac{1}{t_{max}-t_{min}} \sum_{t=t_{min}}^{t=t_{max}} \hat{Z}_{a,t} \tag{19}$$

where $\hat{Z}_{a,t}$ is an estimate of the mortality rate experienced by individuals in age-class a year *t*, and t_{min} and t_{max} are indices of the first- and last-time step in the mortality time series.

Area specific mean mortality

Total mortality rates were compared across areas using an indicator of area specific mean mortality rates. These were calculated as the mean of the abundance weighted mortality rates described above:

$$\bar{Z} = \frac{1}{t_{max} - t_{min}} \sum_{t=t_{min}}^{t=t_{max}} \bar{Z}_t \qquad (20)$$

where $\bar{Z}_t$ is an estimate of the abundance weighted mortality rate (Eq. 16), and t_{min} and t_{max} are indices of the first- and last-time step in the mortality time series.

3.2 Model settings

The models were implemented in STAN, using Hamiltonian Monte Carlo (HMC) for sampling. For each model (i.e. local population), four independent Markov chains were run. Each chain included a burn-in period of 1000 iterations, followed by 1000 iterations kept for posterior analysis. Initial values for the Markov chains were drawn from prior distributions (Eqs. 9-15). The adapt_delta parameter, which controls the target acceptance probability during the adaptation phase and influences the step size taken by the algorithm, was set to 0.95 to reduce the number of divergent transitions. All other settings in STAN were kept at their default settings.

3.3 Model diagnostics

All models had converged as indicated by low Rhat-values (Vehtari et al. 2021), $\hat{R}$<1.01, for all parameters in all models. A few divergent transitions were observed; however, only 4 out of the 11 model runs ended up in any divergent transition, and even in those cases, the number was minimal (at most 4 out of 4000 iterations). We therefore considered these divergent transitions to be a minor issue and proceeded with inference for all models.

3.3.1 Model fit

Estimates of number of female individuals caught per age-class were compared to observed data of the same quantity. This was done using so called Posterior predictive checks where data is simulated from the model and compared to observed data. Posterior predictive checks were conducted for each area and age-class independently, and the general distribution (Appendix 2), the proportion of zeros (Table 3, Appendix 3), and the expected number of female perch caught per net-night and year (Appendix 4) were compared between model simulations and data.

In general, the number of individuals females caught per net-night were well reproduced by the model (Appendix 2). Zooming on a somewhat more detailed level, the average number of female individuals caught per net-night and year was also well reproduced by the model, albeit with some clear discrepancies between model simulations and observed data (Appendix 4). The most notable discrepancy between model simulations and data occurs for the models representing the population dynamics in areas Långvindsfjärden (Appendix 4 [Långvindsfjärden]), Forsmark (Appendix 4 [Forsmark]) and Lagnö (Appendix 4 [Lagnö]). Here, some data points are clearly outside the 90-percent credibility bounds of the predictions. Also, the proportion of zeros in data are not always well reproduced by the models, at least so for the younger age-classes being modelled in some of the areas (Appendix 3, Table 3)

Table 3. Bayesian p-values comparing simulated and observed proportions of cases where zero female perch individuals of a specific age are caught during one gillnet-night. Bayesian p-values are calculated as: $p_B = P(T(y^{rep}) \geq T(y) | \, y)$ *, where T(.) is the proportion of zeros in replicated data simulated from the posterior distribution,* y^{rep}*, and the observed data, y, respectively. Values close to 0 indicate that the model underestimates the proportion of zero catches, values close to 1 indicate that the model overestimates the proportion of zero catches, and values close to 0.5 indicate a relatively good model fit. Hence, values marked in red display* $p_B < 0.05$ *or* $p_B > 0.95$*, that is, area-age-class combinations with at potential lack of fit for the proportion zeros, and values marked in green illustrate area-length-class combinations associated with a potential better fit, that is* $0.05 \leq p_B \leq 0.95$.

Age-class	Rå	Ki	Ho	No	Ga	Lå	Fo	La	As	Kv	To
1			1.00				1.00	1.00		1.00	0.94
2	0.86		0.10	0.61	0.90	1.00	0.00	0.00	0.93	0.01	0.25
3	1.00	0.12	0.00	0.49	0.20	0.01	0.61	0.48	0.35	0.13	0.72
4	0.16	0.60	0.06	0.96	0.61	0.45	0.81	0.61	0.58	0.38	
5	0.02	0.76	0.11		0.45	0.49	0.88	0.91	0.74	0.86	
6	0.16		0.57			0.39	0.87			0.87	
7	0.76					0.93					
8	0.35										

3.3.2 Retrospective patterns

Stability of parameter estimates was investigated using retrospective analyses. To this end, data sets were peeled, that is, the last observation in the time series was sequentially removed from the data set and the model was refitted to these reduced data sets. The procedure was repeated until five time points were removed from the full data set. Using the set of refitted models a metric of retrospective pattern, Mohns rho (ρ_M), was calculated according:

$$\rho_M = \frac{1}{h}\sum_{t=1}^{h}\left(\frac{X_{T-t}-\hat{X}_{T-t}}{\hat{X}_{T-t}}\right) \tag{21}$$

where h is the number of peels, X_{T-t} is the parameter of interest at time *T-t* estimated using the peeled data set, that is, data for the time span *1:T-t*, and $\hat{X}_{T-t}$ is an estimate of the parameter of interest at time *T-t* using the full data set, that is, data for time *1:T*.

The Mohns rho statistic, ρ_M, (Eq. 21) was calculated both for age-class specific mortality rates (Tab. 4) and age-class specific abundances (Tab. 5) as these are the most important model outputs, and medians of the posteriors of the parameters of interest were used in the calculations. Here, we used the 'rule of thumb' for short-lived species suggested by Hurtado-Ferro et al. (2015) (values outside the range (-0.22 to 0.30) corresponds to an undesirable retrospective pattern) to categorize desirable and undesirable retrospective patterns of the parameter estimates. Moreover, the Mohns rho statistic, ρ_M, was complemented with a visual analysis illustrating how parameter estimates respond to sequential removal of data points from the time series (Appendix 5, Appendix 6).

According to the Mohns rho, ρ_M, statistics, retrospective patterns in age-class specific mortality rate estimates were desirable for most of the areas considered in the analysis (Tab. 4). However, for age-class 2 and age-class 4 in Råneå, ρ_M, indicate an undesirable retrospective pattern. Yet, as mortality rates for age-class 2 and age-class 4 in the end of the time series, on which the Mohns rho statistic is based, are very low the statistics is based on near zero statistics, questioning the credibility of the Mohns rho statistics for this case. Further, visual inspection of retrospective patterns in mortality estimates for the Råneå area indicate that there should be no specific problems with parameter estimates of mortality rates for age-class 2 and age-class 4 for this specific case (Appendix 5 [Råneå]). Of larger concern for the Råneå area is likely age-class mortality estimates for age-class 7 and the plus-group, which illustrate a structured retrospective pattern which depends on the number of peels removed from the full data set (Appendix 5 [Råneå]). A similar reasoning, that is, that ρ_M is dominated by near zero values, also hold for age-class specific mortality estimates for age-class 2 and age-class 3 in Holmön (Tab. 4; Appendix 5 [Holmön]). In fact, upon visual inspection age-class specific parameter estimates appear to be relatively stable for all age-classes also for the Holmön data set (Appendix 5 [Holmön]). For Gaviksfjärden, ρ_M indicates that there is an undesirable retrospective pattern in mortality rate for age-class 2 (Tab. 4). Here, the estimate of age-class 2 mortality clearly increases as the time series is peeled (Appendix 5 [Gaviksfjärden]). Hence, for this area mortality rate estimates are clearly unstable, indicating a potential bias in parameter estimates. For Asköfjärden, ρ_M clearly indicates an undesirable retrospective pattern for the mortality of 4-year-olds (Tab. 4). An undesirable pattern in age-class 4 mortality is also clearly observable in the retrospective plot, illustrating that the last data point in the time series is highly influential (Appendix 5 [Asköfjärden]).

According to the Mohns rho, ρ_M, statistic, retrospective patterns in age-class specific abundance estimates were desirable for most of the areas in the analysis (Tab. 5), with two notable exceptions, the plus-group in Asköfjärden and age-class 1 in Kvädöfjärden. However, upon inspection of all retrospective plots for age-class abundances the model gives a good retrospective pattern for all areas, and that the exceptions observed are merely based on near zero statistics.

Table 4. Mohns rho for age-class specific mortality rate. Abbreviations stand for the different areas: Rå- Råneå; Ki – Kinnbäcksfjärden; Ho – Holmön; No – Norrbyn; Ga – Gaviksfjärden; Lå – Långvindsfjärden; Fo – Forsmark; La – Lagnö; As – Asköfjärden; Kv – Kvädöfjärden; To – Torhamn. Cells marked in red correspond to parameter estimates with an undesirable retrospective pattern according to Mohns rho ($\rho_M < -0.22$ or $\rho_M > 0.30$), and green marked cells correspond to parameter estimates with a desirable retrospective pattern ($-0.22 < \rho_M < 0.30$). Multi-mesh gillnet data is not available for years 2019-2020 in Norrbyn, hence ρ_M was not calculated for this area.

Age-class	Rå	Ki	Ho	No	Ga	Lå	Fo	La	As	Kv	To
1			0.20*	-			-0.02*	-0.05*		0.23*	-0.11*
2	0.67*		0.51	-	1.97*	-0.11*	-0.13	-0.00	-0.07*	-0.06	0.02
3	0.22	-0.01*	0.37	-	-0.21	-0.40	-0.02	-0.05	0.02	-0.11	0.02£
4	-0.66	0.06	-0.07	-	0.01	-0.00	-0.04	0.03	2.36	0.21	
5	-0.04	0.06£	0.11	-	0.01£	-0.07	0.04	0.03£	2.36£	-0.03	
6	0.01		0.11£	-		-0.08	0.04£			-0.03£	
7	0.02			-		-0.08£					
8	0.02£			-							

£ Plus-group * The first age-class considered in the respective areas

Table 5. Mohns rho for age-class specific abundance. Abbreviations stand for the different areas: Rå- Råneå; Ki – Kinnbäcksfjärden; Ho – Holmön; No – Norrbyn; Ga – Gaviksfjärden; Lå – Långvindsfjärden; Fo – Forsmark; La – Lagnö; As – Asköfjärden; Kv – Kvädöfjärden; To – Torhamn. Cells marked in red correspond to parameter estimates with an undesirable retrospective pattern according to Mohns rho ($\rho_M < -0.22$ or $\rho_M > 0.30$), and green marked cells correspond to parameter estimates with a desirable retrospective pattern ($-0.22 < \rho_M < 0.30$). Multi-mesh gillnet data is not available for years 2019-2020 in Norrbyn, hence ρ_M was not calculated for this area.

Age-class	Rå	Ki	Ho	No	Ga	Lå	Fo	La	As	Kv	To
1			-0.02*	-			-0.04*	-0.12*		-0.23*	-0.00*
2	-0.12*		-0.05	-	-0.14*	-0.21*	-0.02	-0.02	-0.00*	-0.02	0.03
3	-0.05	0.03*	0.00	-	-0.03	-0.03	-0.05	-0.02	0.15	-0.08	-0.13£
4	0.03	-0.00	-0.03	-	0.05	-0.03	0.03	0.05	-0.08	0.05	
5	0.01	-0.10£	0.03	-	0.01£	-0.00	0.07	-0.04£	-0.84£	-0.10	
6	-0.01		-0.02£	-		0.01	-0.09£			-0.01£	
7	-0.00			-		0.06£					
8	-0.02£			-							

£ *Plus-group* * *The first age-class considered in the respective areas*

3.3.3 Alternative model formulations

Initially, a model based on separable age-class effects and annual mortality was considered (Cook 2013). However, this model was deemed implausible as age-class specific mortality rates likely develop differently over time for different age-classes and are not fully correlated. Hence, a model assuming a total mortality pattern similar to the fishery mortality model by Nielsen & Berg (2014) was considered. Moreover, initially total mortality rates for the plus-group, A_{plus}, were estimated assuming a random walk process a keen to the other age-classes (Eqs. 4-5). However, due to data sparsity, and specifically due to decreases in CPUE over time for older age-classes in many of the areas considered, estimation of total mortality for the plus-group is difficult. Therefore, it was assumed that total mortality for the plus-group ($Z_{A_{plus},t}$) is the same as the mortality for the age-class below (Eq. 6).

3.4 Model results

In the subsections below we first describe patterns in population indicators for each of the areas (Fig. 1) considered in the analysis (subsection 3.4.1). We give a description of how general population indicators (Eqs. 16-18) have changed over time and to what extent these changes are driven by age-class specific abundances and age-class specific mortality rates (Eqs. 2-5). Next, we summarize, using mean total mortality rates (Eqs. 19-20), how total mortality differs across areas (subsection 3.4.2).

3.4.1 Area specific results

Råneå

The model suggests that female abundance has increased since 2017 (p for linear trend < 0.01) and is now in a state similar to the record high population size observed in 2006 and 2013 (Fig. 2a). According to the model, this result does not stem from an increase in recruitment (p for linear trend = 0.19) (Fig. 2c) but rather to a decline in the total mortality of perch individuals in the area (p for linear trend = 0.02) (Fig. 2b). This decline in total mortality is specifically driven by a decrease in the mortality of relatively young female individuals, that is, for age-classes 2-5 (Appendix 7 [Råneå]).

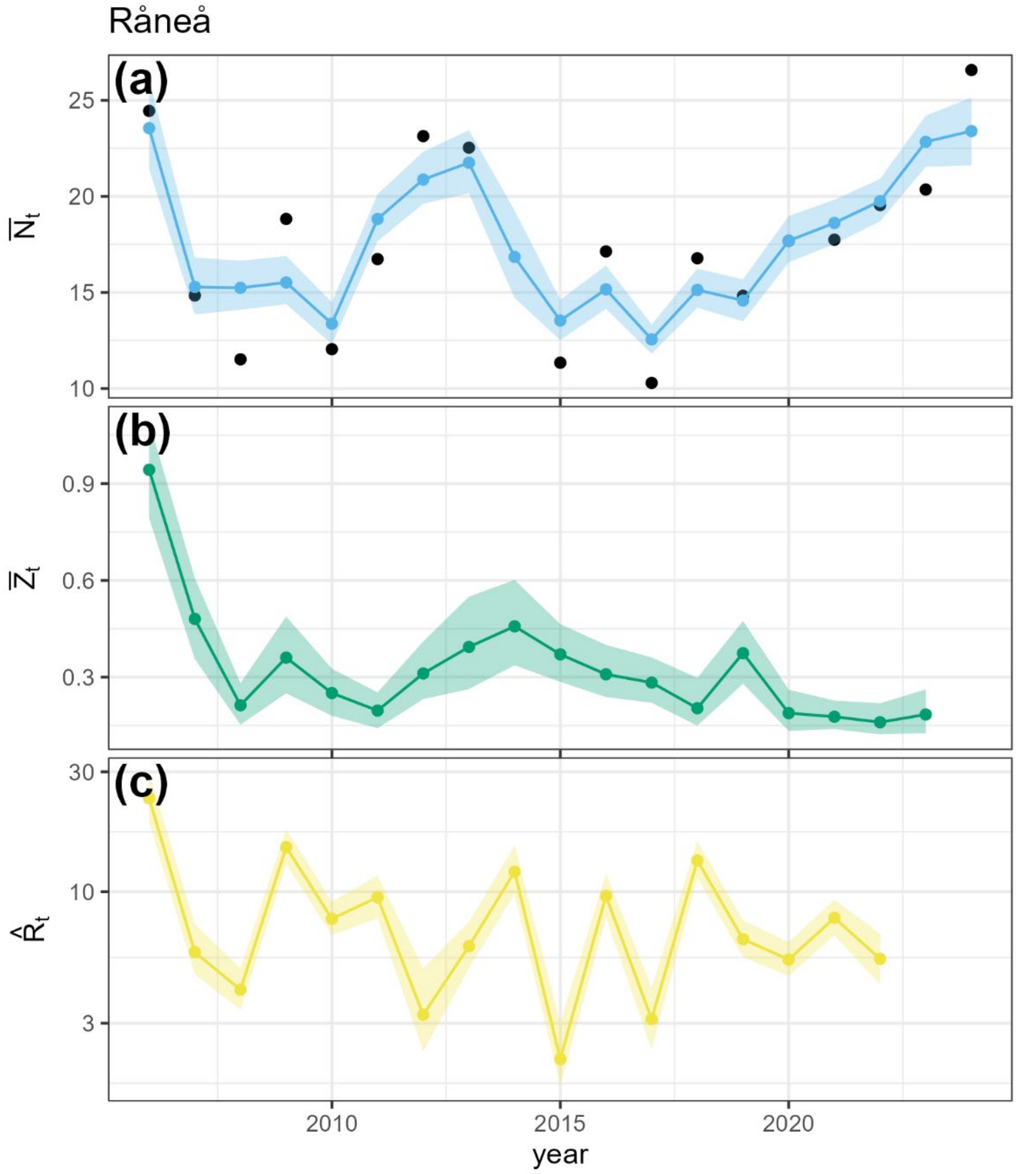

Figure 2. Temporal development of population indicators in Råneå. ***(a)*** *Total number of females of age 2 and older caught per net and night,* $\overline{N}_t$ *(Eq. 17). The light-blue line with points illustrates medians of the posterior distribution, ribbons displays 90 % credibility intervals of the posterior distribution, and black dots illustrate the mean number of females caught annually per net and night.* ***(b)*** *Abundance weighted mean annual mortality rate,* $\bar{Z}_t$ *(Eq. 16).* ***(c)*** *Back-calculated recruitment index,* $\hat{R}_t$ *(Eq. 18). As only female individual of age 2 year and older are included in the analysis, recruitment can only be estimates for years* T_{start} *: (*T_{final}*-2), where* T_{start} *is the first year with abundance observations and* T_{final} *is last year with abundance observations.*

Kinnbäcksfjärden

For Kinnbäcksfjärden there is no clear trend in abundance over time (p for linear trend = 0.45) (Fig. 3a). However, there appears to be a small positive trend in the total mortality rate for perch in this area (p for linear trend < 0.01) (Fig. 3b), specifically driven by an increase in the mortality rate of 3-year-olds (p for linear trend < 0.01) (Appendix 7 [Kinnbäcksfjärden]). According to the model, the increasing trend in total mortality may have been counteracted by an increase in recruitment (p for linear trend = 0.067) (Fig. 3c), leading to a relatively stable population dynamics in the abundance of females three years old and older (Fig. 3a).

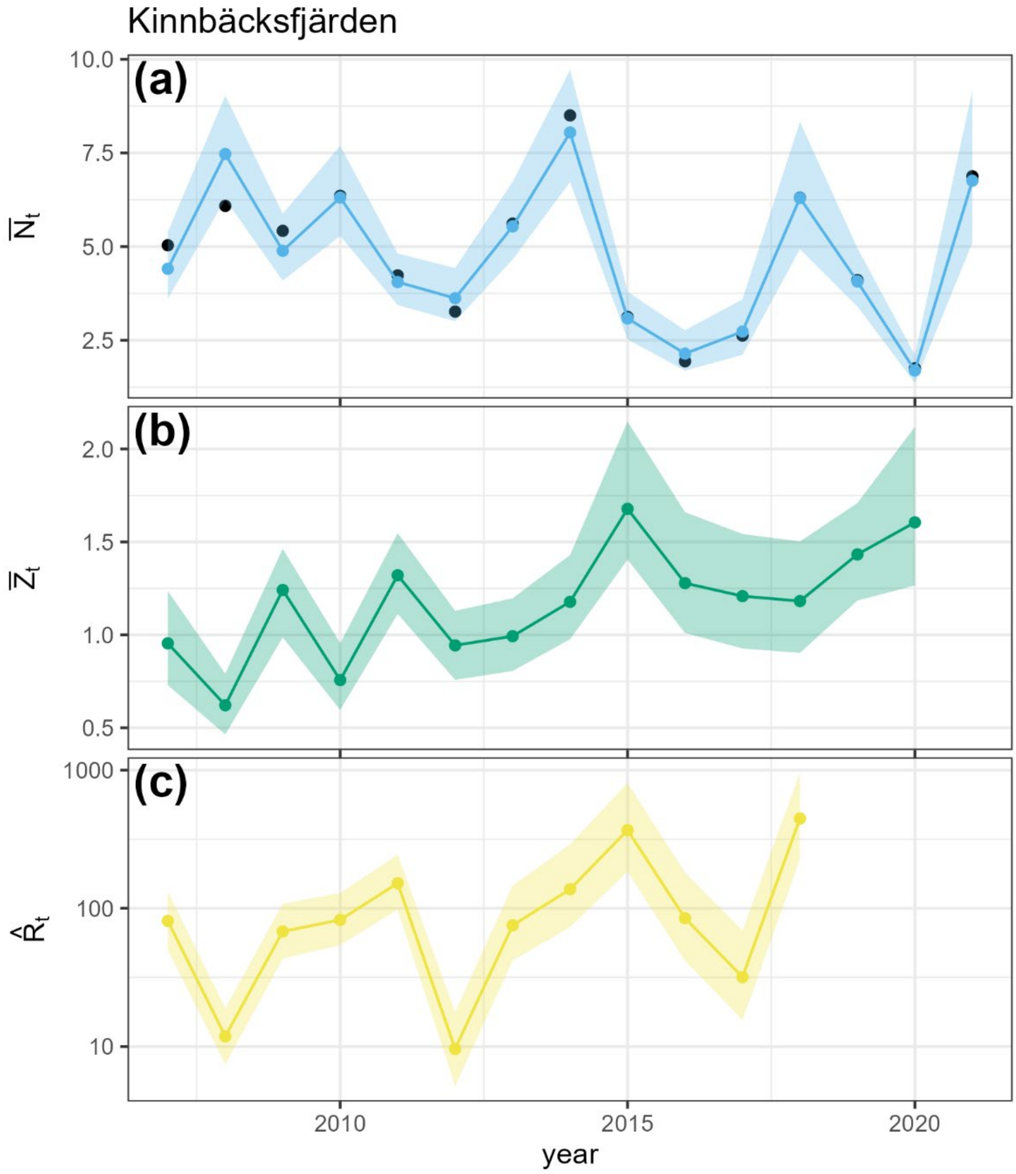

Figure 3. Temporal development of population indicators in Kinnbäcksfjärden. ***(a)*** *Total number of females of age 3 and older caught per net and night, $\overline{N}_t$ (Eq. 17). The light-blue line with points illustrates medians of the posterior distribution, ribbons display 90 % credibility intervals of the posterior distribution, and black dots illustrate the mean number of females caught annually per net and night.* ***(b)*** *Abundance weighted mean annual mortality rate, $\bar{Z}_t$ (Eq. 16).* ***(c)*** *Back-calclulated recruitment index, $\hat{R}_t$ (Eq. 18). As only individual of age 3 year and older are included in the analysis, recruitment can only be estimates for years T_{start} : (T_{final}-3), where T_{start} is the first year with abundance observations and T_{final} is last year with abundance observations.*

Holmön

In the Holmön area, neither female abundance (Fig. 4a), recruitment (Fig. 4c) nor total mortality (Fig. 4b) display any clear pattern over time (p for linear trend for all indicators > 0.05). Instead, the dynamics of the three population indicators appear relatively erratic. Population dynamics in this area is driven by strong cohorts. For example, for the year-classes born in 2003, 2013 and 2018 (Fig. 4c), cohorts can readily be followed by following how the number of individuals per age-class change over time (Appendix 4 [Holmön]).

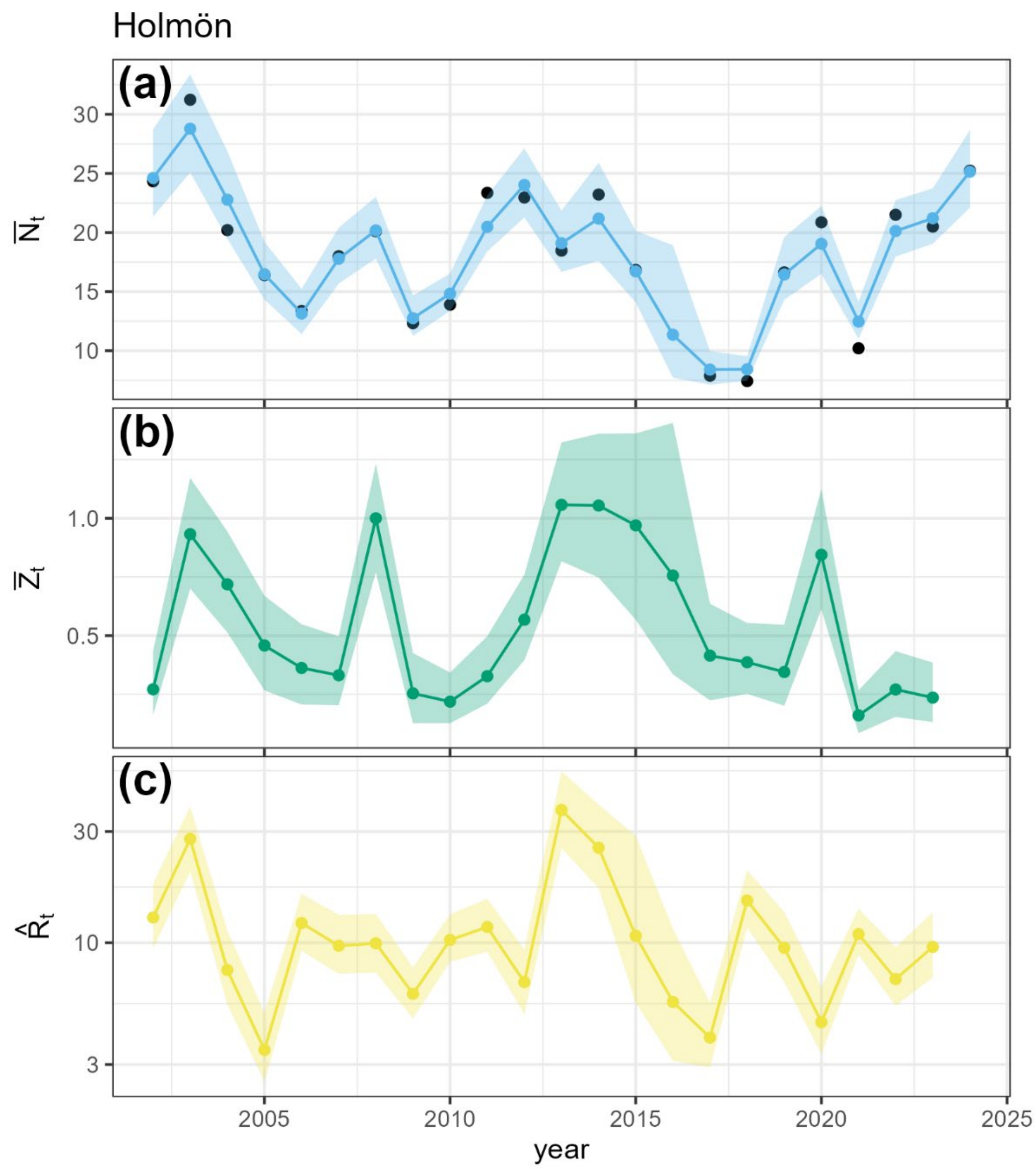

Figure 4. Temporal development of population indicators in Holmön. ***(a)*** *Total number of females of age 1 and older caught annually per net and night, $\overline{N}_t$ (Eq. 17). The light-blue line with points illustrates medians of the posterior distribution, ribbons display 90 % credibility bounds of the posterior distribution, and black dots illustrate the mean number of females caught annually per net and night.* ***(b)*** *Abundance weighted mean annual mortality rate, $\bar{Z}_t$ (Eq. 16).* ***(c)*** *Back-calculated recruitment index, $\hat{R}_t$ (Eq. 18). As only individual of age 1 year and older are included in the analysis, recruitment can only be estimates for years T_{start} : (T_{final}-1), where T_{start} is the first year with abundance observations and T_{final} is last year with abundance observations.*

Norrbyn

The total abundance of females in Norrbyn display two clear peaks, one in year 2005 and another in 2013 (Fig. 5a). These peaks are likely driven by strong cohorts, recruiting to the population in years 2003 and 2011, respectively (Fig. 5c; Appendix 4 [Norrbyn]). According to the model, there was also a peak in recruitment in 2014 (Fig. 5c), however, this peak does not give rise to a strong cohort, potentially due to a subsequent high mortality in 2014 (Fig. 5b). In terms of total mortality, no clear pattern over time is observed, neither with respect to the general mortality experienced by individuals (p for linear trend = 0.27) (Fig. 5b), nor with respect to age-class specific mortality rates (Appendix 7 [Norrbyn]). Moreover, for Norrbyn, predictions in the end of the time series are highly uncertain (Fig. 5) due to lack of data for years 2019-2020.

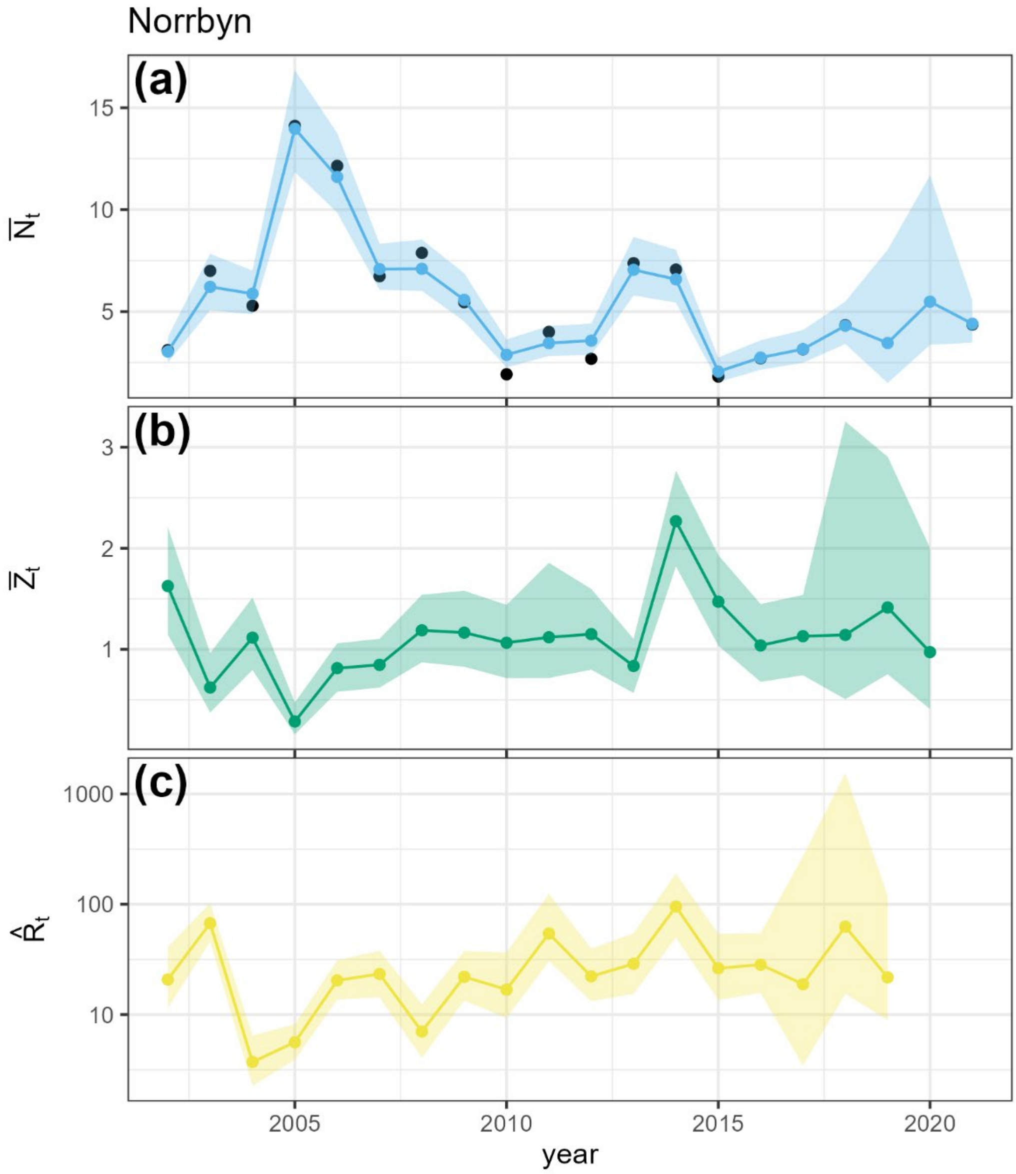

Figure 5. Temporal development of population indicators in Norrbyn. ***(a)*** *Total number of females of age 2 and older caught annually per net and night, $\overline{N}_t$ (Eq. 17). The light-blue line with points illustrates medians of the posterior distribution, ribbons display 90 % credibility bounds of the posterior distribution, and black dots illustrate the mean number of females caught annually per net and night.* ***(b)*** *Abundance weighted mean annual mortality rate, $\bar{Z}_t$ (Eq. 16).* ***(c)*** *Back-calculated recruitment index, $\hat{R}_t$ (Eq. 18). As only individual of age 2 year and older are included in the analysis, recruitment can only be estimates for years T_{start} : (T_{final}-2), where T_{start} is the first year with abundance observations and T_{final} is last year with abundance observations.*

Gaviksfjärden

In Gaviksfjärden, the peak in abundance of females in 2014 (Fig. 6a) appears to be driven by two subsequent strong cohorts, year-classes born in 2011 and 2012 (Fig. 6c), giving rise to a high total abundance of females (Fig. 6a) dominated by young individuals (Appendix 4 [Gaviksfjärden]). Further, there are additional strong year-classes born in 2007, 2015 and 2018 (Fig. 6c) that can readily be followed in age-class specific female abundances (Appendix 4 [Gaviksfjärden]). Total mortality displays no pattern over time (p for linear trend = 0.81) (Fig. 6b), but the mortality rate for the youngest age-class, that is, 2-year-olds has decreased somewhat over time (p for linear trend < 0.01) (Appendix 7 [Gaviksfjärden]).

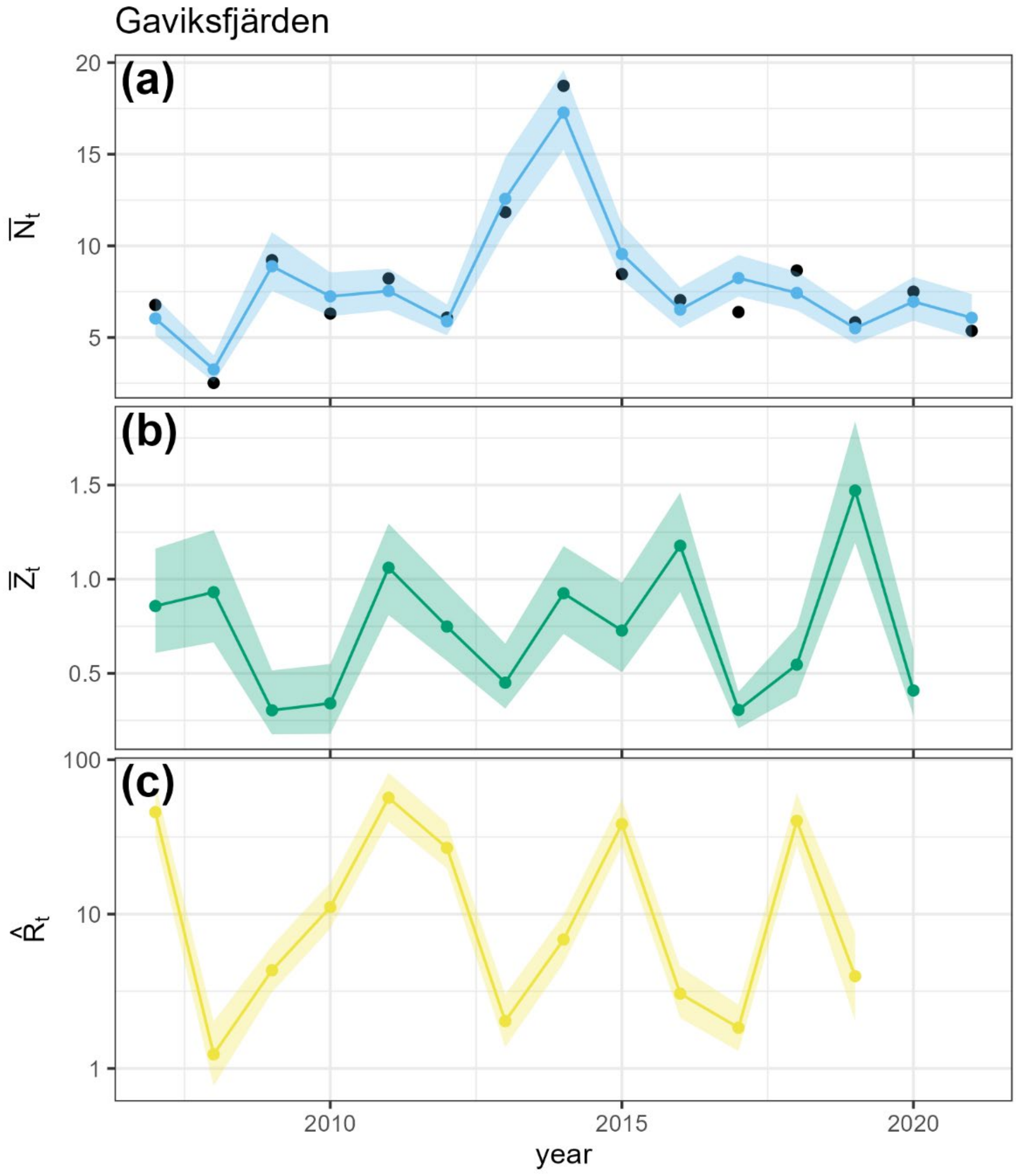

Figure 6. Temporal development of population indicators in Gaviksfjärden. ***(a)*** *Total number of females of age 2 and older caught annually per net and night, $\overline{N}_t$ (Eq. 17). The light-blue line with points illustrates medians of the posterior distribution, ribbons display 90 % credibility bounds of the posterior distribution, and black dots illustrate the mean number of females caught annually per net and night.* ***(b)*** *Abundance weighted mean annual mortality rate, $\bar{Z}_t$ (Eq. 16).* ***(c)*** *Back-calculated recruitment index, $\hat{R}_t$ (Eq. 18). As only individual of age 2 year and older are included in the analysis, recruitment can only be estimates for years T_{start} : (T_{final}-2), where T_{start} is the first year with abundance observations and T_{final} is last year with abundance observations.*

Långvindsfjärden

The abundance of female perch in Långvindsfjärden has been relatively stable over time (Fig. 7a), but for the last years in the time series abundances have increased, likely due to a very strong year-class born in 2018 (Fig. 7c) and low total mortality in 2019-2020 (Fig. 7b). This year-class dominates the total population size due to the recruitment of 2-year-olds to the population in 2020 (Appendix 4 [Långvindsfjärden]). For other years, there is no clear pattern as to whether strong year-classes contribute significantly to the total abundance, although recruitment peaks (Fig. 7c) give rise to strong year-classes (Appendix 4 [Långvindsfjärden]). Total mortality rate does not display any clear trend (p for linear trend = 0.60) (Fig. 7b), however time trends indicate that mortality rates for older individuals have increased over time (p values for linear trends age classes 4 and above < 0.1) (Appendix 7 [Långvindsfjärden]).

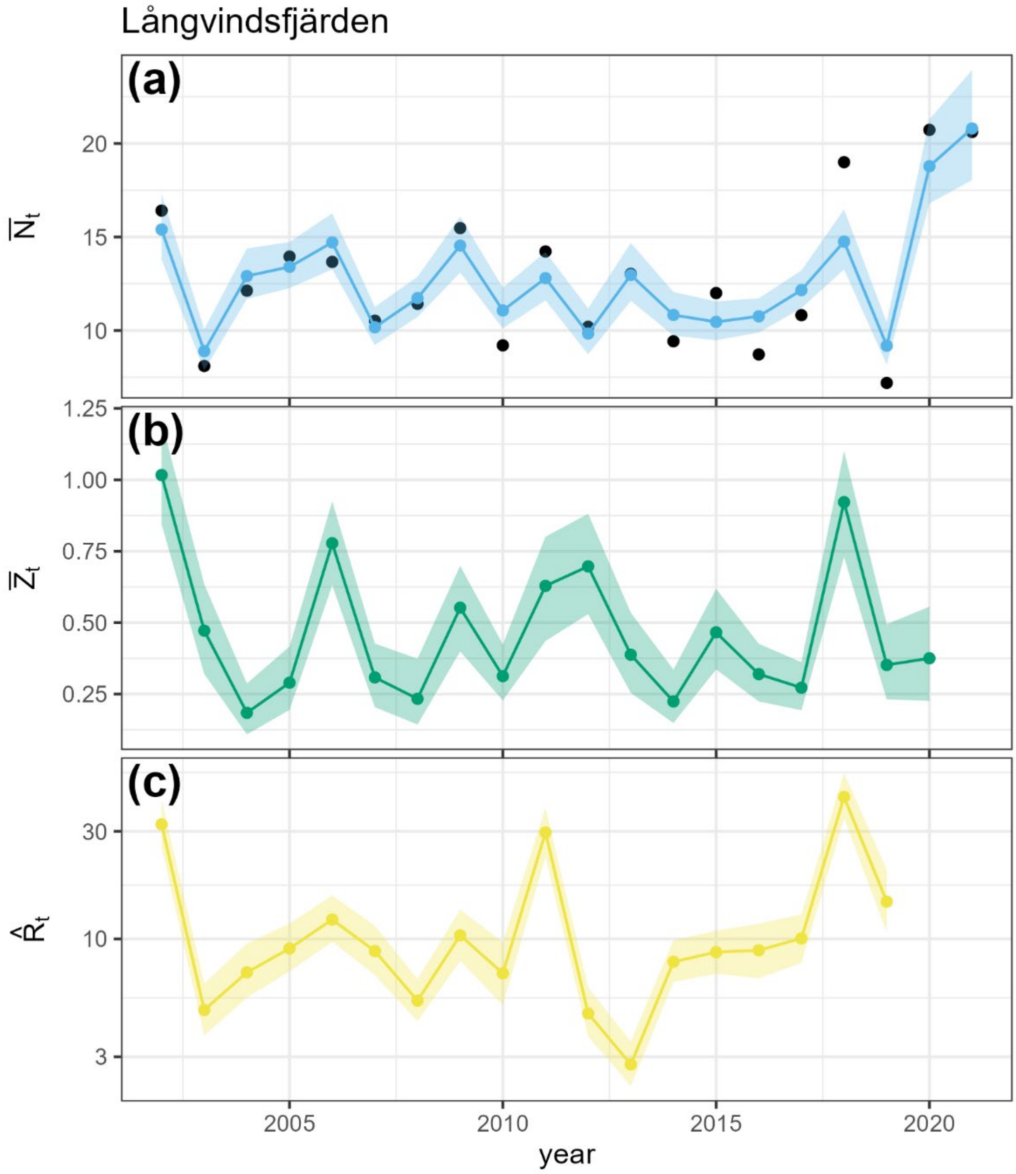

Figure 7. Temporal development of population indicators in Långvindsfjärden. ***(a)*** *Total number of females of age 2 and older caught annually per net and night, $\overline{N}_t$ (Eq. 17). The light-blue line with points illustrates medians of the posterior distribution, ribbons display 90 % credibility bounds of the posterior distribution, and black dots illustrate the mean number of females caught annually per net and night.* ***(b)*** *Abundance weighted mean annual mortality rate, $\bar{Z}_t$ (Eq. 16).* ***(c)*** *Back-calculated recruitment index, $\hat{R}_t$ (Eq. 18). As only individual of age 2 year and older are included in the analysis, recruitment can only be estimates for years T_{start} : (T_{final}-2), where T_{start} is the first year with abundance observations and T_{final} is last year with abundance observations.*

Forsmark

In the Forsmark area, two clear peaks in total abundance of females are observed, one peak after year 2011 and another one but comparably lower peak after year 2018 (Fig. 8a). These peaks likely result from strong recruitment in 2010, 2018, 2019 and 2021 (Fig. 8c). Although the recruitment peak was lower in year 2011 as compared to the recruitment peaks during the latter years (2018, 2019 and 2021) (Fig. 8c), total female perch abundance was anyhow higher during 2012-2014 compared to the later years (Fig. 8a). This result likely stems from the fact that there is a tendency that total mortality has increased over time (p for linear trend = 0.11) (Fig. 8b). Increasing mortality might hence counteract the effects of an increasing recruitment and increasing mortality is specifically pronounced for older age-classes (p for linear trends for age-classes 3 and above < 0.01) (Appendix 7 [Forsmark]).

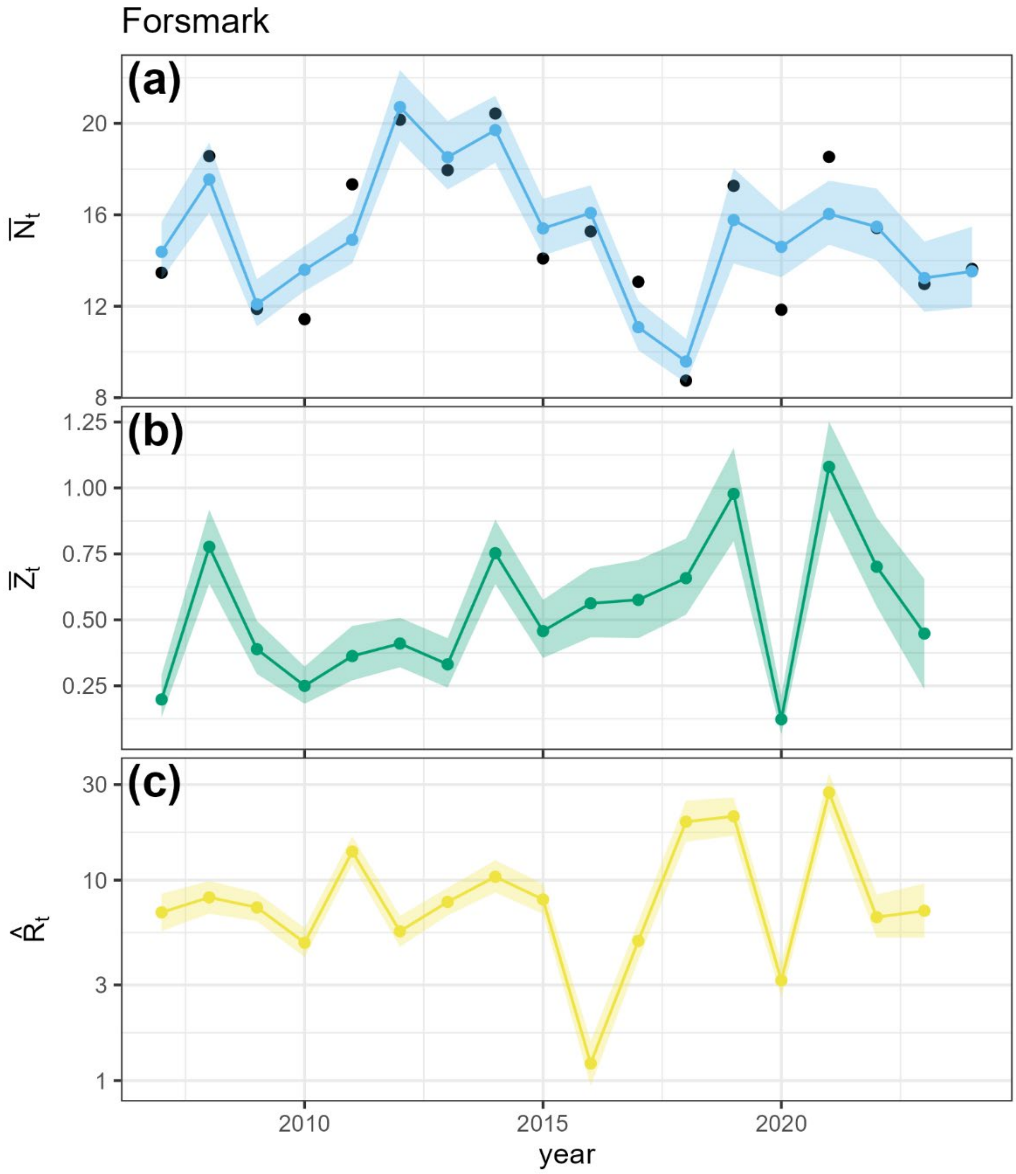

Figure 8. Temporal development of population indicators in Forsmark. ***(a)*** *Total number of females of age 1 and older caught annually per net and night, $\overline{N}_t$ (Eq. 17). The light-blue line with points illustrates medians of the posterior distribution, ribbons display 90 % credibility bounds of the posterior distribution, and black dots illustrate the mean number of females caught annually per net and night.* ***(b)*** *Abundance weighted mean annual mortality rate, $\bar{Z}_t$ (Eq. 16).* ***(c)*** *Back-calculated estimate of annual recruitment, $\hat{R}_t$ (Eq. 18). As only individual of age 1 year and older are included in the analysis, recruitment can only be estimates for years T_{start} : (T_{final}-1), where T_{start} is the first year with abundance observations and T_{final} is last year with abundance observations.*

Lagnö

In the Lagnö area, total abundance of females has been relatively stable over time, with a notable decrease during the years 2014-2017 (Fig. 9a). This dip in total abundance likely results from a relatively low recruitment during 2012-2015 (Fig. 9c), and a subsequent increase in total mortality (Fig. 9b). In the end of the time series total population size is high due to high recruitment (Fig. 9c), but the abundance is dominated by young individuals (Appendix 4 [Lagnö]), as older individuals have experienced an increasing mortality over time (Appendix 7 [Lagnö]).

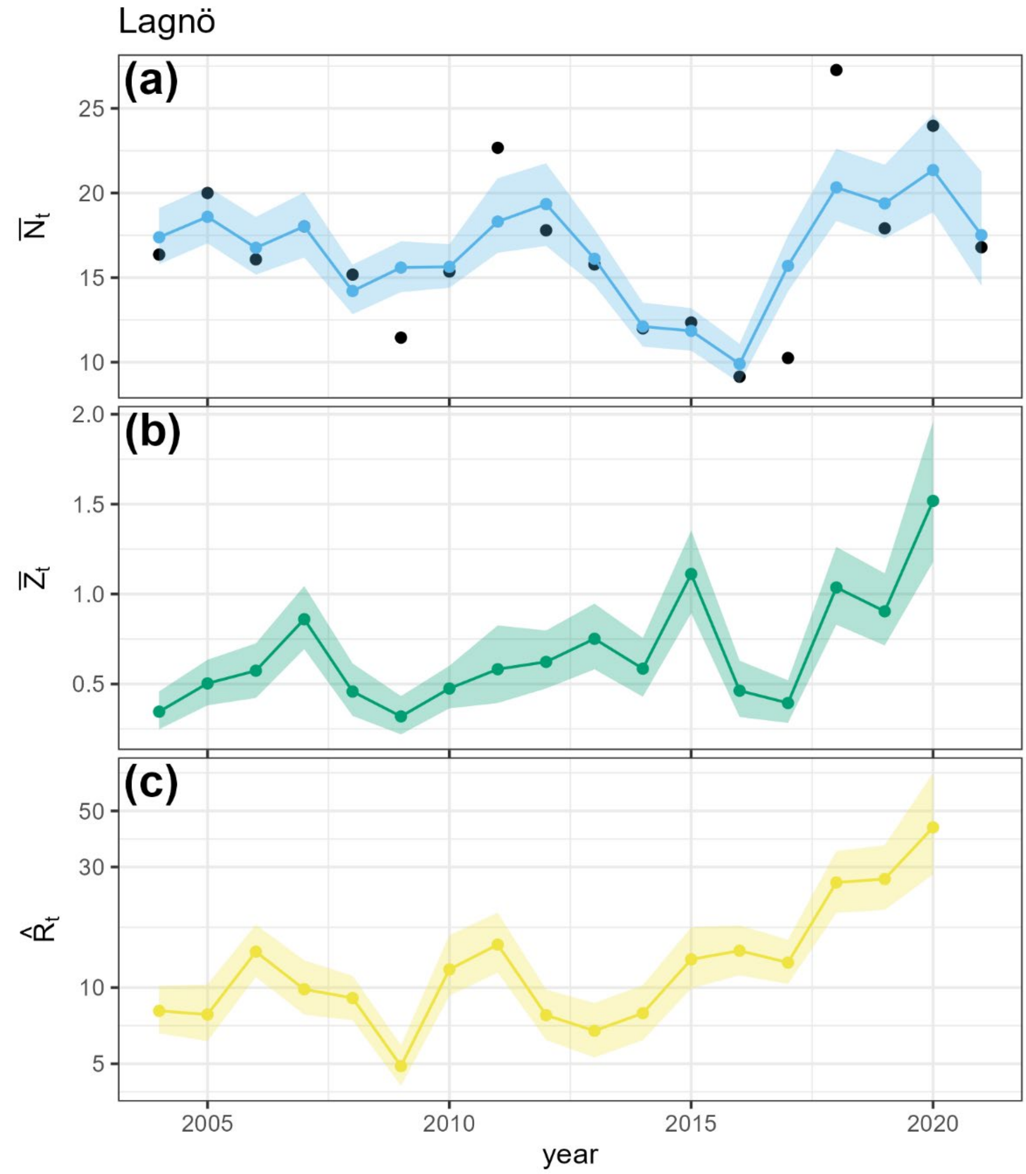

*Figure 9. Temporal development of population indicators in Lagnö. **(a)** Total number of females of age 1 and older caught annually per net and night, $\bar{N}_t$ (Eq. 17). The light-blue line with points illustrates medians of the posterior distribution, ribbons display 90 % credibility bounds of the posterior distribution, and black dots illustrate the mean number of females caught annually per net and night. **(b)** Abundance weighted mean annual mortality rate, $\bar{Z}_t$ (Eq. 16). **(c)** Back-calculated recruitment index, $\hat{R}_t$ (Eq. 18). As only individual of age 1 year and older are included in the analysis, recruitment can only be estimates for years T_{start} : (T_{final}-1), where T_{start} is the first year with abundance observations and T_{final} is last year with abundance observations.*

Asköfjärden

In Asköfjärden, a major shift in female population dynamics appears to have occurred around year 2015 (Fig. 10). This shift in dynamics is governed by a drastic increase in total mortality (p for linear trend < 0.01) (Fig. 10b), an increase in mortality rate which is specifically pronounced for age-classes 2 and 3 (p for linear trends < 0.01) (Appendix 7 [Asköfjärden]) and corresponds to a total mortality (yr^{-1}) at around 85-95 % in the end of the time series. In fact, there are almost no individuals observed for age-classes above age 2 in the end of the time series (Appendix 4 [Asköfjärden]). However, future will tell whether the recruitment peak in 2022 (Fig. 10c) has given rise to a strong year-class that will increase the abundance of all age-classes in the area (Appendix 4 [Asköfjärden]) as indicated by total female abundance in 2024 (Fig. 10a).

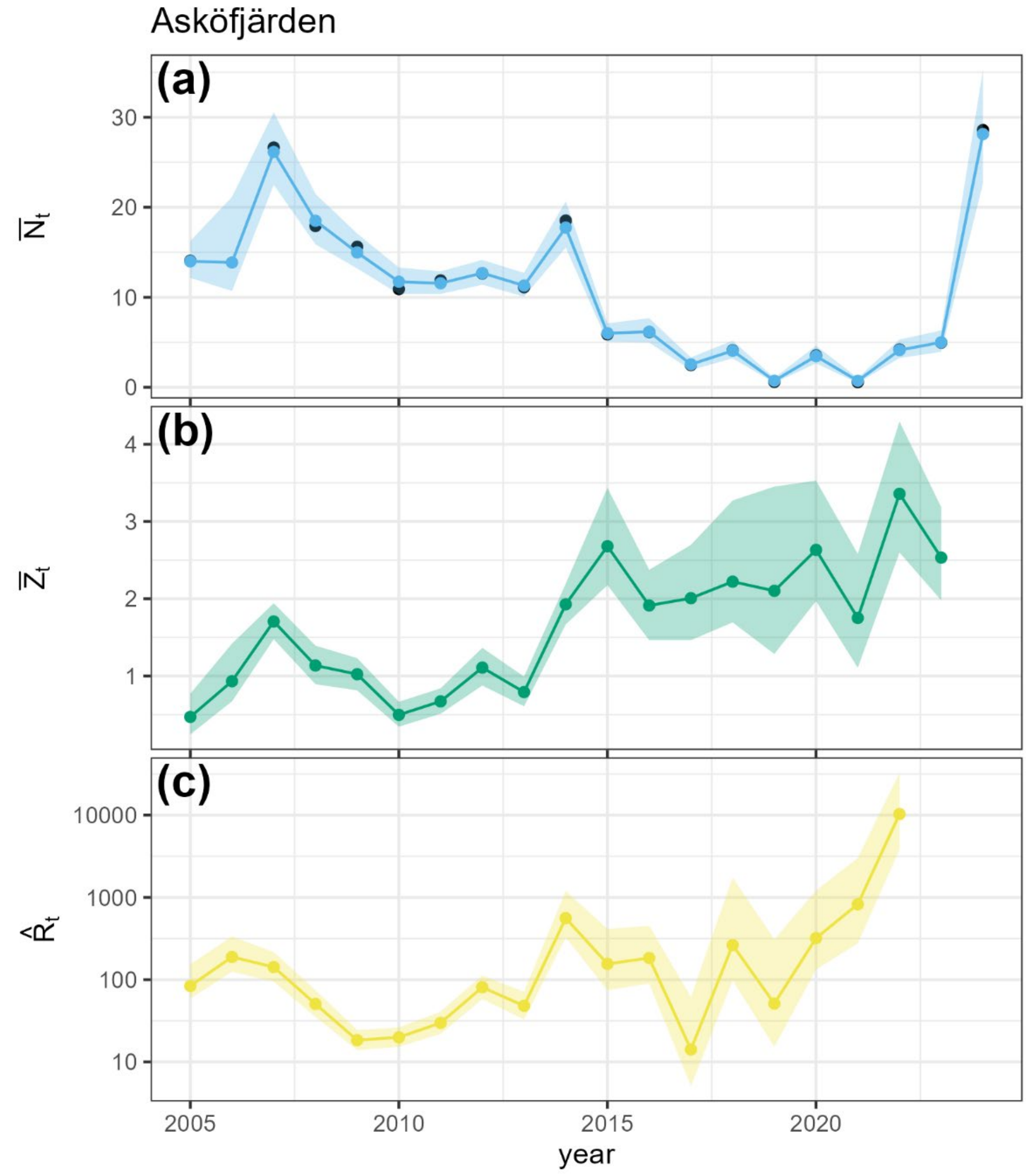

*Figure 10. Temporal development of population indicators in Asköfjärden. **(a)** Total number of females of age 2 and older caught annually per net and night, $\overline{N}_t$ (Eq. 17). The light-blue line with points illustrates medians of the posterior distribution, ribbons display 90 % credibility intervals of the posterior distribution, and black dots illustrate the mean number of females caught annually per net and night. **(b)** Abundance weighted mean annual mortality rate, $\bar{Z}_t$ (Eq. 16). **(c)** Back-calculated recruitment index, $\hat{R}_t$ (Eq. 18). As only individual of age 2 year and older are included in the analysis, recruitment can only be estimates for years T_{start} : (T_{final}-2), where T_{start} is the first year with abundance observations and T_{final} is last year with abundance observations.*

Kvädöfjärden

In Kvädöfjärden there are no clear patterns with regards to effect of recruitment and mortality on the total abundance of female perch (Fig. 11). Similar to many of the other areas, strong recruitment pulses, for example the three highest recruitment peaks observed in the time series (year 2002, 2006 and 2018 in Fig. 11c), give rise to strong cohorts that can readily be observed in time series of age-class specific abundances (Appendix 4 [Kvädöfjärden]). There is no clear trend in total mortality (p linear trend = 0.08), except that mortality appears to fluctuate to a larger extent during recent years as compared to in the beginning of the time series (Fig. 11b). In this area, mortality of young individuals (age-class 1) appears to have decreased over time (p linear trend < 0.01), whereas no clear patterns are observed for other age-classes (Appendix 7 [Kvädöfjärden]).

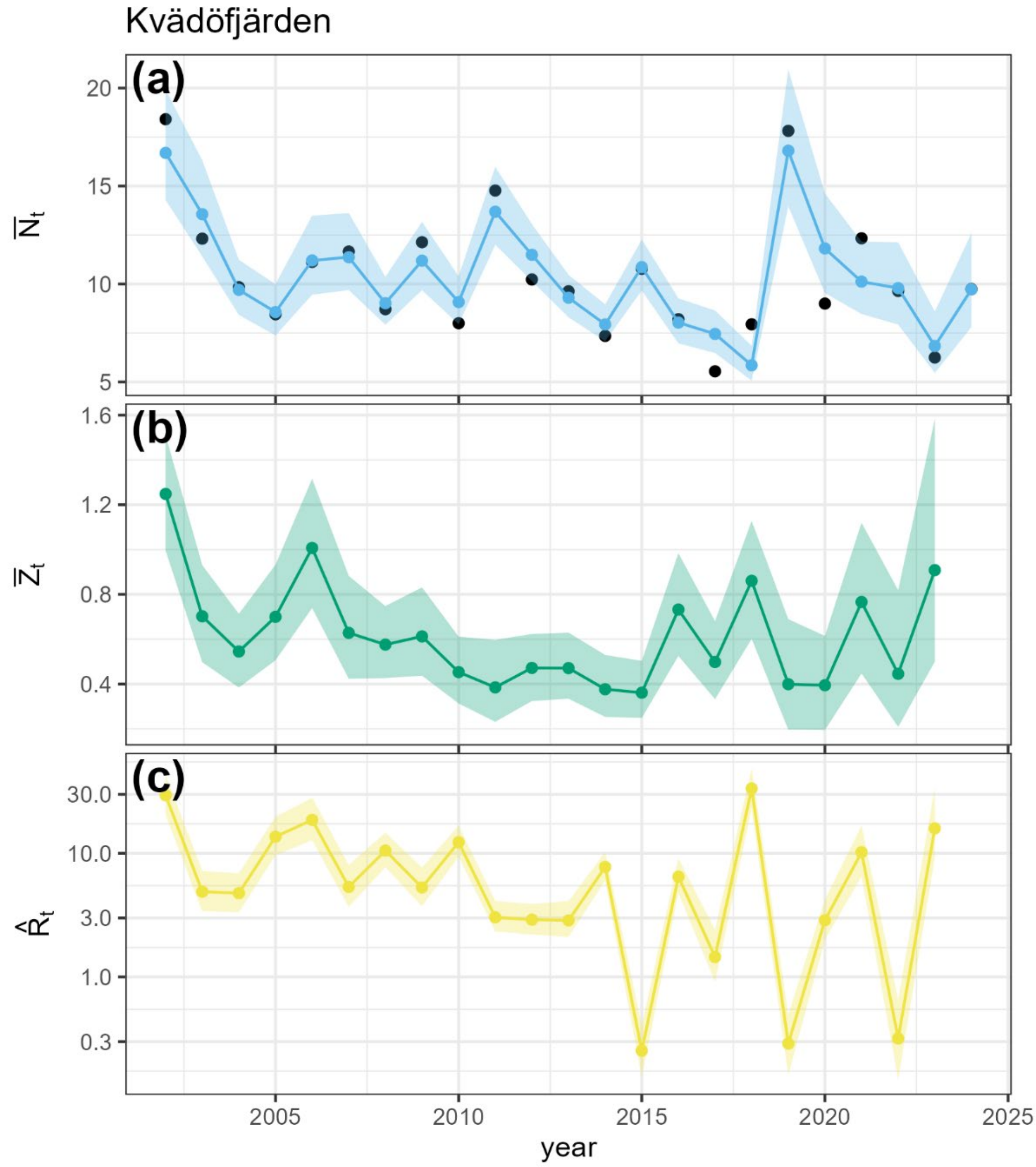

Figure 11. Temporal development of population indicators in Kvädöfjärden. ***(a)*** *Total number of females of age 1 and older caught annually per net and night,* $\overline{N}_t$ *(Eq. 17). The light-blue line with points illustrates medians of the posterior distribution, ribbons display 90 % credibility intervals of the posterior distribution, and black dots illustrate the mean number of females caught annually per net and night.* ***(b)*** *Abundance weighted mean annual mortality rate,* $\bar{Z}_t$ *(Eq. 16).* ***(c)*** *Back-calculated recruitment index,* $\hat{R}_t$ *(Eq. 18). As only individual of age 1 year and older are included in the analysis, recruitment can only be estimates for years* T_{start} *:* $(T_{final}$*-1), where* T_{start} *is the first year with abundance observations and* T_{final} *is last year with abundance observations.*

Torhamn

In the Torhamn area, model results indicate that abundance of females has decreased over time (p linear trend = 0.09) and are specifically low during the most recent years (Fig. 12a). This decrease in abundance may result from an increased mortality over time (p linear trend = 0.07) (Fig. 12b), which to some extent is counteracted by a similar development in recruitment (Fig. 12c). Although mortality is highly variable between years in this area, mortality rates for the oldest age-classes, that is, age-class 2 and the plusgroup have clearly increased (p linear trend < 0.01) (Appendix 7 [Torhamn]). As for many other areas analysed, recruitment peaks, as for example the two highest recruitment peaks observed in 2004 and 2018, give rise to strong and readily observable cohorts in age-class abundance plots (Appendix 4 [Torhamn]).

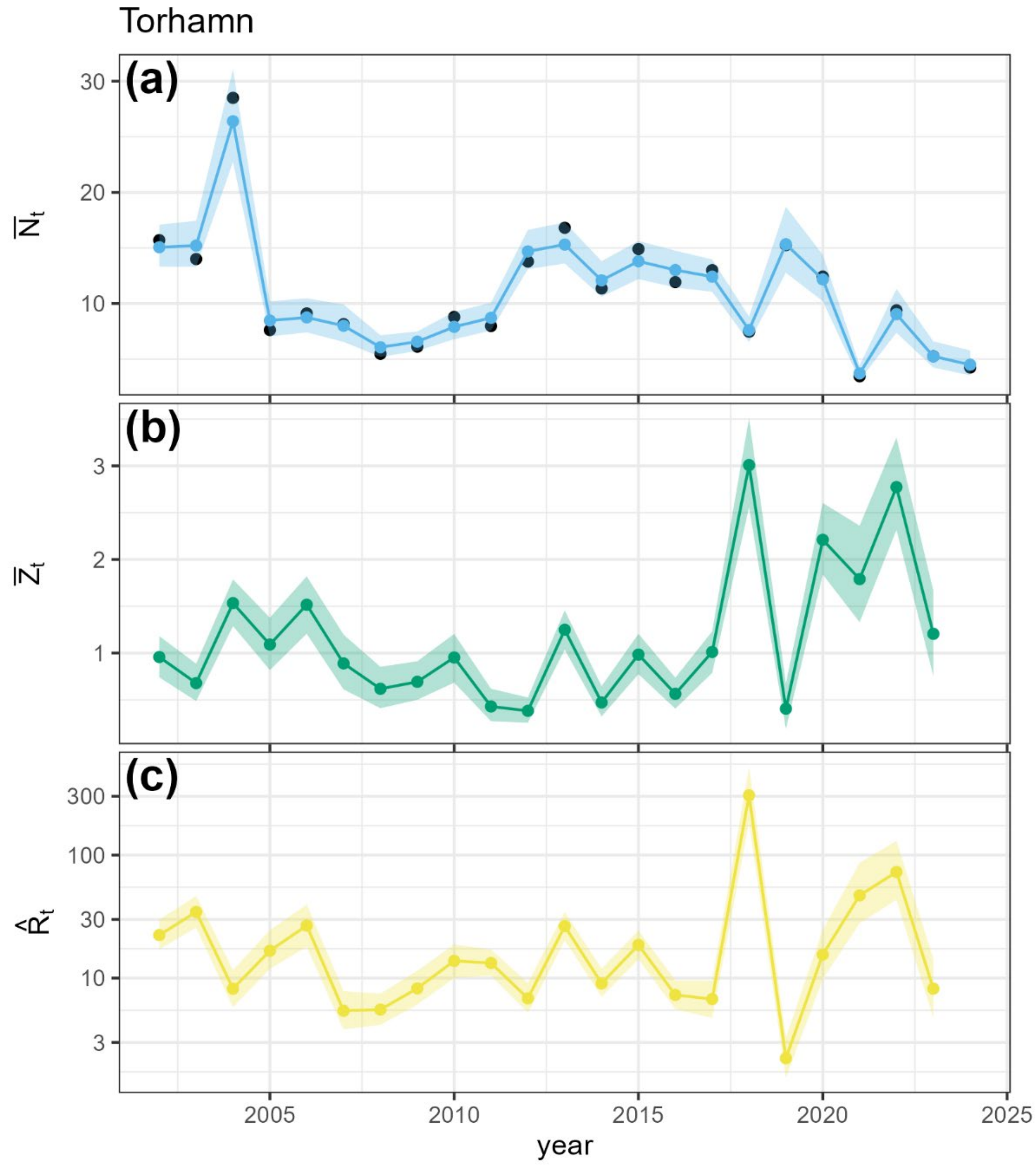

Figure 12. Temporal development of population indicators in Torhamn. ***(a)*** *Total number of females of age 1 and older caught annually per net and night, $\bar{N}_t$ (Eq. 17). The light-blue line with points illustrates medians of the posterior distribution, ribbons display 90 % credibility intervals of the posterior distribution, and black dots illustrate the mean number of females caught annually per net and night.* ***(b)*** *Abundance weighted mean annual mortality rate, $\bar{Z}_t$ (Eq. 16).* ***(c)*** *Back-calculated recruitment index, $\hat{R}_t$ (Eq. 18). As only individual of age 1 year and older are included in the analysis, recruitment can only be estimates for years T_{start} : (T_{final}-1), where T_{start} is the first year with abundance observations and T_{final} is last year with abundance observations.*

3.4.2 General results

Implementations of the age-based perch model revealed several general patterns. First, we note that the dynamics of female perch in most areas is dominated by successful recruitment years, giving rise to strong cohorts that sometimes dominate the total female abundance over multiple years. Second, we note that mortality rates appear to have been relatively stable, i.e. fluctuating stochastically around some mean level, in all northern areas (areas in the Gulf of Bothnia) except Kinnbäcksfjärden where an increasing trend over time is observed, whereas in the southern areas, i.e. for areas in the Baltic Proper, most areas display an increasing total mortality over time, with a notable exception, Kvädöfjärden, which displays an erratic mortality pattern during the most recent years. The increasing trend in mortality rate is in many areas associated with a general change in the age-structure of the populations, where the number of old individuals has decreased considerably (Appendix 4). Third, the model clearly suggests that total mortality increases with perch age, irrespective of the specific area being considered (Appendix 8). Fourth, overall, the models suggest that the mean total mortality is relatively high in all areas ($Z \approx 0.3$-1.3 (derived using Eq. 20), subpanel “Total” in Fig. 13). It is unclear to what extent there is any spatial pattern in mean abundance weighted mortality rates (Eq. 20) or mean age-specific mortality rates (Eq. 19) across the different areas, but a simple linear regression analysis does not reject the null hypothesis of no relationship between latitude and abundance weighted mortality across areas ($p = 0.38$) (Fig. 13).

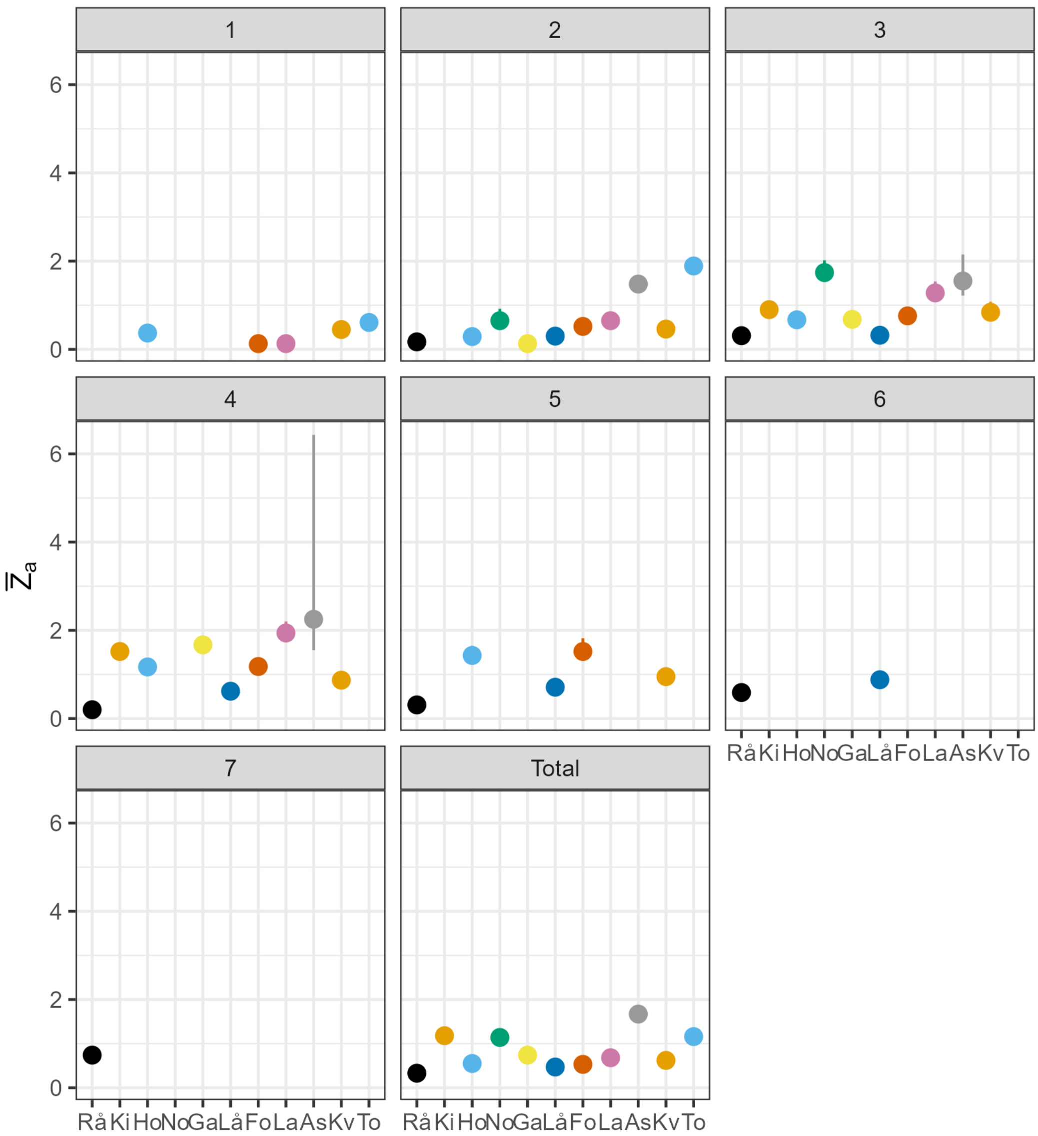

Figure 13. Comparison of area specific mortality rates. Subpanels show mean age-class specific mortality rate (Eq. 19) for each age-class (indexed in subpanel headings), and the area specific mean mortality (Eq. 20; indexed with the heading Total). Subpanels are ordered such that the northernmost area Råneå (Rå) is displayed as the leftmost point with uncertainty interval (in black) and the southernmost area Torhamn (To) is displayed as the rightmost point with uncertainty interval (in light-blue). Points represent medians of the posterior distribution and vertical lines represent 90 % credibility intervals. Abbreviations stand for: Rå – Råneå; Ki – Kinnbäcksfjärden; Ho – Holmön; No – Norrbyn; Ga – Gaviksfjärden; Lå – Långvindsfjärden; Fo – Forsmark; La – Lagnö; As – Asköfjärden; Kv – Kvädöfjärden; To – Torhamn.

3.5 Concluding remarks and recommendations

In this report we developed an age-based model that can be used to estimate the temporal development of various indicators for local perch populations along the Swedish Baltic Sea coast. The model uses as input, standardized multi-mesh gillnet monitoring data together with age-length information from subsamples of individuals caught in the gillnets. In many ways, the sampling protocol follows standard sampling conducted in many fishery programs. However, despite the wealth of data, no population dynamic model for perch, based on Nordic coastal multi-mesh gillnet data, has yet so far been developed. In this contribution, we developed a population dynamic model that can readily be used to estimate various important population indicators for perch.

In earlier studies (Appelberg et al. 2020, Bolund et al. 2025), total mortality of local perch populations along the Baltic Sea coast were estimated using a steady-state age-distribution assumption (Millar 2015, Nelson 2019). These analyses specifically assume that total mortality does not depend on age neither time. By contrast, we here developed a model which specifically estimates age-class specific mortality, abundance of females of different age-classes and a recruitment index, which hence can give a more detailed picture of the development of local perch populations along the Baltic Sea coast. Nevertheless, although the methods used by Bolund et al. (2025), who also estimated total mortality for the areas considered here, differ to the approach taken here, the general trends in total mortality observed using the two approaches is similar. Moreover, the magnitude in total mortality as estimated by Bolund et al. (2025) and Appelberg et al. (2020), are also similar to the magnitude of mortality rates estimated here. However, above the contribution by Appelberg et al. (2020) and Bolund et al. (2025), the current model can readily be used to estimate time-varying trends in age-class specific mortality rates and abundances, as clearly exemplified for the area Lagnö where an increasing total mortality over time (Fig. 9b) is driven by an increased mortality of older age-classes (Appendix 7 [Lagnö]). In fact, estimates of age-class specific mortality appears to be lacking for the European perch in general (Ning et al. 2025). Moreover, uncertainty follows naturally for any parameter of interest from the population dynamic model developed here.

Although it would be technically straightforward to extend the model to also include the effects of commercial and recreational fishing, and the effect of predation mortality, we have not included such factors here due to poor quality of spatio-temporally resolved data on both sources of mortality (see for example Bolund et al 2025). Instead, we here estimate total mortality, i.e. mortality originating from any potential source, such as fishery mortality, predation mortality or any other natural mortality sources. One drawback with this approach is that it is not possible to estimate total population size. If detailed information on the yearly outtake from various sources such as total consumption by important predators and total catches in the fishery, it would be possible to estimate total population size (Baranov 1918) and potentially also give catch recommendations. Nevertheless, such an assessment will not be possible to conduct for the local populations investigated here unless a detailed study, focusing on for example mark-recapture of PIT-tags in cormorant colonies (See e.g. Veneranta. et al. 2020) and detailed questionnaires on the recreational fishery, in some of the areas is conducted. However, such studies are likely not possible to conduct on a large scale, and an assessment of the total mortality is currently the best approach to consider.

Another important factor affecting population size is recruitment. To this end, we have here assumed that recruitment is completely random, following a lognormal process, and hence does not depend on the population size. Commonly applied fishery models often include some type of stock-recruitment function describing how recruitment relate to the spawning stock biomass, i.e. the biomass of spawning individuals in the stock. Unfortunately, gonad development has not been assessed in August when the test fishing is conducted. Hence, it is not possible to estimate spawning population biomass in these areas and to couple population dynamics to recruitment. However, it has been shown that temperature during the first year is a strong determinant of cohort strength (Kjellman et al. 2003, Linløkken 2023). Hence, it would be interesting to couple a temperature index, for example degree days, to recruitment in the current model. This could be done using a time lagged recruitment model, where spring and summer temperature year $t\text{-}A_{min}$ affects abundance of the first age-class considered year t. Importantly, if such a model was tested and deemed useful, it could be used to make forecasts on the current years' population size using temperature information from the same year.

Applications of the perch model on local populations along the Swedish Baltic Sea coast revealed a result that was unexpected on beforehand. We found that total mortality (mortality caused by any factor e.g., $Z = M + F$, natural mortality plus fishery induced mortality) increases with perch age. By contrast, theory suggest that natural mortality (M) should decrease with fish size/age (Lorenzen et al. 2022, Lorenzen 2022). There are several potential explanations for why this contradictory result may have emerged in the models. First, although multi-mesh gillnets and the depth stratified sampling procedure are amended to give a representative picture of the size structure and abundance of the fish community (Holmqvist et al. 2003), both indirect methods, methods estimating relative size selectivity using catches in various mesh sizes (Appelberg et al. 1995) and direct methods (Prchalova et al. 2009), that is, methods estimating size selectivity comparing the size distribution among the individuals caught to the true size distribution, show that the multi-mesh gillnets similar to the Nordic multi-mesh gillnets used here have a higher selectivity for large than small perch individuals. This suggests that small (young) individuals are underrepresented in the gillnets in relation to large (old) individuals, implying a steeper CPUE-age-catch-curve (i.e. number of individuals caught per age-class as a function of age) when selectivity is controlled for compared to when selectivity is not controlled for, and hence a higher mortality rate for younger age-classes than what is currently observed. This could potentially reduce, alternatively neutralise, the general increase in mortality with age observed here. Hower, for size/age classes considered here, controlling for selectivity may not affect the catch estimates largely (Prchalova et al. 2009). Second, it may be so that fishery induced mortality is size selective. However, as the commercial perch fishery along the Swedish coast is relatively minor, this may not be a very strong driver to this end, except potentially locally (Bolund et al. 2025). Recreational fishing, which has been suggested to be a larger driver of perch populations than the commercial fishery (Fiskbarometern 2024) and tends to target larger sized perch than what is caught in monitoring (Flink et al. 2024), may be a factor contributing to the observed result. Thus, overall fishery induced mortality, may at least partially, be a factor that have affected the observed result of a general increase in total mortality with perch age. Third, predation by large efficient predators may affect the mortality rate per age-classes differently than the general theoretical expectation (Lonrenzen et al. 2022, Lorenzen 2022) as large predators are likely not part of data sets used for modelling the general relationship between fish age/size and natural mortality (e.g. Lorenzen et al. 2022, Lorenzen 2022), hence large predation effects may counterbalance the expected decrease in natural mortality with age. The most significant predators on perch along the Baltic Sea coast are seals and cormorants, of which cormorants are estimated to be the most important predator (Hanson et al. 2018). Further, as the number of cormorants has increased significantly in recent years (Lundström 2024), and the total consumption by cormorants has been estimated larger than the total catches in the commercial and recreational fishing (Hanson et al. 2018) along the Swedish Baltic Sea coast, they deserve specific attention. However, as studies suggest that cormorants feed preferentially on specific size ranges of perch (Östman et al. 2013), this would suggest that the predation by cormorants would lead to a higher total mortality for certain age-classes and not a consistent pattern displaying increasing mortality with age. Furthermore, in some of the areas investigated here, there are no cormorants, or at least very few cormorants, but still the same total mortality age relationship is observed across all areas. Hence, the predation pressure by large predators alone does not explain the general result of an increasing total mortality with age. Fourth, as perch may utilize different habitats during ontogeny the age-structure caught in Nordi multi-mesh gillnets may not truly represent the underlying age-structure of the population, in effect leading to erroneous mortality estimates. In summary, the consistent age- total mortality relationship observed in all areas investigated here likely results from multiple factors, or some other factors not addressed here, and the specific importance of these factors is hard to disentangle.

Overall, the model presented here is useful for estimating time-varying natural mortality for local perch populations along the Swedish Baltic Sea coast. Although the model could be extended in many ways, with for example a temperature driven recruitment function and with estimates of outtake from fisheries and natural predators, the current implementation could nevertheless be used to estimate one of the key parameters needed in the assessment of nationally managed populations in Sweden. Above estimating instantaneous total mortality, the model can be used to generate new insights into population dynamics, such as, to what extent different age-classes are differently affected by mortality as well as how age-class specific abundances vary over time. Parameters are additionally estimated in a Bayesian framework, enabling the possibility to quantify the reliability of parameter estimates.

4. Forecasts

4.1 Methods

One-step-ahead forecast accuracy was measured using mean absolute scalable error (MASE) (Hyndman & Koehler 2006, Carvalho et al. 2021). This forecast accuracy metric measures how much better or worse forecast the model produces in comparison to a naïve prediction. The naïve prediction in this case is a random walk, which assumes that abundance at time *t* equals abundance at time *t-1*, i.e. the expected value of a random walk is that the abundance this year should be the same as the abundance for the previous year. MASE compares mean forecast errors for a few pre-specified time steps, i.e. mean of the absolute errors, to the mean absolute errors of the naïve in sample predictions, such that:

$$MASE = \frac{\frac{1}{h}\sum_{t=T-h+1}^{T}|\tilde{y}_t - y_t|}{\frac{1}{h}\sum_{t=T-h+1}^{T}|y_t - y_{t-1}|} \quad (18)$$

where $\tilde{y}_t$ is the one-step-ahead prediction of the model fitted to data up to time t-1, y_t is the observed data at time *t*, *h* is the number of one-step-ahead predictions used in the calculation, and T is the number of time points in the full time series. Predictions, $\tilde{y}_t$, were based on the median posterior predictions, and observations, y_t, based on the mean number of individuals caught year *t*. MASE values >1 indicate that the model forecasts in general are worse than a naïve random walk, whereas MASE values <1 indicate that model forecasts are more accurate than a random walk.

The age-structured model considered in this report is not build to produce forecasts of abundance for the first age-class in the models (a naïve forecast to this end could however be produced by setting $\tilde{y}_t = e^{\mu_{\ln}(N_{A_{min}})}$ (Eq. 2), but this is by necessity a very uniformed prediction). Hence, forecast accuracy was only assessed for age-classes above the minimum age-class, A_{min}, considered in each area.

4.2 Results

In general, model forecasts for the last five years of data in each area were relatively accurate, with MASE values < 1. However, a few exceptions clearly exist. For example, in Lagnö, forecast accuracy is almost two times worse that the random walk expectation. A likely reason to this is the large shift in age-structure of the population observed in the end of this time series (Appendix 4 [Lagnö]). For Asköfjärden, another notable exception (Tab. 1), it is likely so that the low abundance across almost all age-classes in the model (Appendix 4 [Asköfjärden]) leads to a near zero statistic, which may lead to an instability in the MASE statistic. For Forsmark and Kvädöfjärden, the relatively bad forecast accuracy observed for age-class 5 and the plus group, respectively, likely results simply from bad forecast accuracy.

Table 1. One-step-ahead forecast accuracy for different survey areas and age-classes. Numbers show mean absolute scalable errors (MASE). Values highlighted in green corresponds to MASE values < 1(i.e. forecasts that are more accurate than a naïve random walk prediction) and values highlighted in red correspond to MASE values > 1 (i.e. forecasts that are less accurate than a naïve random walk prediction). Abbreviations stand for: Rå- Råneå; Ki – Kinnbäcksfjärden; Ho – Holmön; No – Norrbyn; Ga – Gaviksfjärden; Lå – Långvindsfjärden; Fo – Forsmark; La – Lagnö; As – Asköfjärden; Kv – Kvädöfjärden; To – Torhamn.

Age-class	Rå	Ki	Ho	No	Ga	Lå	Fo	La	As	Kv	To
1			*				*	*		*	*
2	*		0.34	*	*	*	0.60	0.80	*	0.18	0.75
3	0.39	*	0.40	0.57	0.33	0.76	0.90	1.94	1.35	0.28	0.32£
4	0.62	0.19	0.43	0.52£	0.11	0.82	0.62	1.68	0.47	0.23	
5	0.11	0.43£	0.22		0.55£	0.90	1.28	0.53£	1.04£	0.14	
6	0.10		0.68£			0.27	0.72£			1.09£	
7	0.23					0.73£					
8	0.89£										

£ *Plus-group* * *The first age-class considered in the respective areas*

5. Biological reference points

The status of coastal fish communities is included in the Swedish national reporting to EU for the Marine Strategy Framework Directive (Havs- och vattenmyndigheten 2024) and the follow up of the Baltic Sea Action Plan with HELCOM (HELCOM 2023a). Within these status assessments perch population abundance and size structure are evaluated against quantitative threshold values defined as representing good environmental status.

In short, for perch abundance, the status is evaluated against survey area-specific threshold values derived from the temporal dynamics of perch abundances within survey sites (HELCOM 2023b). The logic behind the choice of area-specific threshold values for perch abundance is the local population structure observed for coastal perch and the substantial natural gradient in absolute population abundance observed for perch populations along the Baltic Sea coast (Östman et al. 2017). The site-specific threshold values are derived using the ASCETS methodology (Östman et al. 2020) where the temporal dynamics and variability of abundance data during a pre-defined reference period (for perch 10-15 years prior to the assessment period that in this case covers the latest six years of the time-series) is compared to a reference period defined by expert judgement as representing either good or poor environmental status (Östman et al. 2020).

To assess the status of the size structure of perch populations, a gear-specific but Baltic-wide threshold value of the indicator L90 is used (HELCOM 2023c). The rationale for this is limited variability across areas and over time in the size of perch in the Baltic Sea (HELCOM 2023c). The indicator L90 represents the length of the perch at the 90th percentile in the monitored populations size distribution. For the Nordic multi-mesh gillnets used in this study, the threshold value for good environmental status of perch L90 is set to 25 cm in the Baltic Sea (HELCOM 2023c; Bolund et al. in prep).

6. Model code

The model was fitted in STAN and implemented in R (R Core Team 2024) through the R-package cmdstanR (Gabry et al. 2024). Custom code for implementing the age-based model, diagnostic checks, and background data analyses are provided through an open github repository:
https://github.com/torbjornsaterberg/Perch_coastal_model

7. References

Appelberg, M., Berger, H. M., Hesthagen, T. et al. (1995). Development and intercalibration of methods in Nordic freshwater fish monitoring. *Water, Air, and Soil Pollution*, 85, 401–406. https://doi.org/10.1007/BF00476862

Baranov, F. I. (1918). On the question of the biological basis of fisheries. *Izvestiya*, 1: 81–128.

Bergek, S., & Björklund, M. Cryptic barriers to dispersal within a lake allow genetic differentiation of Eurasian perch. *Evolution*, 61(8), 2035–2041, https://doi.org/10.1111/j.1558-5646.2007.00163.x

Bergström, U., Olsson, J., Casini, M., Eriksson, B. K., Fredriksson, R., Wennhage, H., & Appelberg, M. (2015). Stickleback increase in the Baltic Sea – A thorny issue for coastal predatory fish. *Estuarine, Coastal and Shelf Science*, 163(B), 134–142. https://doi.org/10.1016/j.ecss.2015.06.017

Bolund, E., Olsson, J., Svensson, F., Wennhage, H. 2024. Faktablad för att bedöma indikator för god miljöstatus enligt havsmiljöförordningen - 1.2J Förekomst av nyckelart av fisk i kustvatten. https://www.havochvatten.se/download/18.1d23b59c190125a43f2e9570/1719557060312/1-2j-forekomst-av-nyckelart-av-fisk-i-kustvatten.pdf

Bolund, E., Olsson, J. 2024. Faktablad för att bedöma indikator för god miljöstatus enligt havsmiljöförordningen - 1.3E Storleksfördelning av kustfiskarter. https://www.havochvatten.se/download/18.1d23b59c190125a43f2e9575/1719557060406/1-3e-storleksfordelning-av-kustfiskarter.pdf

Bolund, E., Andersson, M. L., Olin, A., Bergström, L., & Olsson, J. (2025). Påverkansanalys kustfisk – Analys av geografiska samband mellan påverkansfaktorer och statusbedömningar. *Aqua reports* 2025:4. Uppsala: Institutionen för akvatiska resurser. https://doi.org/10.54612/a.7nvktgh84i

Böhling, P. & Lehtonen, H. (1984). Effect of environmental factors on migrations of perch (Perca fluviatilis L.) tagged in the coastal waters of Finland. *Finnish Fisheries Research*, 5, 31–40.

Cook, R. M. (2013). A fish stock assessment model using survey data when estimates of catch are unreliable. *Fisheries Research*, 143, 1–11. https://doi.org/10.1016/j.fishres.2013.01.003

Eklöf, J. S., Sundblad, G., Erlandsson, M. et al. (2020). A spatial regime shift from predator to prey dominance in a large coastal ecosystem. *Communications Biology*, 3, 459. https://doi.org/10.1038/s42003-020-01180-0

Estlander, S., Kahilainen, K. K., Horppila, J., Olin, M., Rask, M., Kubečka, J., Peterka, J., Říha, M., Huuskonen, H., & Nurminen, L. (2017). Latitudinal variation in sexual dimorphism in life-history traits of a freshwater fish. *Ecology and Evolution*, 7, 665–673. https://doi.org/10.1002/ece3.2658

Fiskbarometern (2024). *Fiskbarometern (Abborre) 2024*. https://fiskbarometern.se/rapport/2024/species/Abborre

FISKERIVERKET (2003). Strategi för ett samordnat nationellt/regionalt övervakningsprogram för kustfisk i Bottniska viken. *Fiskeriverket informerar* 2003:5, 1–46. https://www.diva-portal.org/smash/get/diva2:657936/FULLTEXT01

Flink, H., Sundblad, G., Merilä, J., & Tibblin, P. (2024). Recreational fisheries selectively capture and harvest large predators. *Fish and Fisheries*, 25, 793–805. https://doi.org/10.1111/faf.12839

Gabry, J., Češnovar, R., Johnson, A., & Bronder, S. (2024). *cmdstanr: R Interface to 'CmdStan'*. R package version 0.8.1.9000. https://github.com/stan-dev/cmdstanr

Hall, M., Koch-Schmidt, P., Larsson, P., Tibblin, P., Yıldırım, Y. & Sunde, J. (2022) Reproductive homing and fine-scaled genetic structuring of anadromous Baltic Sea perch (*Perca fluviatilis*). *Fisheries Management and Ecology*, 29, 586–596. https://doi.org/10.1111/fme.12542

Hansson, S., Bergström, U., Bonsdorff, E., Härkönen, T., Jepsen, N., Kautsky, L., Lundström, K., Lunneryd, S.-G., Ovegård, M., Salmi, J., Sendek, D., & Vetemaa, M. (2018). Competition for the fish – fish extraction from the Baltic Sea by humans, aquatic mammals, and birds. *ICES Journal of Marine Science*, 75(3), 999–1008. https://doi.org/10.1093/icesjms/fsx207

Havs- och vattenmyndigheten. (2020). Undersökningstyp: Provfiske i Östersjön – Djupstratifierat provfiske med nordiska kustöversiktsnät. version 1.4 [PDF]. https://www.havochvatten.se/download/18.19a8b87f170646960b9dedc4/1708688519369/undersokningstyp-provfiske-i-ostersjon-version-1-4.pdf

Havs- och Vattenmyndigheten. (2024). Marin strategi för Nordsjön och Östersjön 2024-2029. 2024:12. https://www.havochvatten.se/download/18.60662d6719060e439995beef/1723711349019/rapport-2024-12-marin-strategi-nordjon-ostersjon.pdf

Heibo, E., Magnhagen, C., & Vøllestad, L.A. (2005). LATITUDINAL VARIATION IN LIFE-HISTORY TRAITS IN EURASIAN PERCH. *Ecology*, 86, 3377-3386. https://doi.org/10.1890/04-1620

HELCOM. (2023a). State of the Baltic Sea. Third HELCOM holistic assessment 2016-2021. Baltic Sea Environment Proceedings n°194.

HELCOM. (2023b). Abundance of coastal fish key species**.** HELCOM core indicator report. Online. 2025-11-14, https://indicators.helcom.fi/indicator/coastal-fish-key-species/

HELCOM (2023c). Size structure of coastal fish (Coastal fish size). HELCOM core indicator report. Online. 2025-11-14,.

Hurtado-Ferro, F., Szuwalski, C. S., Valero, J. L., Anderson, S. C., Cunningham, C. J., Johnson, K. F., Licandeo, R., McGilliard, C. R., Monnahan, C. C., Muradian, M. L., Ono, K., Vert-Pre, K. A., Whitten, A. R., & Punt, A. E. (2015). Looking in the rear-view mirror: bias and retrospective patterns in integrated, age-structured stock assessment models. *ICES Journal of Marine Science*, 72(1), 99–110. https://doi.org/10.1093/icesjms/fsu198

Huss, M., Lindmark, M., Jacobson, P., van Dorst, R. M., & Gårdmark, A. (2019). Experimental evidence of gradual size-dependent shifts in body size and growth of fish in response to warming. *Global Change Biology*, 25, 2285–2295. https://doi.org/10.1111/gcb.14637

ICES. (2020). Workshop on Catch Forecast from Biased Assessments (WKFORBIAS; outputs from 2019 meeting). *ICES Scientific Reports*, 2:28, 38 pp. https://doi.org/10.17895/ices.pub.5997

Järv, L. (2000). Migrations of the perch (*Percha fluviatilis* L.) in the coastal waters of western Estonia. *Proc. Estonian Acad. Sci. Biol. Ecol.*, 49 (3), 270-276.

Kjellman, J., Lappalainen, J., Urho, L., & Hudd, R. (2003). Early determination of perch and pikeperch recruitment in the northern Baltic Sea. *Hydrobiologia*, 495, 181–191. https://doi.org/10.1023/A:1025480105775

Kokkonen, E., Heikinheimo, O., Pekcan-Hekim, Z. *et al.* (2019). Effects of water temperature and pikeperch (*Sander lucioperca*) abundance on the stock–

recruitment relationship of Eurasian perch (*Perca fluviatilis*) in the northern Baltic Sea. *Hydrobiologia,* 841, 79–94. https://doi.org/10.1007/s10750-019-04008-z

Jørgensen, C., & Holt, R. E. (2013). Natural mortality: Its ecology, how it shapes fish life histories, and why it may be increased by fishing. *Journal of Sea Research*, 75, 8–18. https://doi.org/10.1016/j.seares.2012.04.003

Karlsson, M., Ragnarsson Stabo, H., Petersson, E., Carlstrand, H., & Thörnqvist, S. (2014). Nationell plan för kunskapsförsörjning om fritidsfiske inom fisk-, havs- och vattenförvaltningen. *Aqua reports* 2014:12. Sveriges lantbruksuniversitet, Drottningholm. 71 s.

Larsson, S., Sundblad, G., Gustafsson-Renes, S., Bergström, L., Dannewitz, J., Valentinsson, D., Wennhage, H., Bolund, E., Holmgren, K. (2024). Bedömning av status för nationellt förvaltade fisk- och skaldjursbestånd. *Aqua notes* 2024:13. Uppsala: Institutionen för akvatiska resurser. https://doi.org/10.54612/a.4knd3ar0hg

Linløkken, A. N. (2023). Temperature Effects on Recruitment and Individual Growth of Two Antagonistic Fish Species, Perch *Perca fluviatilis* and Roach *Rutilus rutilus*, from a Climate Change Perspective. *Fishes*, 8, 295. https://doi.org/10.3390/fishes8060295

Lindmark, M., Karlsson, M., & Gårdmark, A. (2023). Larger but younger fish when growth outpaces mortality in heated ecosystem. *eLife*, 12, e82996. https://doi.org/10.7554/eLife.82996

Lindmark, M., Ohlberger, J., & Gårdmark, A. (2025). Stronger effect of temperature on body growth in cool than in warm populations suggests lack of local adaptation. *Ecography*, e07518. https://doi.org/10.1002/ecog.07518

Lorenzen, K. (2022). Size- and age-dependent natural mortality in fish populations: Biology, models, implications, and a generalized length-inverse mortality paradigm. *Fisheries Research*, 255, 106454. https://doi.org/10.1016/j.fishres.2022.106454

Lorenzen, K., Camp, E. V., & Garlock, T. M. (2022). Natural mortality and body size in fish populations. *Fisheries Research*, 252, 106327. https://doi.org/10.1016/j.fishres.2022.106327

Mustamäki, N., Jokinen, H., Scheinin, M., Bonsdorff, E., Mattila, J., Seasonal small-scale variation in distribution among depth zones in a coastal Baltic Sea fish assemblage. *ICES Journal of Marine Science*, 72 (8), 2374–2384. https://doi.org/10.1093/icesjms/fsv068

Nielsen, A., & Berg, C. W. (2014). Estimation of time-varying selectivity in stock assessments using state-space models. *Fisheries Research*, 158, 96–101. https://doi.org/10.1016/j.fishres.2014.01.014

Ning, N., Barlow, C., Baumgartner, L.J. et al. (2025). A global review of the biology and ecology of the European perch, *Perca fluviatilis*. *Rev Fish Biol Fisheries,* 35, 587–618. https://doi.org/10.1007/s11160-025-09924-z

Ogle, D. H., Doll, J. C., Wheeler, A. P., & Dinno, A. (2025). *FSA: Simple Fisheries Stock Assessment Methods*. R package version 0.9.6. https://CRAN.R-project.org/package=FSA

Olsson, J., Mo, K., Florin, A.-.-B., Aho, T. and Ryman, N. (2011). Genetic population structure of perch *Perca fluviatilis* along the Swedish coast of the Baltic Sea. *Journal of Fish Biology,* 79, 122-137. https://doi.org/10.1111/j.1095-8649.2011.02998.x

Östman, Ö., Boström, M. K., Bergström, U., Andersson, J., & Lunneryd, S.-G. (2013). Estimating Competition between Wildlife and Humans – A Case of Cormorants and Coastal Fisheries in the Baltic Sea. *PLoS ONE*, 8(12), e83763. https://doi.org/10.1371/journal.pone.0083763

Östman, Ö., Lingman, A., Bergström, L. and Olsson, J. (2017). Temporal development and spatial scale of coastal fish indicators in reference ecosystems: hydroclimate and anthropogenic drivers. *J Appl Ecol*, 54, 557-566. https://doi.org/10.1111/1365-2664.12719

Östman, Ö., Bergström, L., Leonardsson, K., Gårdmark, A., Casini, M., Sjöblom, Y., Haas, F., Olsson, J. (2020). Analyses of structural changes in ecological time series (ASCETS). *Ecological Indicators*, 116, 106469. https://doi.org/10.1016/j.ecolind.2020.106469.

Prchalová, M., Kubečka, J., Říha, M., Mrkvička, T., Vašek, M., Jůza, T., Kratochvíl, M., Peterka, J., Draštík, V., & Křížek, J. (2009). Size selectivity of standardized multimesh gillnets in sampling coarse European species. *Fisheries Research*, 96(1), 51–57. https://doi.org/10.1016/j.fishres.2008.09.017

R Core Team. (2024). *R: A Language and Environment for Statistical Computing*. Vienna: R Foundation for Statistical Computing. https://www.R-project.org/

Salmi, J. A., Auvinen, H., Raitaniemi, J., Kurkilahti, M., Lilja, J., & Maikola, R. (2015). Perch (*Perca fluviatilis*) and pikeperch (*Sander lucioperca*) in the diet of the great cormorant (*Phalacrocorax carbo*) and effects on catches in the Archipelago Sea, Southwest coast of Finland. *Fisheries Research*, 164, 26–34. https://doi.org/10.1016/j.fishres.2014.10.011

Statistics Sweden. Recreational fishing. https://www.scb.se/en/finding-statistics/statistics-by-subject-area/agriculture-forestry-and-fishery/fishery/recreational-fishing/

Söderberg K. 2006. Provfiske i Östersjöns kustområden – Djupstratifierat provfiske med Nordiska kustöversiktsnät. (Test fishing in the coastal areas of the Baltic Sea – Depth stratified test fishing with Nordic coastal multi-mesh gillnets). In Swedish.

Vehtari, A., Gelman, A., Simpson, D., Carpenter, B., & Bürkner, P. C. (2021). Rank-normalization, folding, and localization: An improved R-hat for assessing convergence of MCMC. *Bayesian Analysis*, 16(2), 667–718. https://doi.org/10.1214/20-BA1221

Veneranta, L., Heikinheimo, O., & Marjomäki, T. J. (2020). Cormorant (*Phalacrocorax carbo*) predation on a coastal perch (*Perca fluviatilis*) population: estimated effects based on PIT tag mark-recapture experiment. *ICES Journal of Marine Science*, 77(7–8), 2611–2622. https://doi.org/10.1093/icesjms/fsaa148

Acknowledgement

First, we would like to thank all skilled personnel involved in collecting the standardized multi-mesh gillnet data. Thanks to all people involved in the individual data collection. We would like to thank Magnus Appelberg for discussions and helpful comments. Also, the two reviewers Mikko Olin and Szymon Smolinski provided critical and helpful comments that improved the manuscript. Thanks SLUs environmental monitoring program "Kust och Hav" for funding to develop the models, and the Swedish Agency for Marine and Water Management for funding for writing the report.

Appendix 1 – Catch-curves

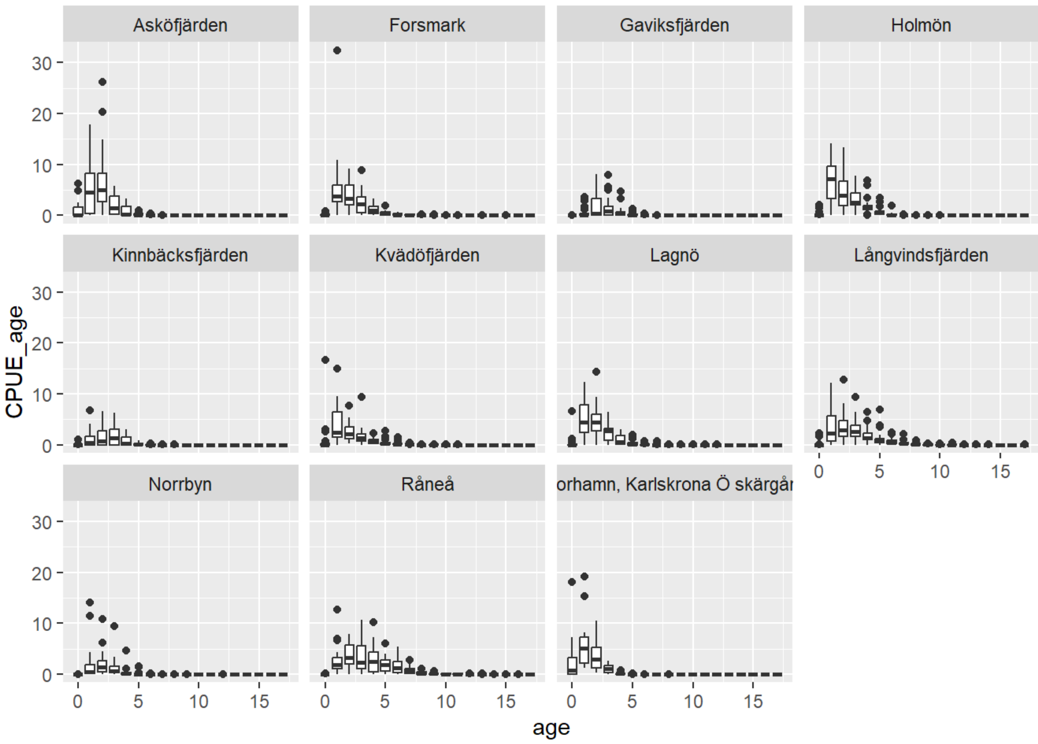

Appendix 1. Catch-curves. This figure shows the distribution of the number of female perch of age a caught per net and night in the Nordic multi-mesh gillnets deployed annually in August. Y-axis shows the number of females caught and x-axis display age-classes. Points show outliers, horizontal lines in each box shows medians, the lower and upper limit of the box displays the 25th and 75th quantiles, respectively.

Appendix 2 - Posterior predictive check (distribution of abundance per age-class)

This appendix shows distributions of number of individuals of age-class a caught per gillnet-night (in orange) and posterior simulations (yrep) of the same quantity.

Density age-group 1 Råneå

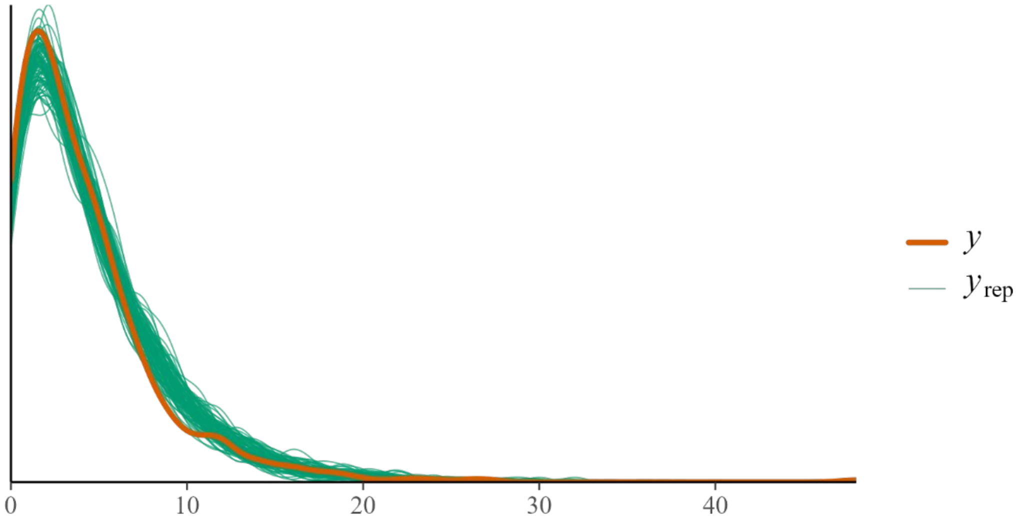

Density age-group 2 Råneå

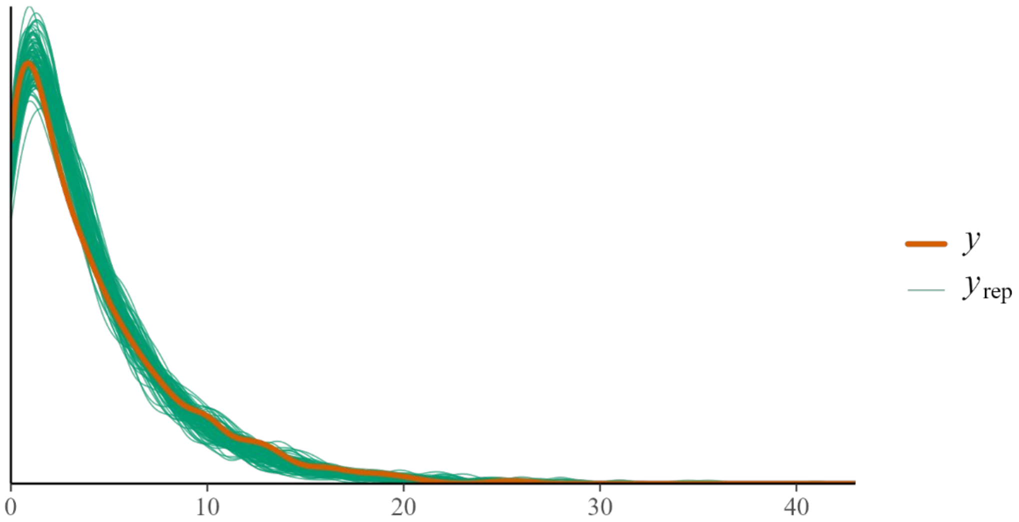

Density age-group 3 Råneå

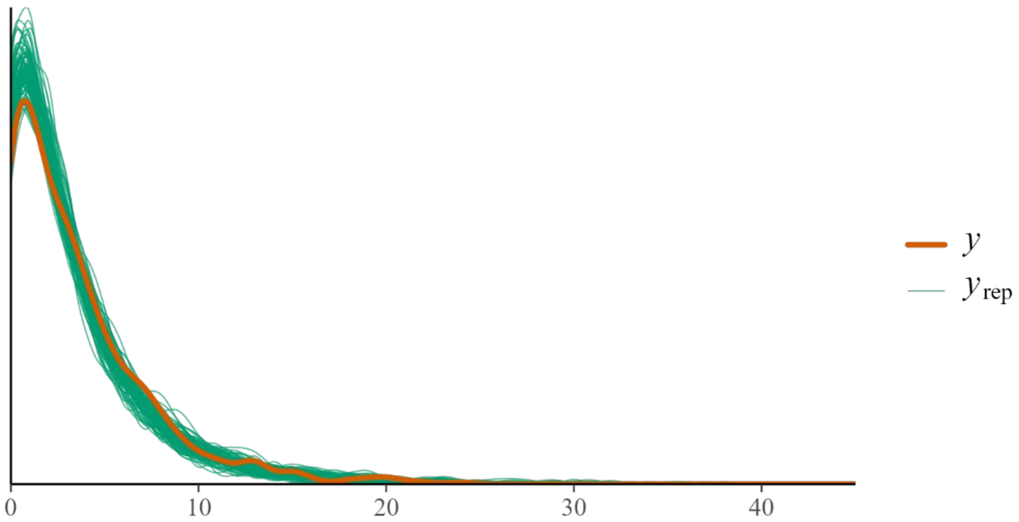

Density age-group 4 Råneå

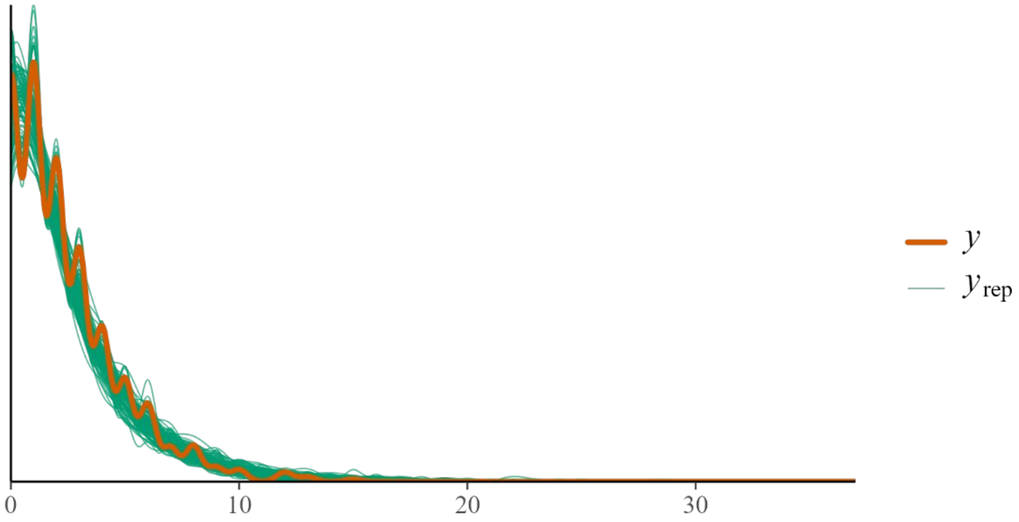

Density age-group 5 Råneå

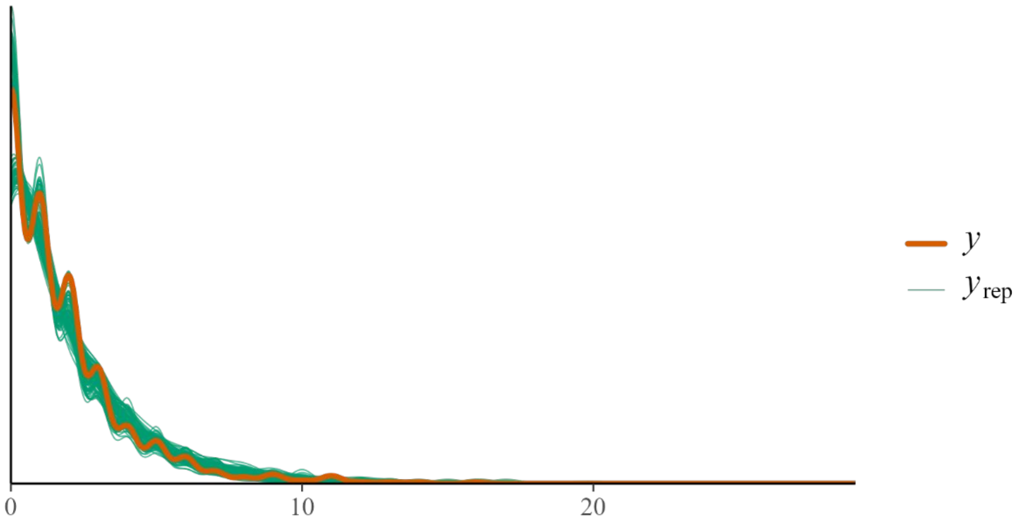

Density age-group 6 Råneå

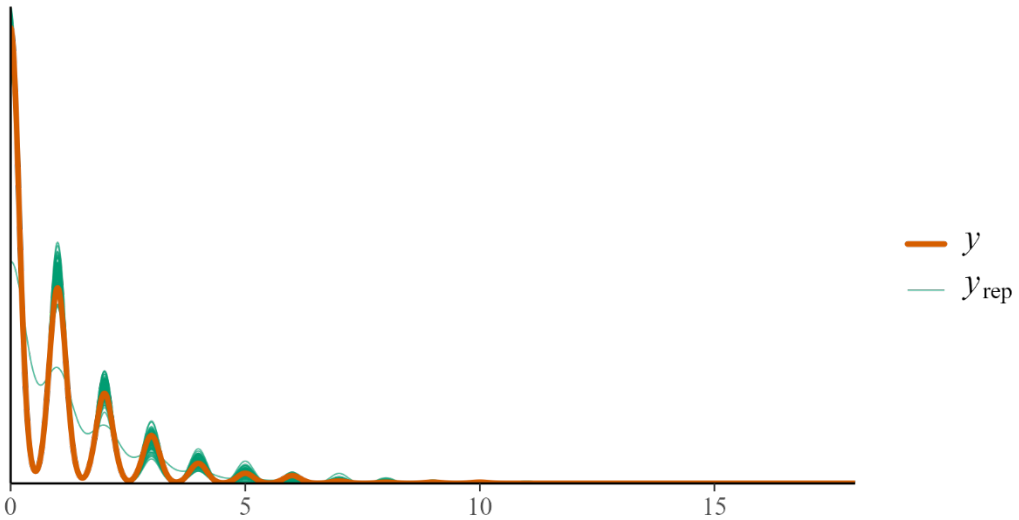

Density age-group 7 Råneå

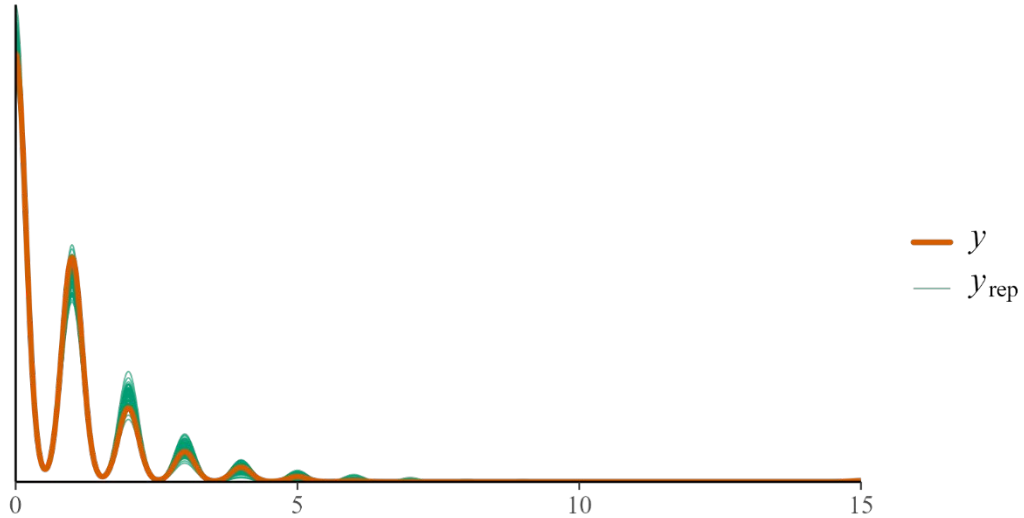

Density age-group 1 Kinnbäcksfjärden

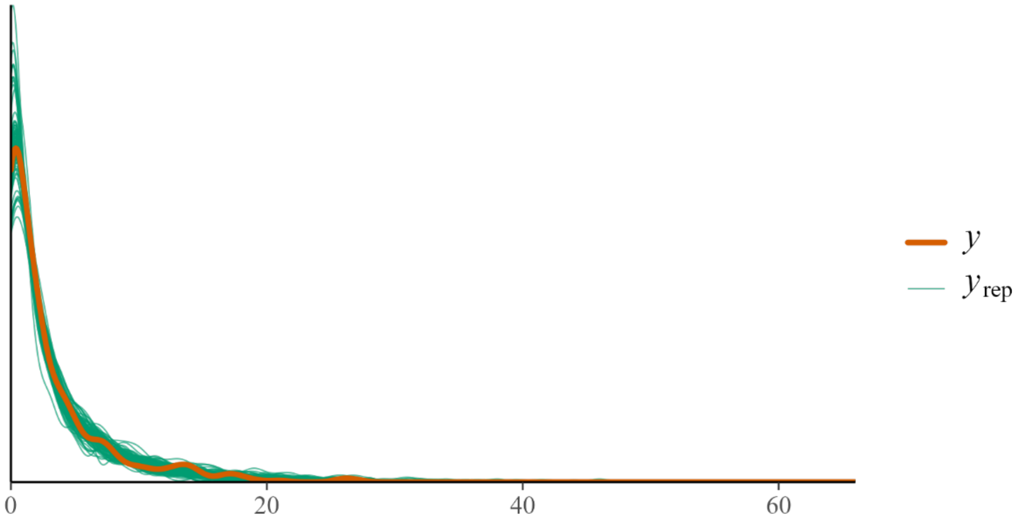

Density age-group 2 Kinnbäcksfjärden

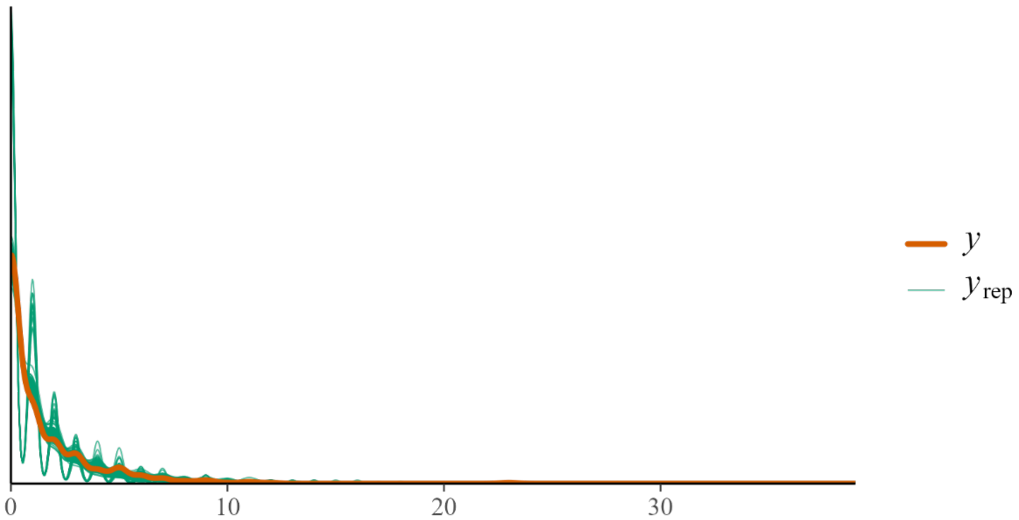

Density age-group 3 Kinnbäcksfjärden

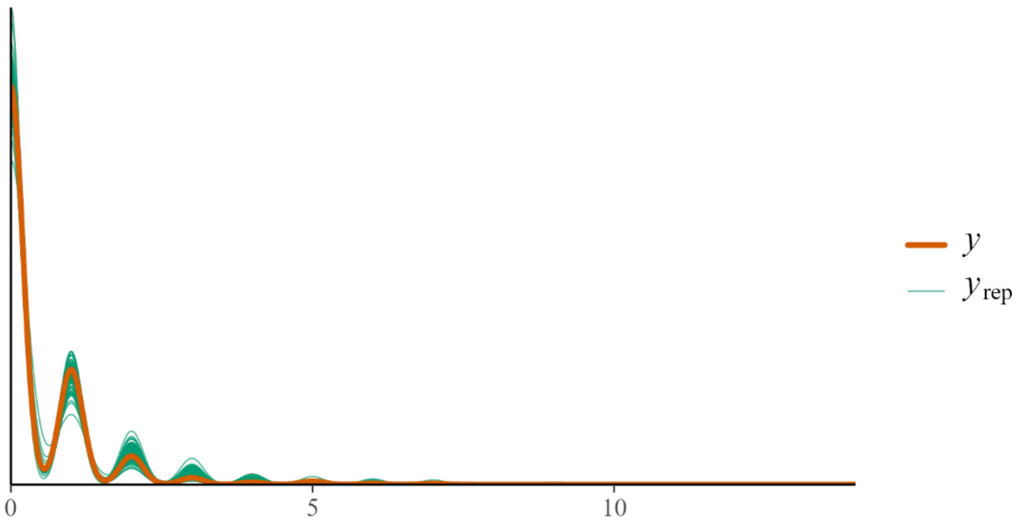

Density age-group 1 Holmön

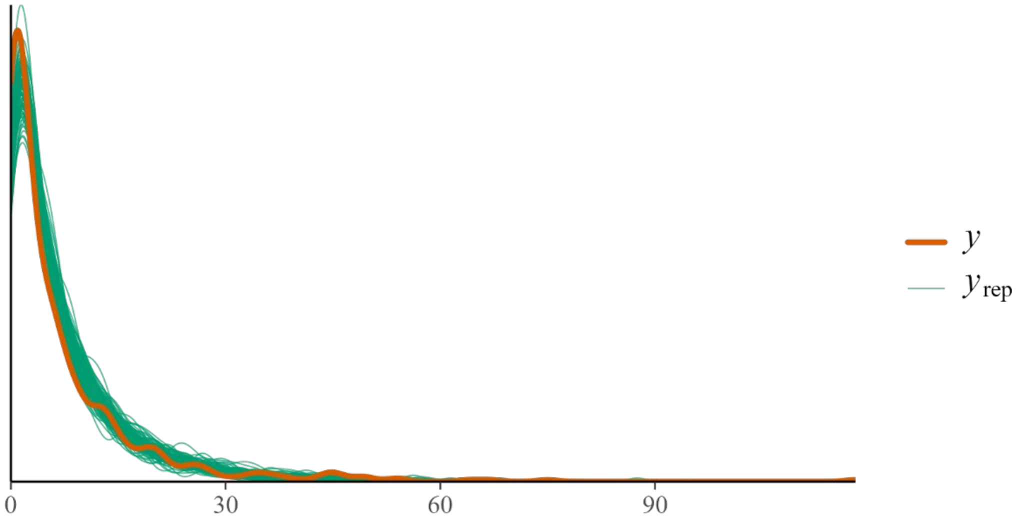

Density age-group 2 Holmön

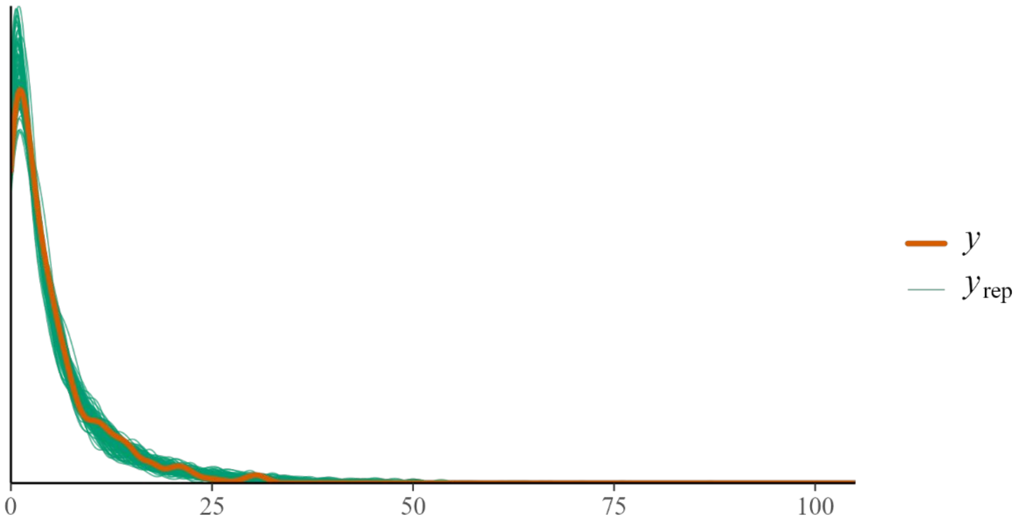

Density age-group 3 Holmön

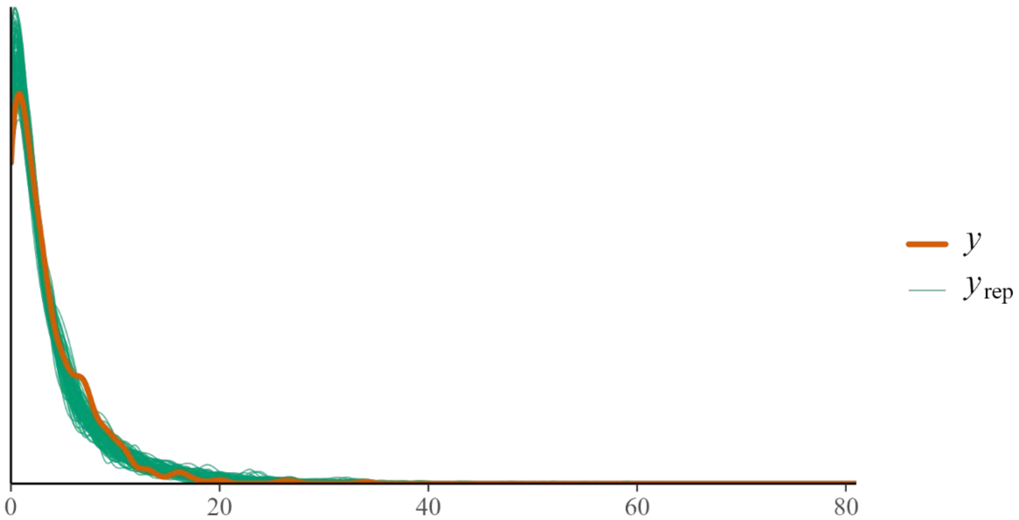

Density age-group 4 Holmön

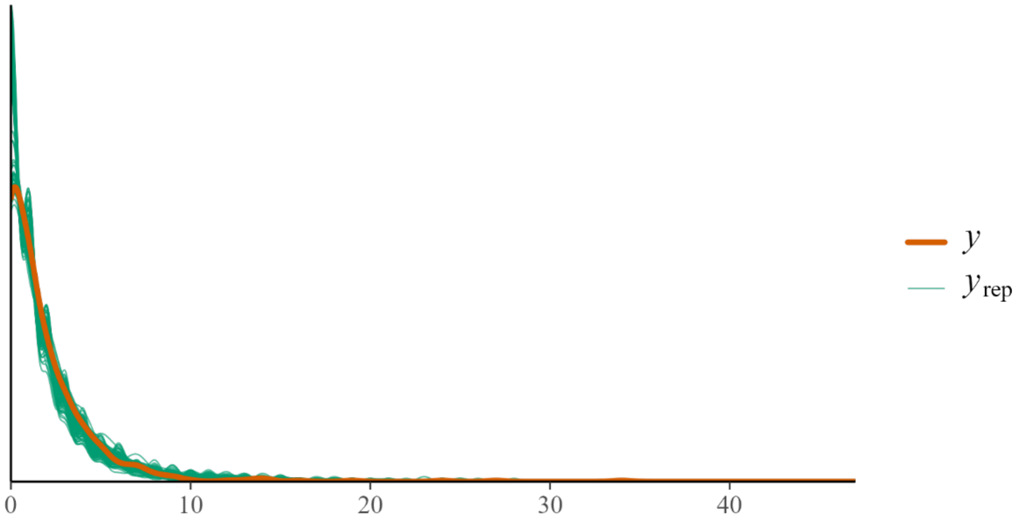

Density age-group 5 Holmön

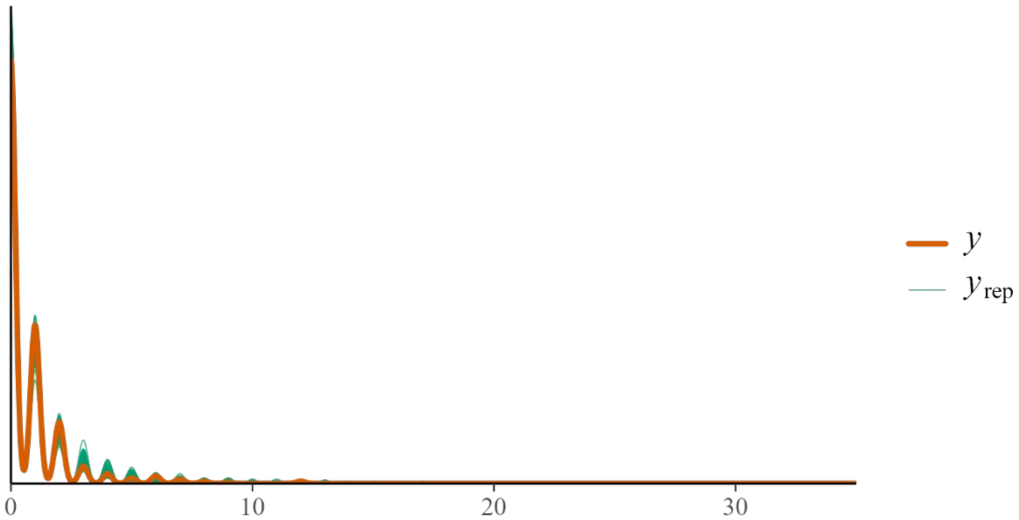

Density age-group 6 Holmön

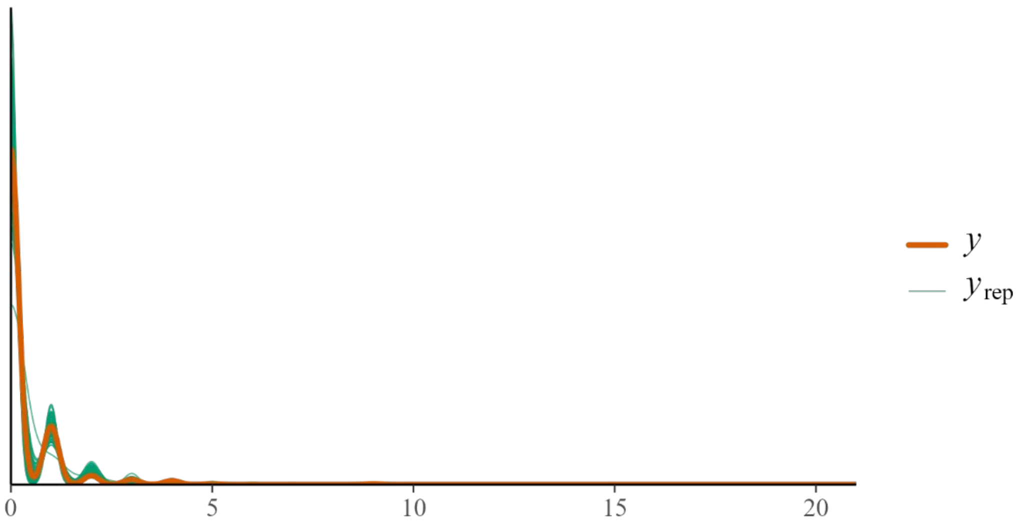

Density age-group 1 Norrbyn

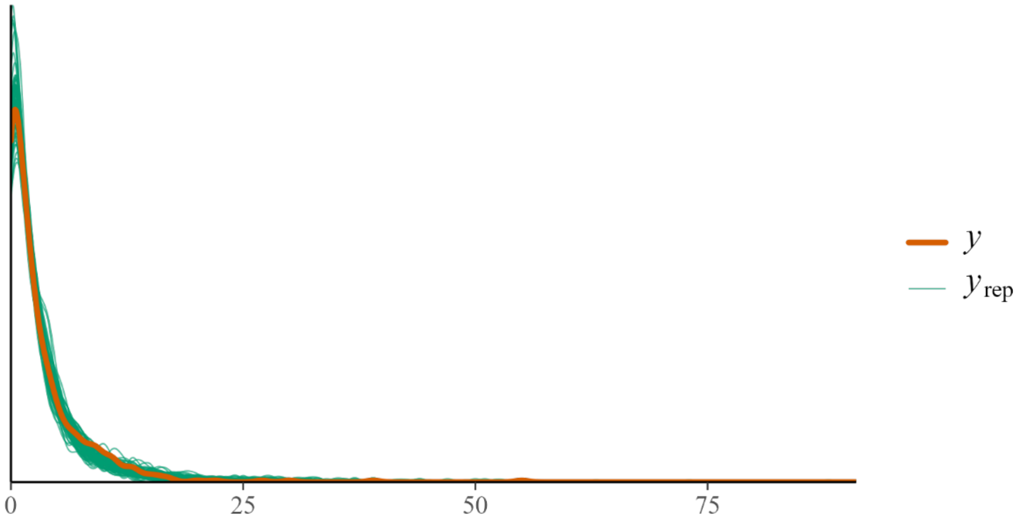

Density age-group 2 Norrbyn

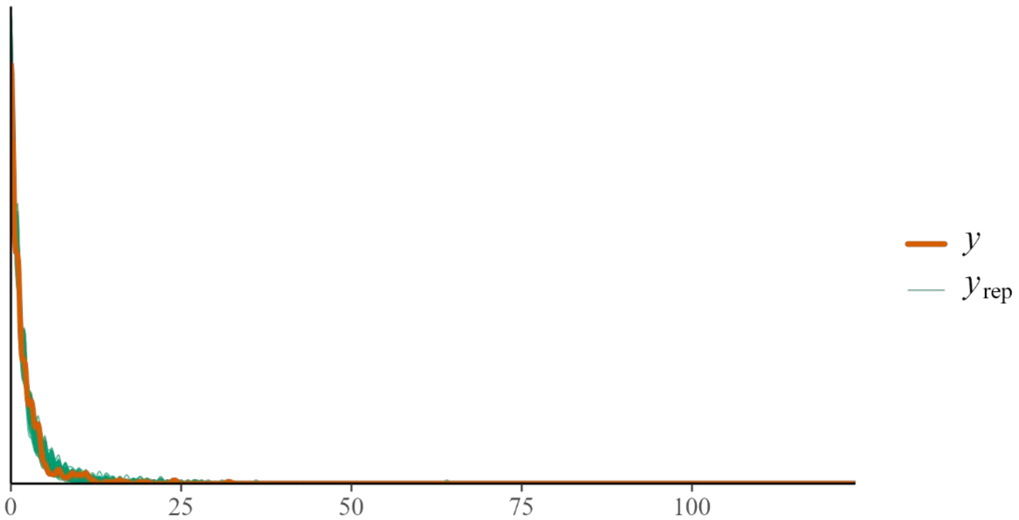

Density age-group 3 Norrbyn

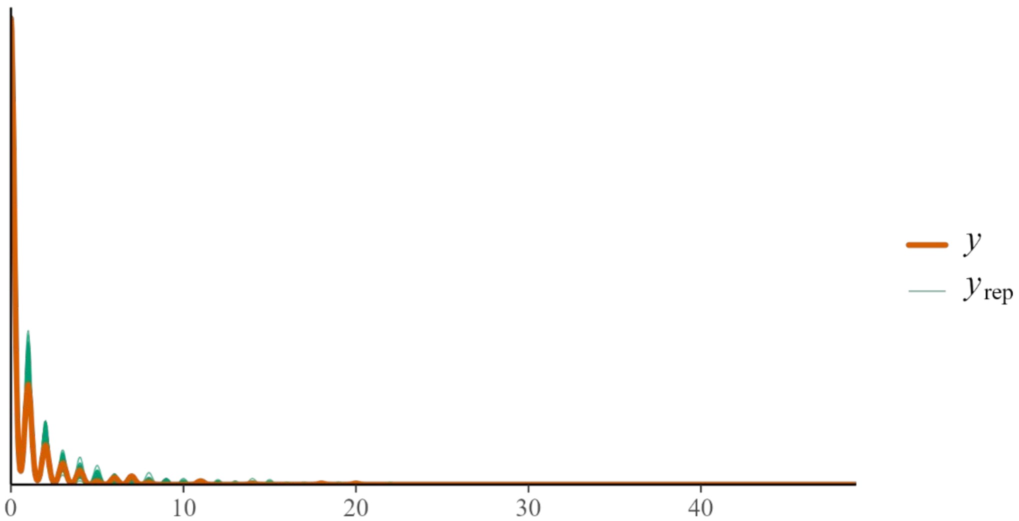

Density age-group 1 Gaviksfjärden

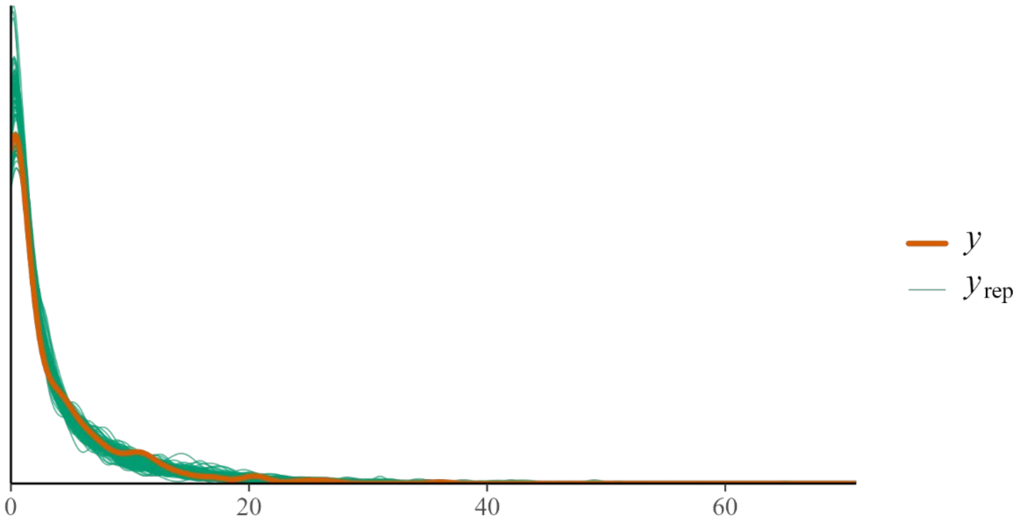

Density age-group 2 Gaviksfjärden

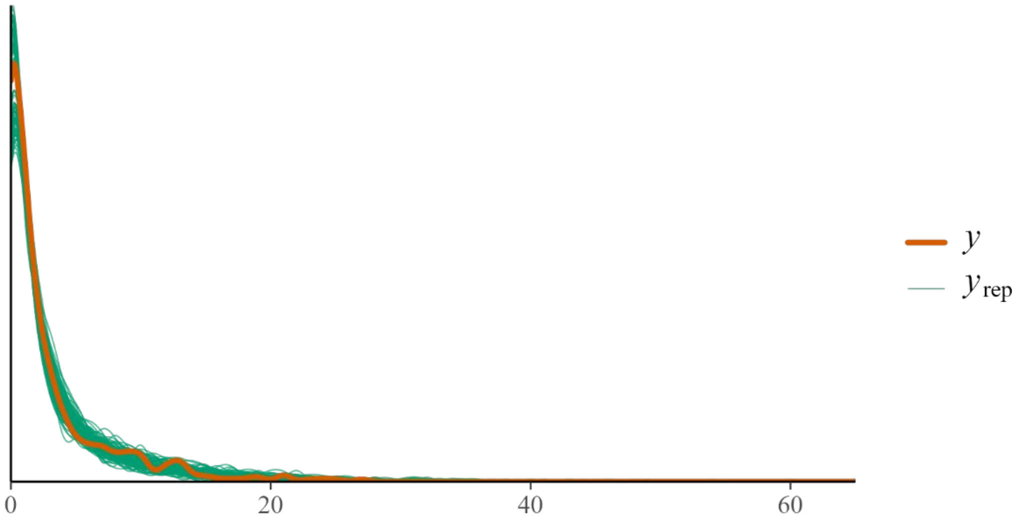

Density age-group 3 Gaviksfjärden

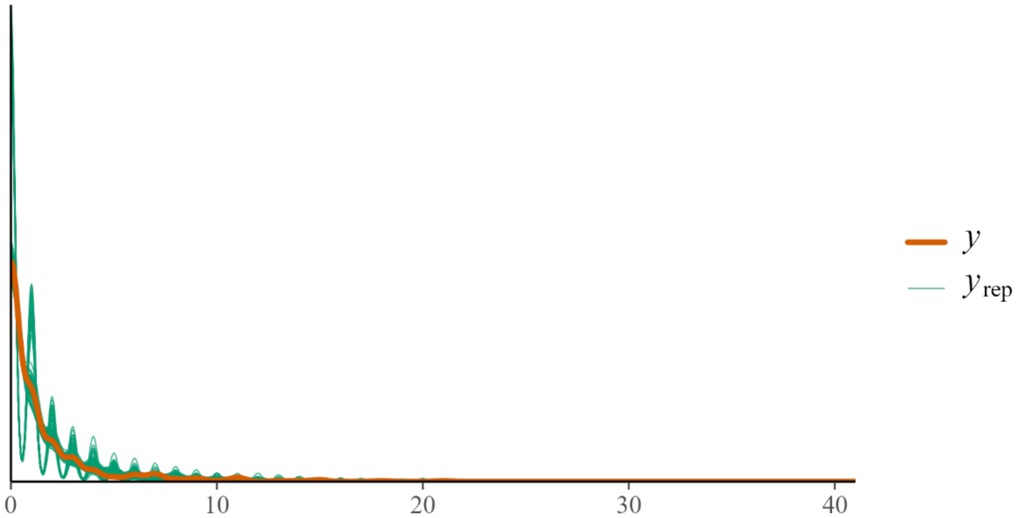

Density age-group 4 Gaviksfjärden

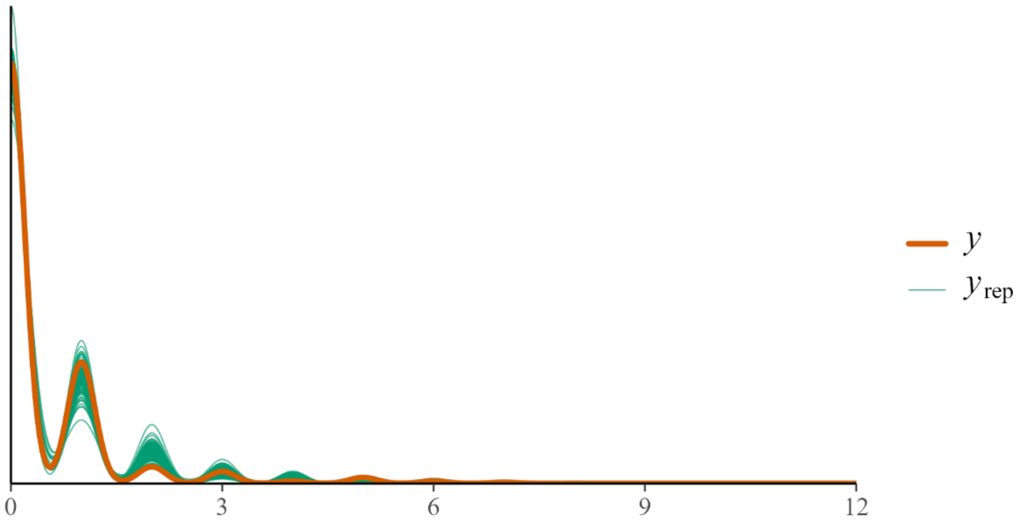

Density age-group 1 Långvindsfjärden

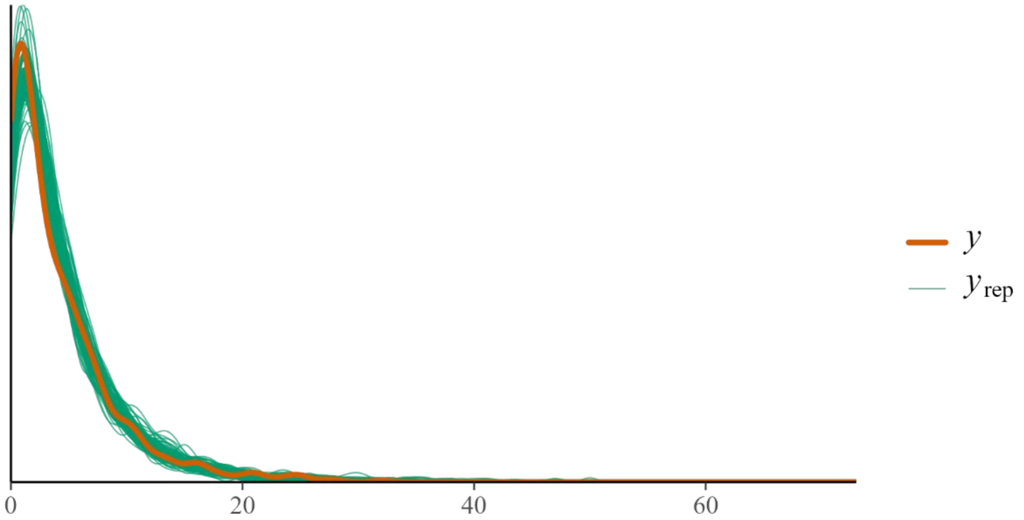

Density age-group 2 Långvindsfjärden

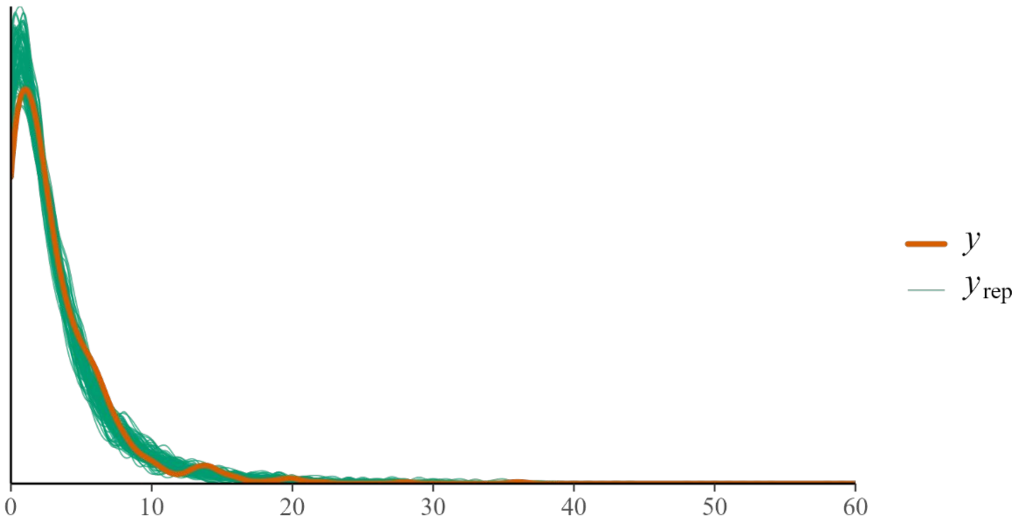

Density age-group 3 Långvindsfjärden

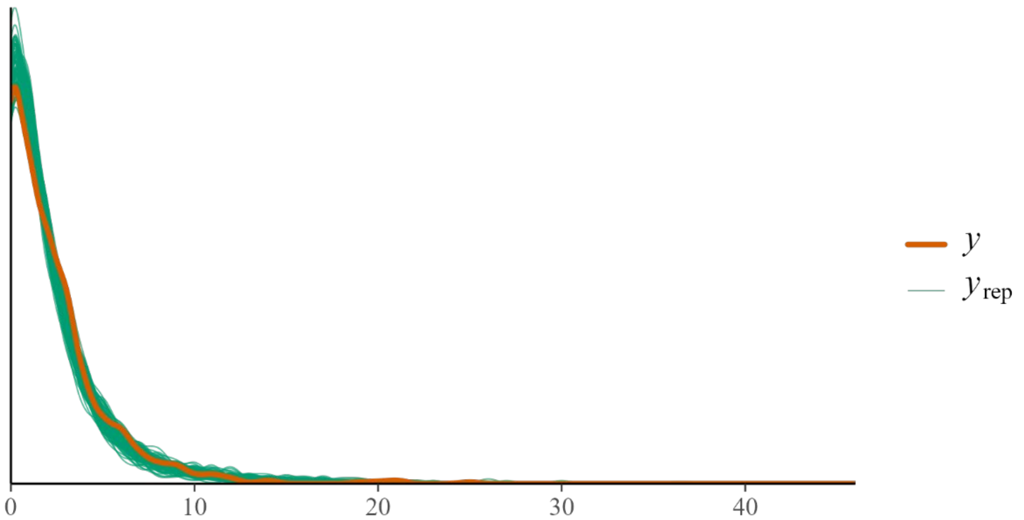

Density age-group 4 Långvindsfjärden

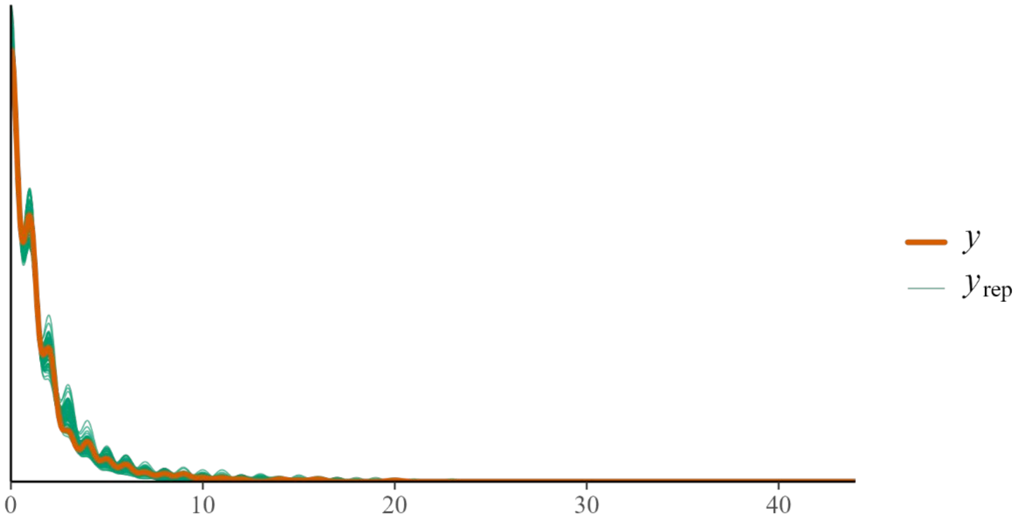

Density age-group 5 Långvindsfjärden

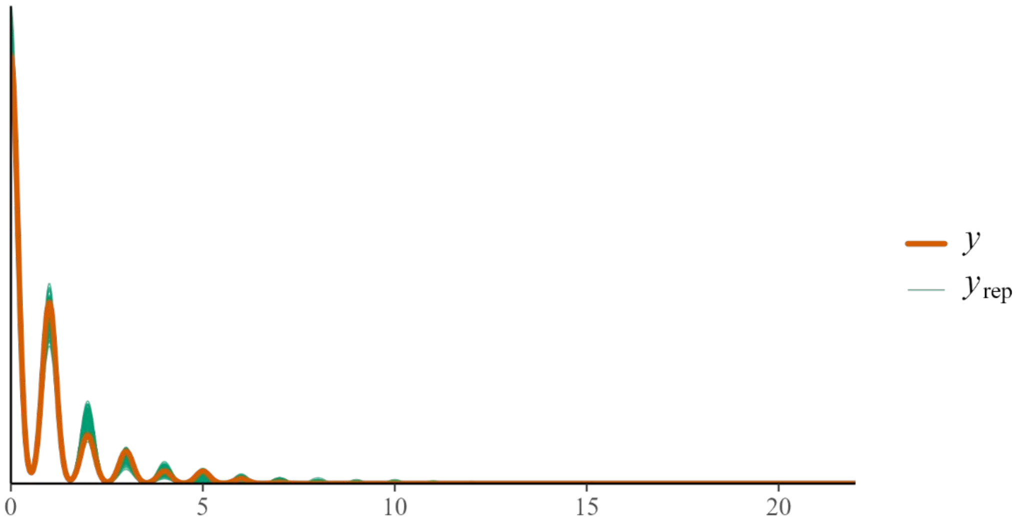

Density age-group 6 Långvindsfjärden

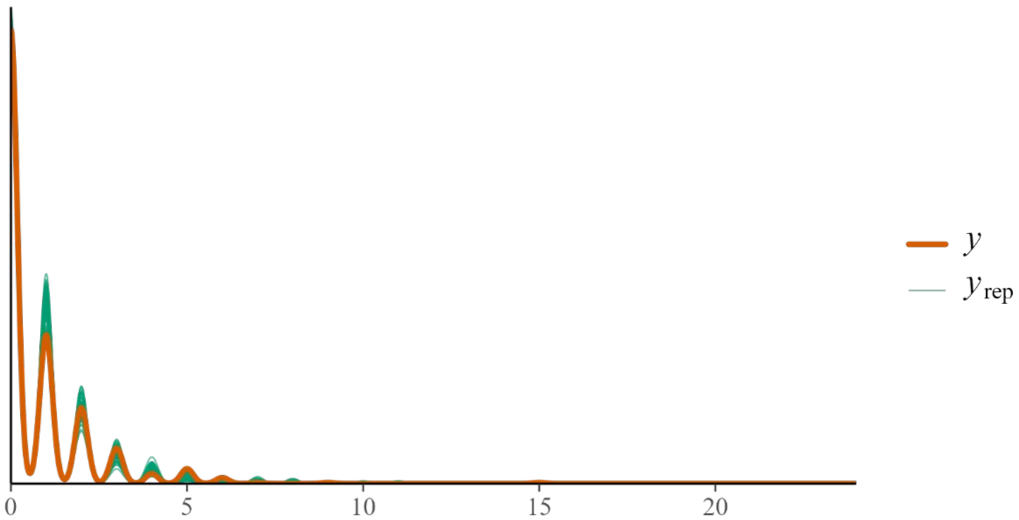

Density age-group 1 Forsmark

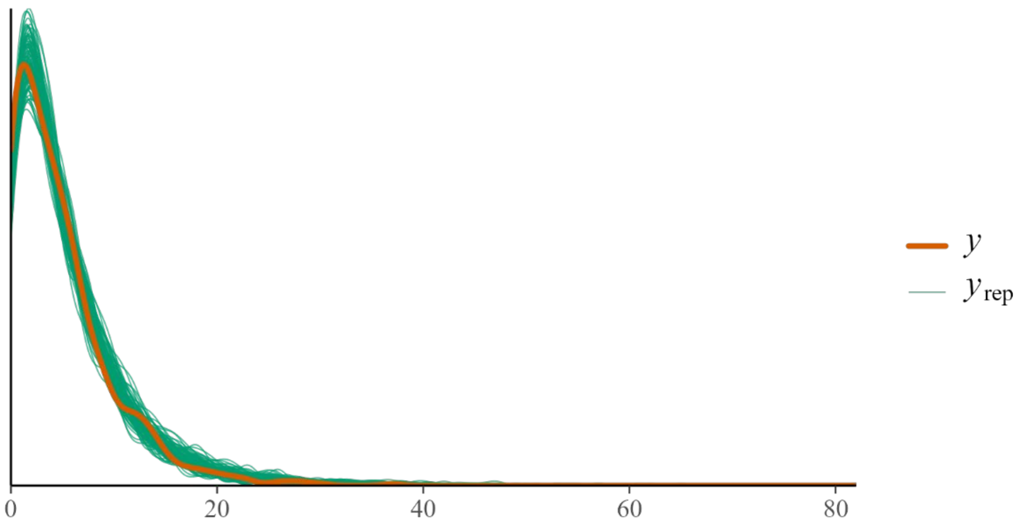

Density age-group 2 Forsmark

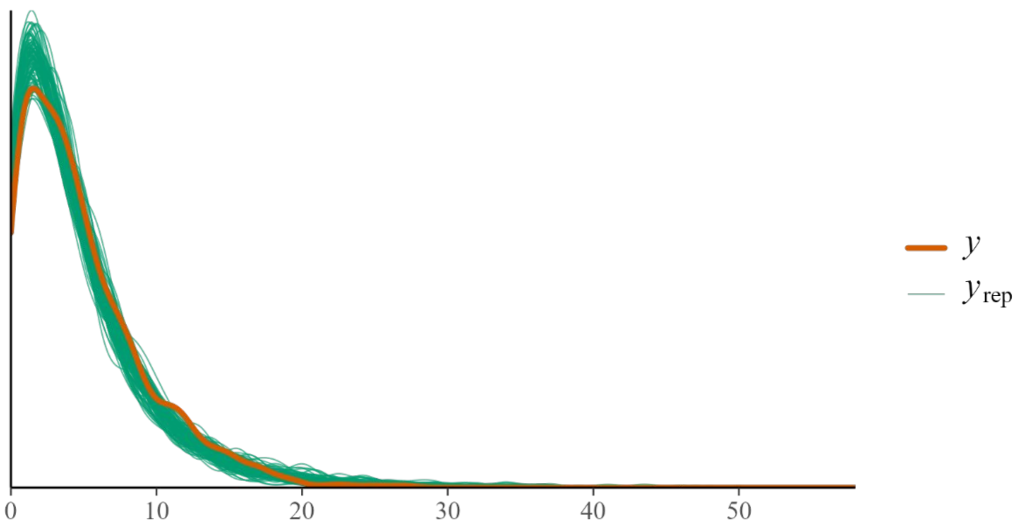

Density age-group 3 Forsmark

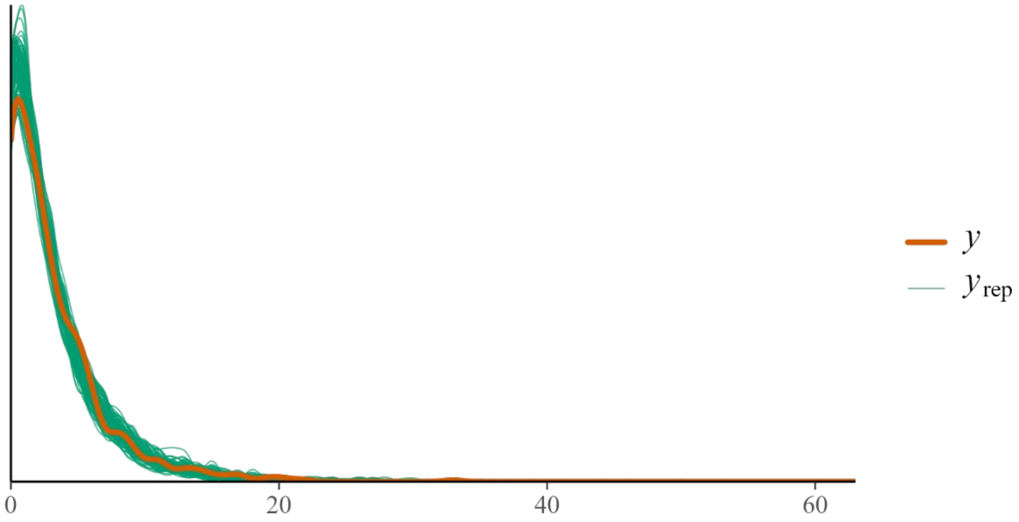

Density age-group 4 Forsmark

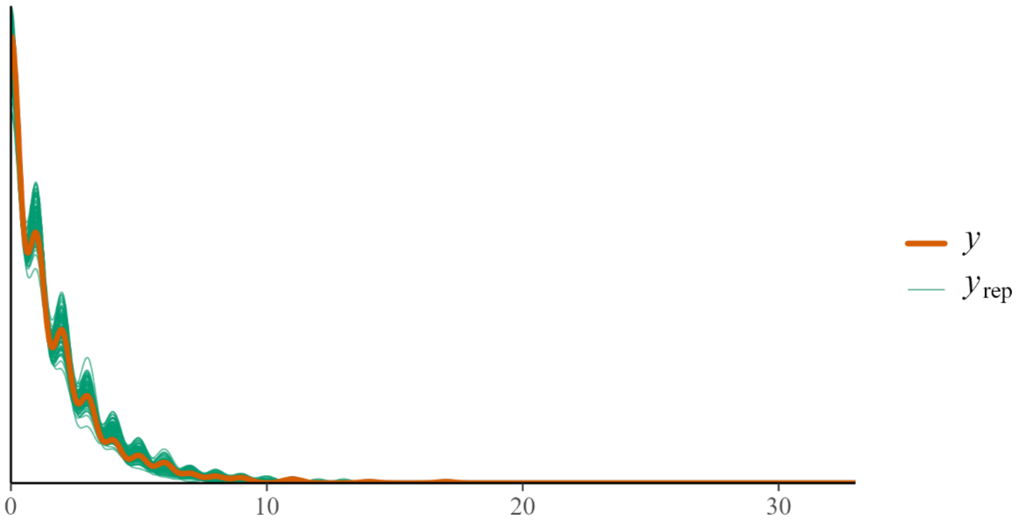

Density age-group 5 Forsmark

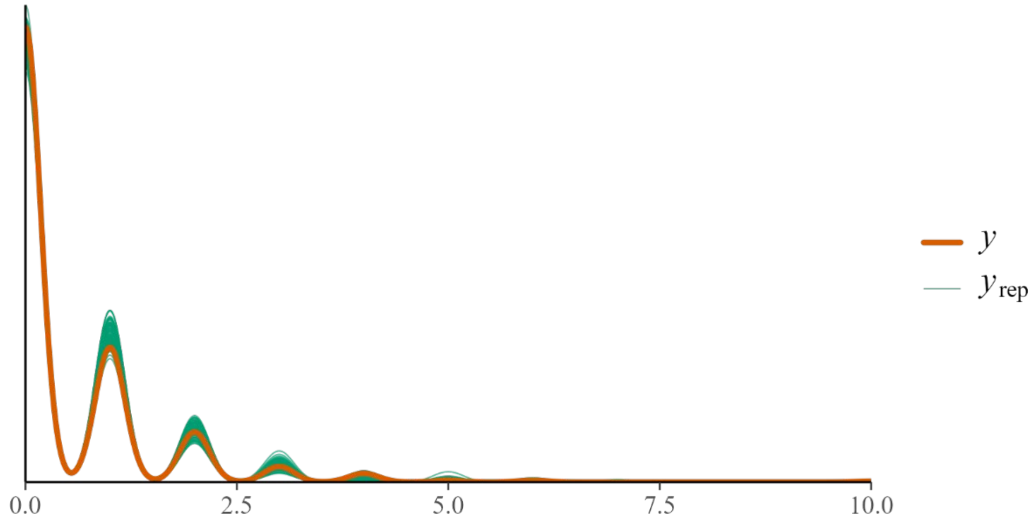

Density age-group 6 Forsmark

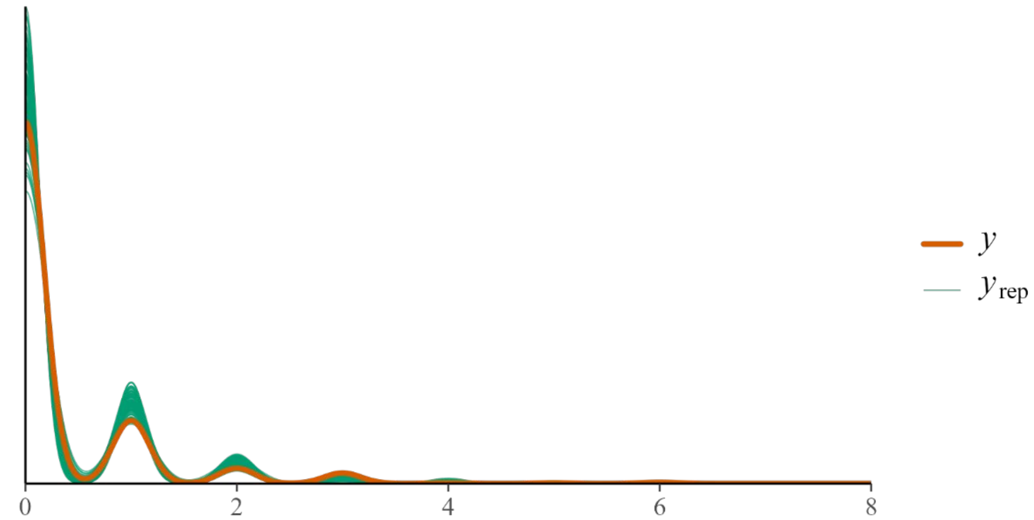

Density age-group 1 Lagnö

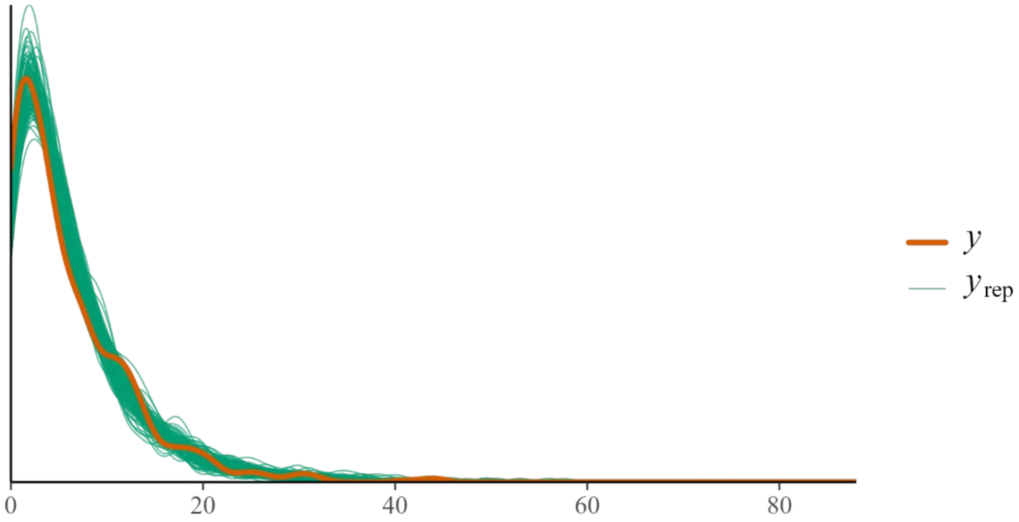

Density age-group 2 Lagnö

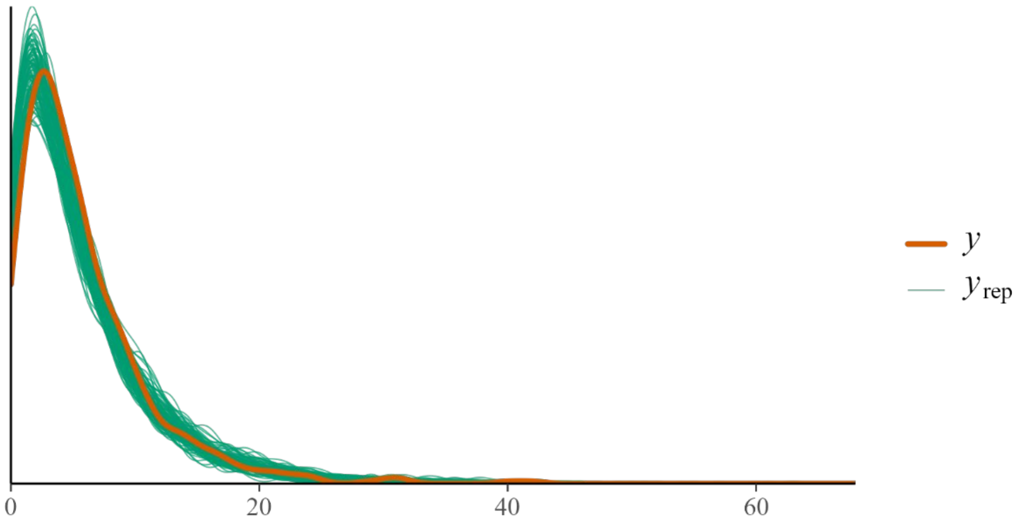

Density age-group 3 Lagnö

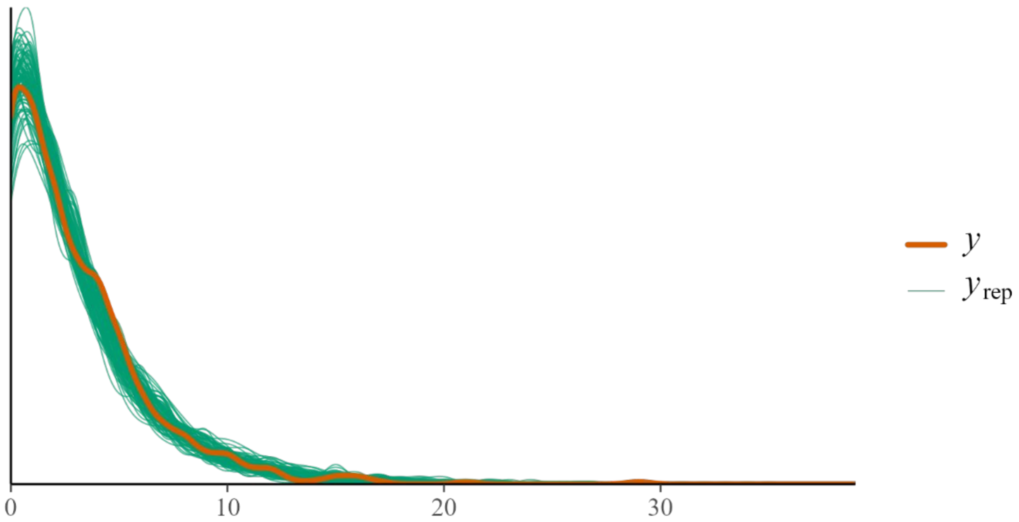

Density age-group 4 Lagnö

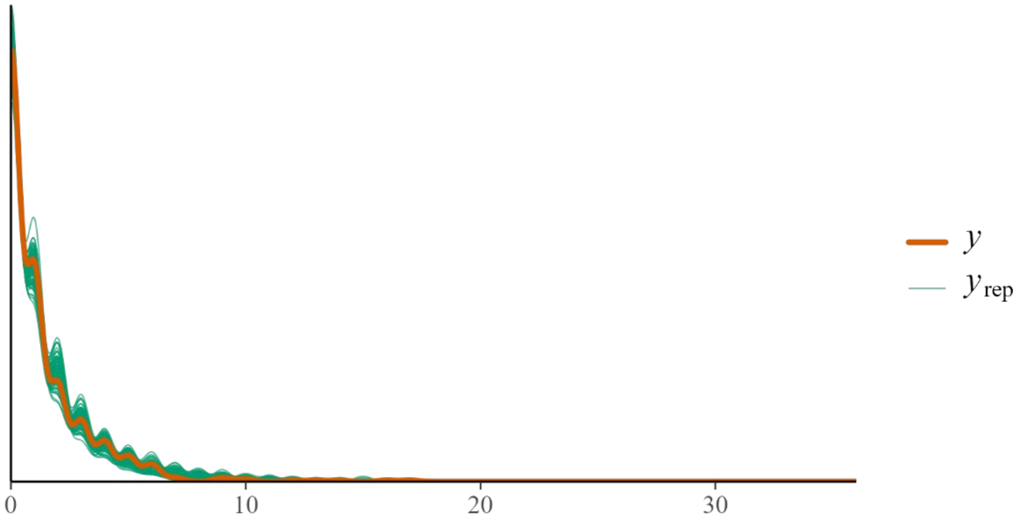

Density age-group 5 Lagnö

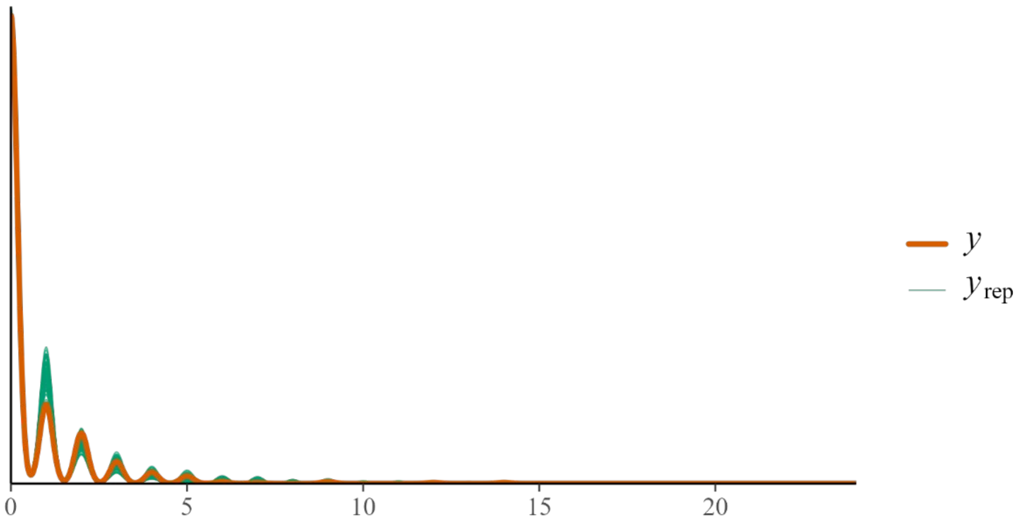

Density age-group 1 Asköfjärden

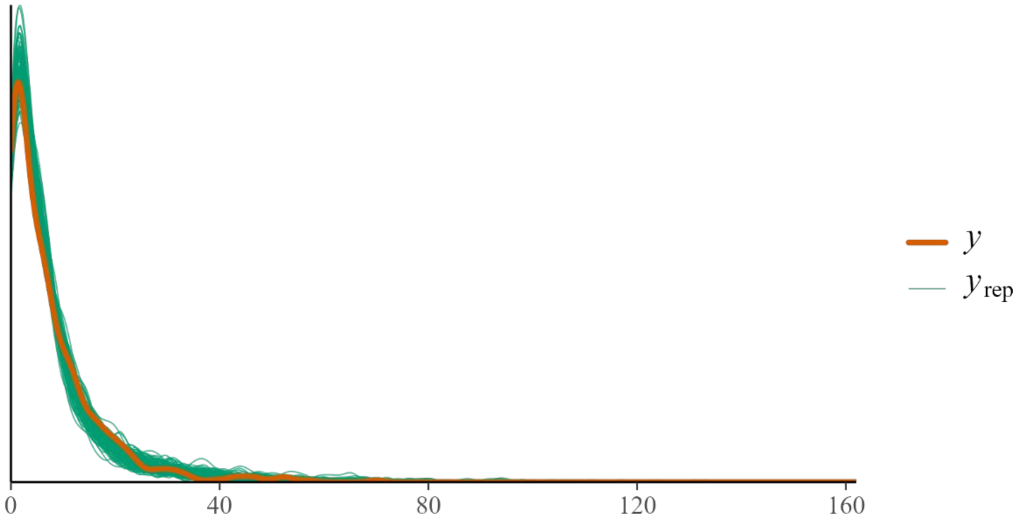

Density age-group 2 Asköfjärden

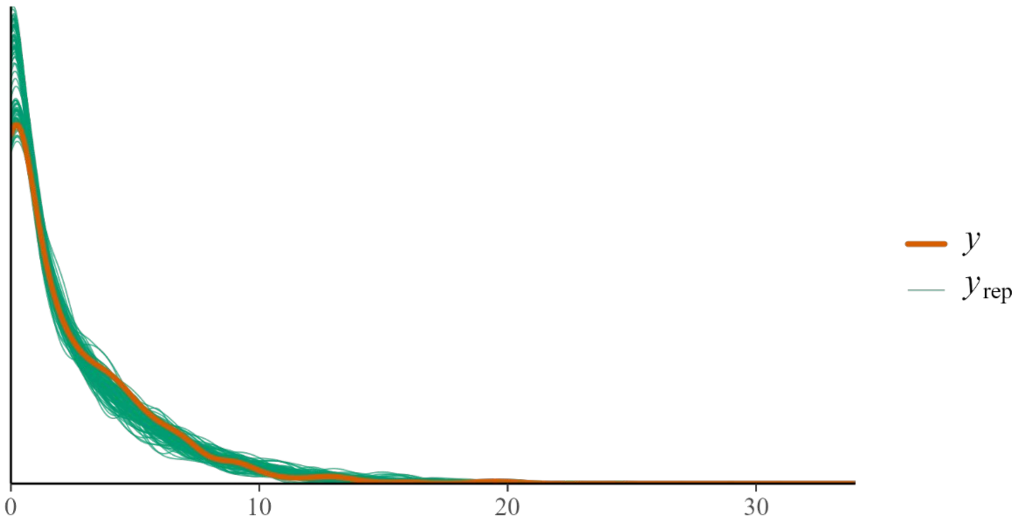

Density age-group 3 Asköfjärden

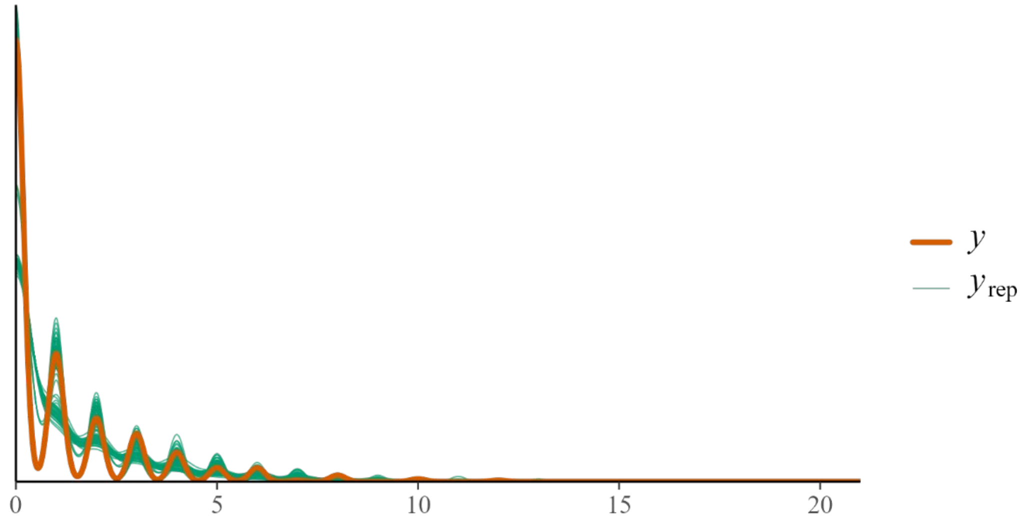

Density age-group 4 Asköfjärden

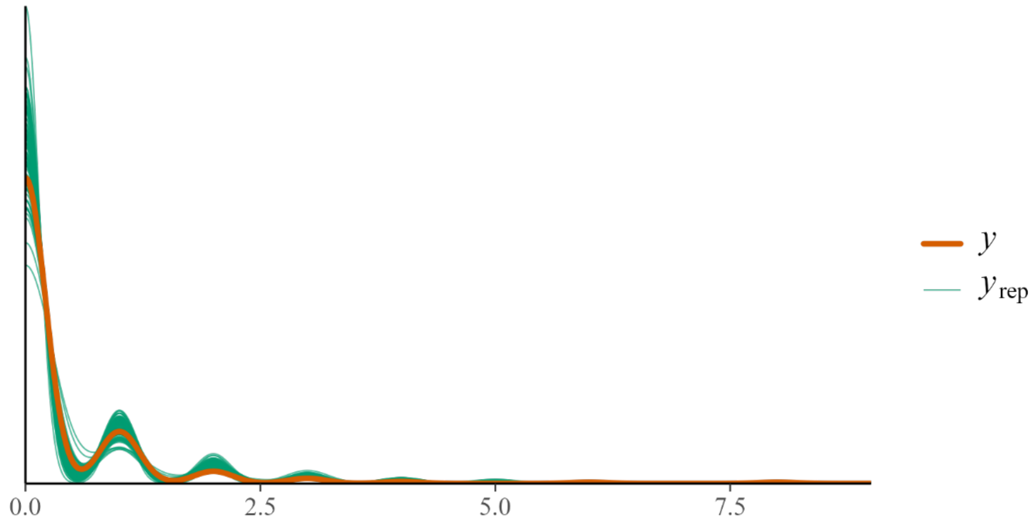

Density age-group 1 Kvädöfjärden

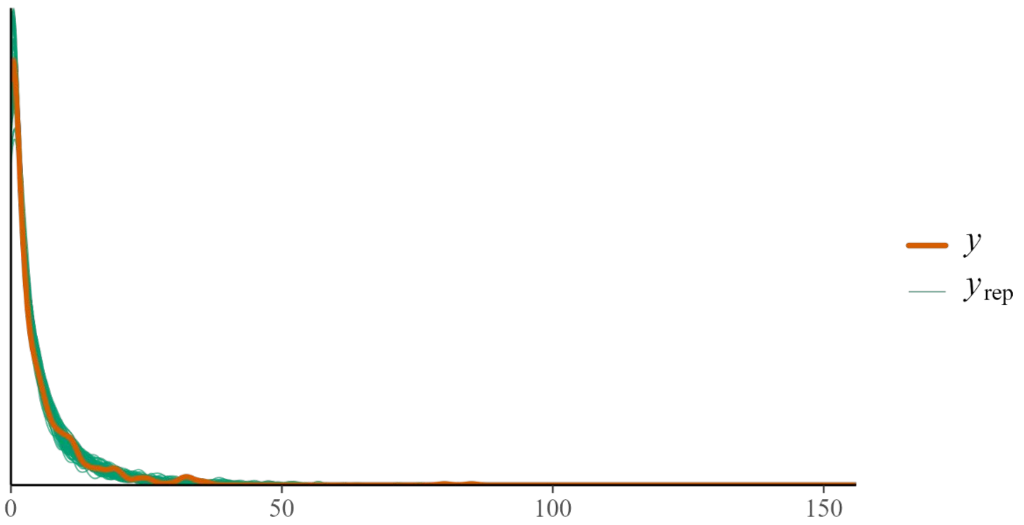

Density age-group 2 Kvädöfjärden

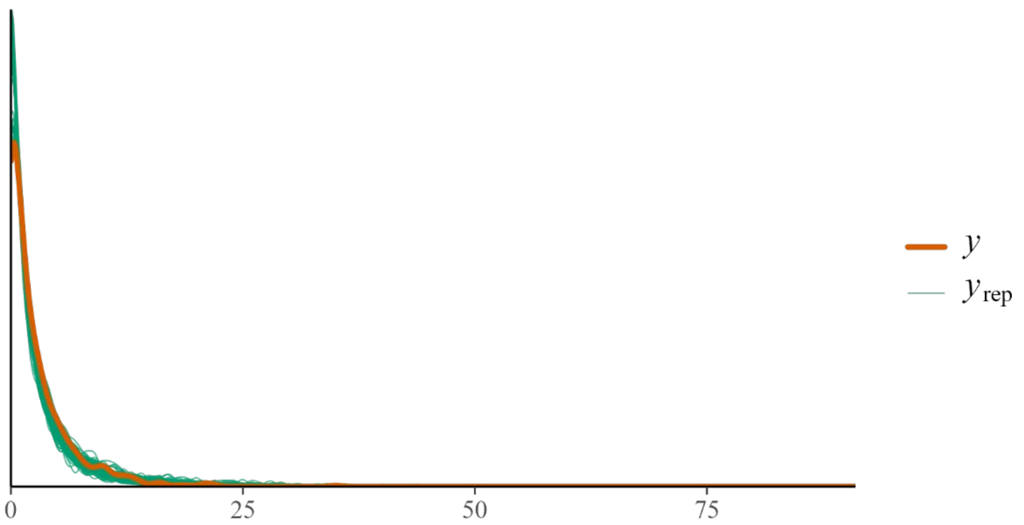

Density age-group 3 Kvädöfjärden

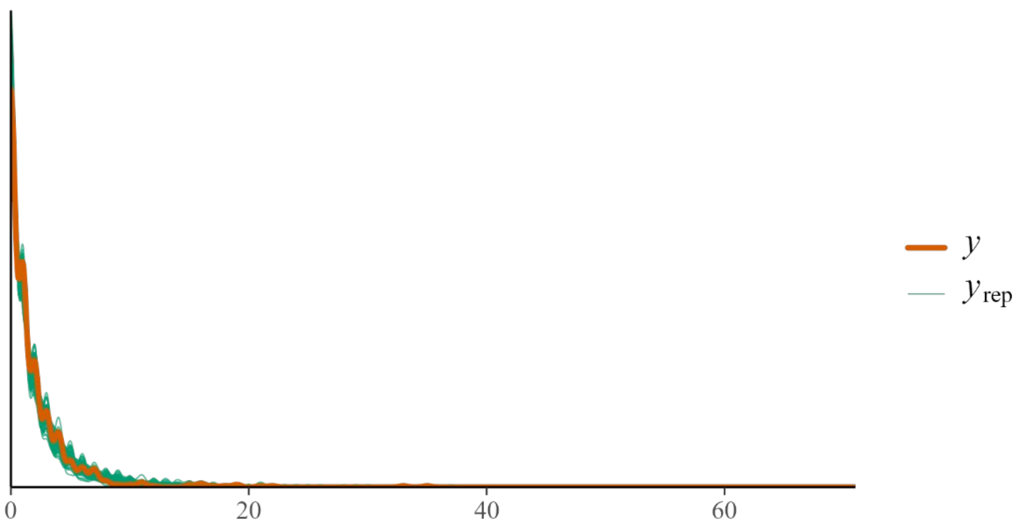

Density age-group 4 Kvädöfjärden

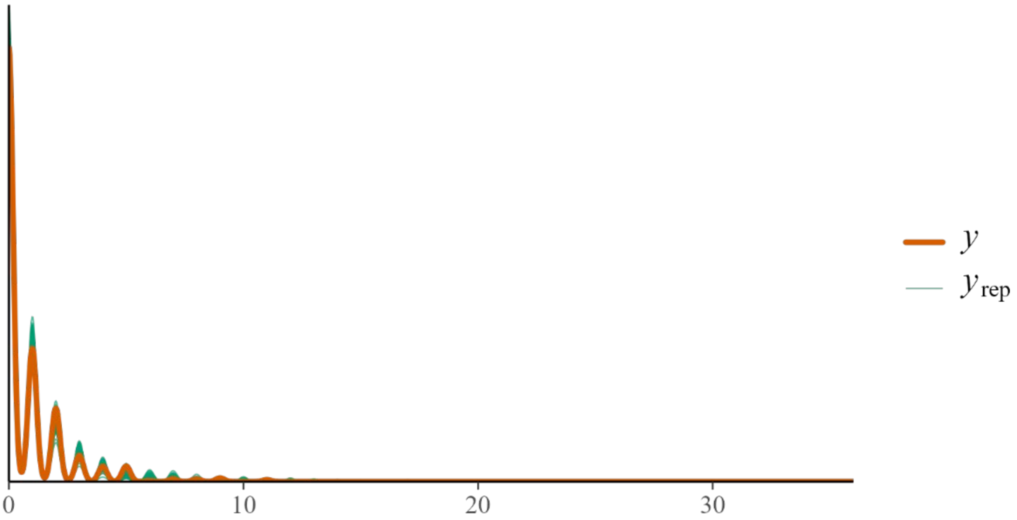

Density age-group 5 Kvädöfjärden

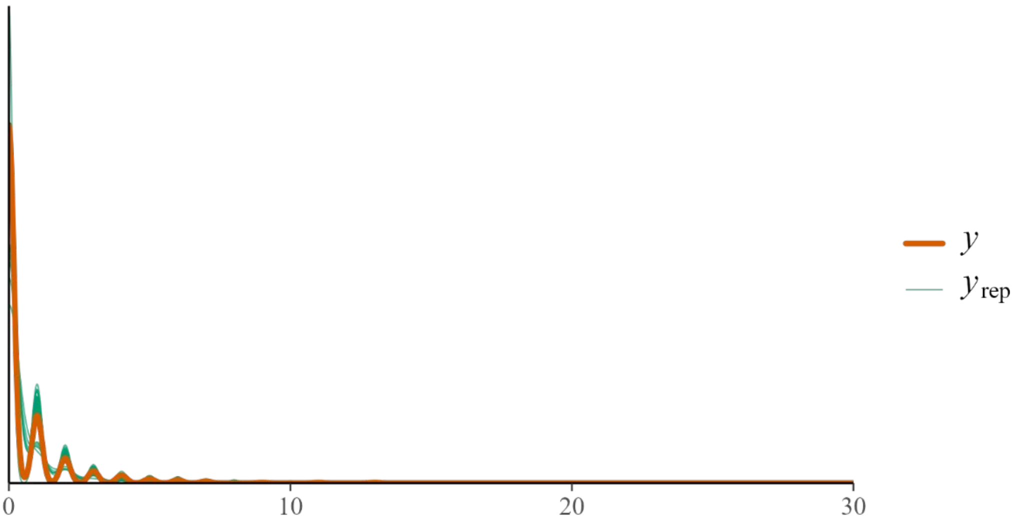

Density age-group 6 Kvädöfjärden

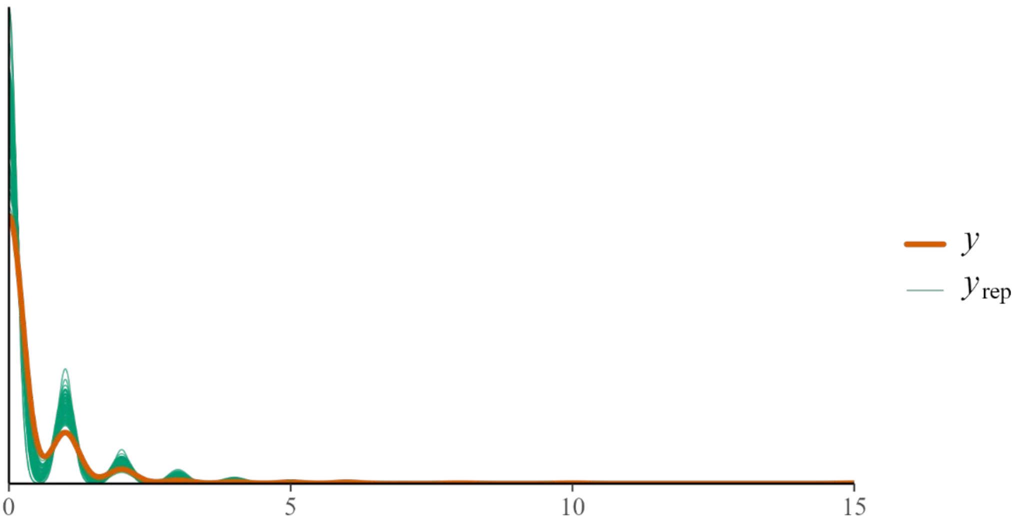

Density age-group 1 Torhamn

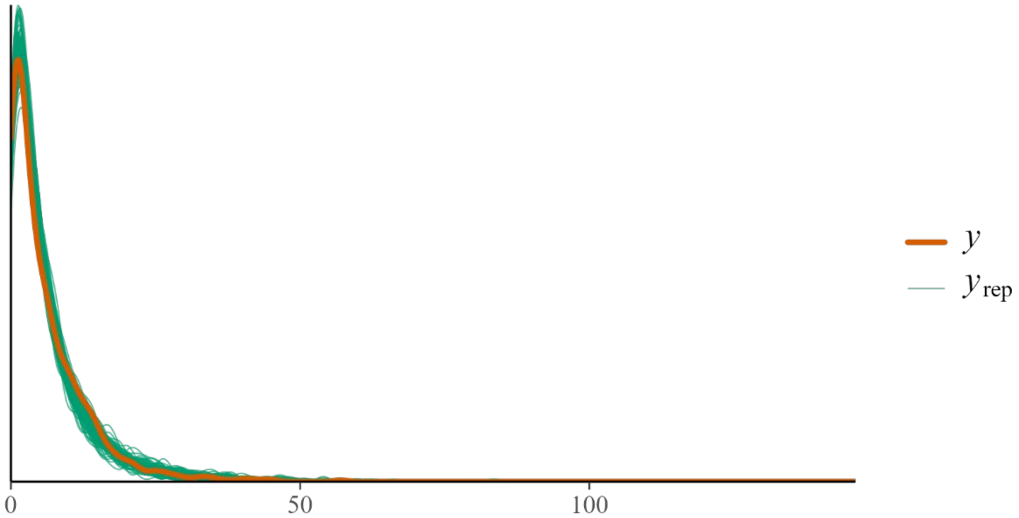

Density age-group 2 Torhamn

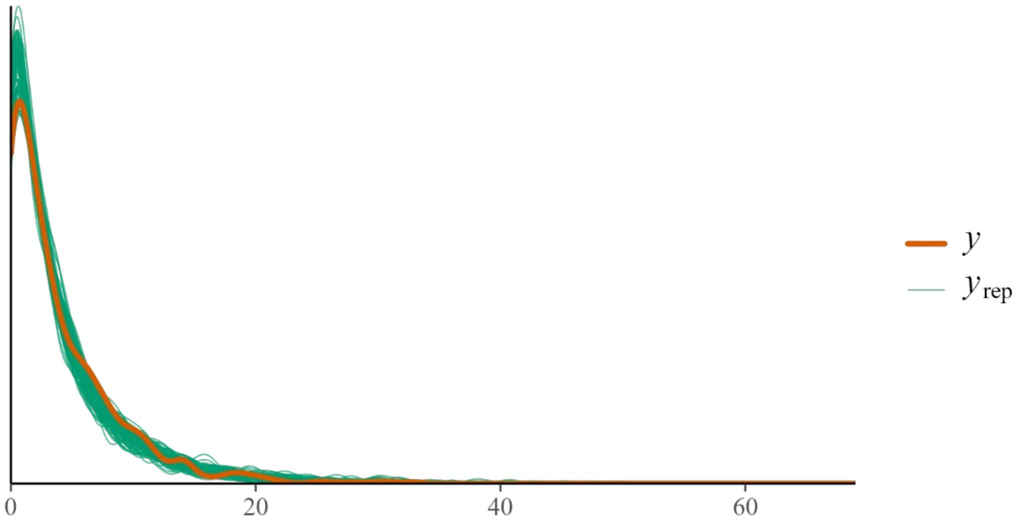

Density age-group 3 Torhamn

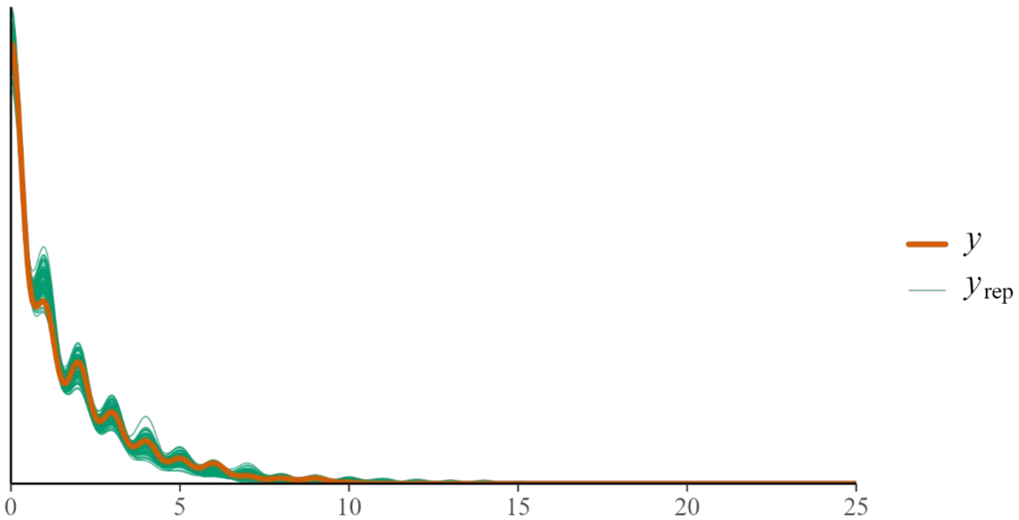

Appendix 3 - Posterior predictive check (proportion zeros per age-class)

This appendix shows the proportion of cases where no individuals of age-class a are caught in gillnets (in orange), and the distribution of the same quantity simulated using the posterior distribution (blue bars).

Proportion zeros age-group 1 Råneå

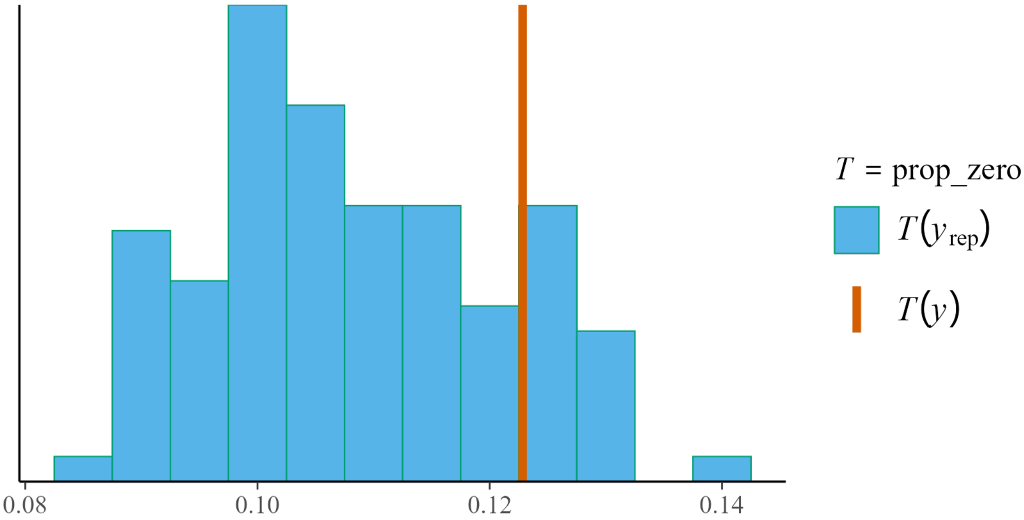

Proportion zeros age-group 2 Råneå

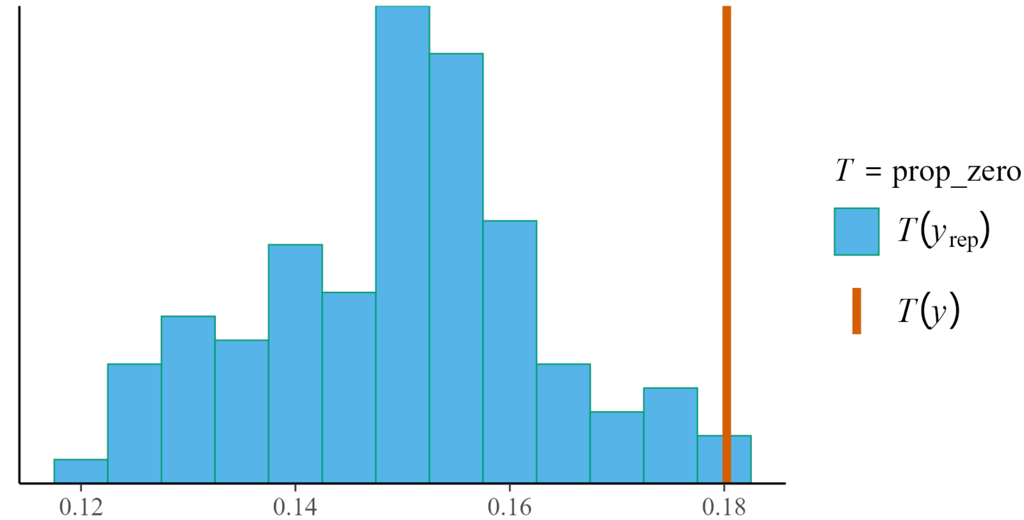

Proportion zeros age-group 3 Råneå

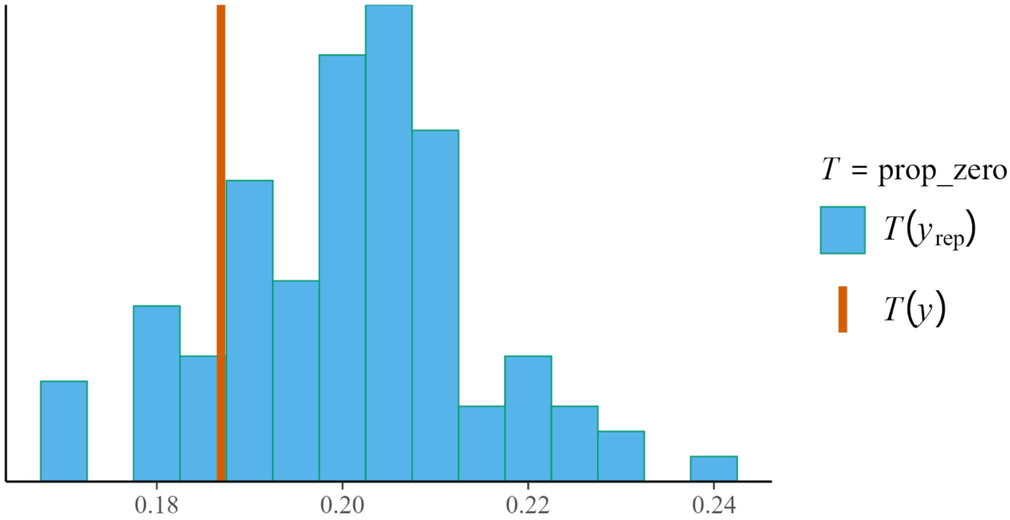

Proportion zeros age-group 4 Råneå

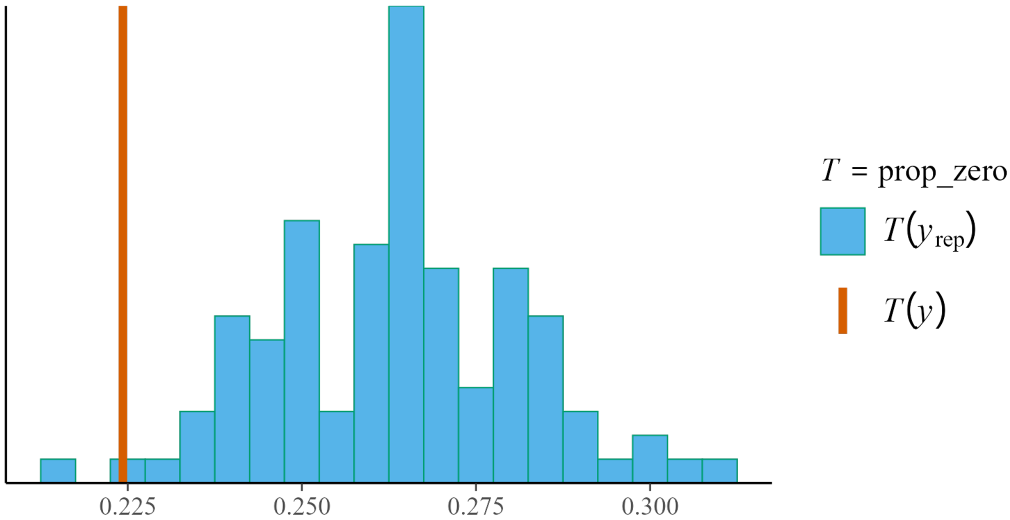

Proportion zeros age-group 5 Råneå

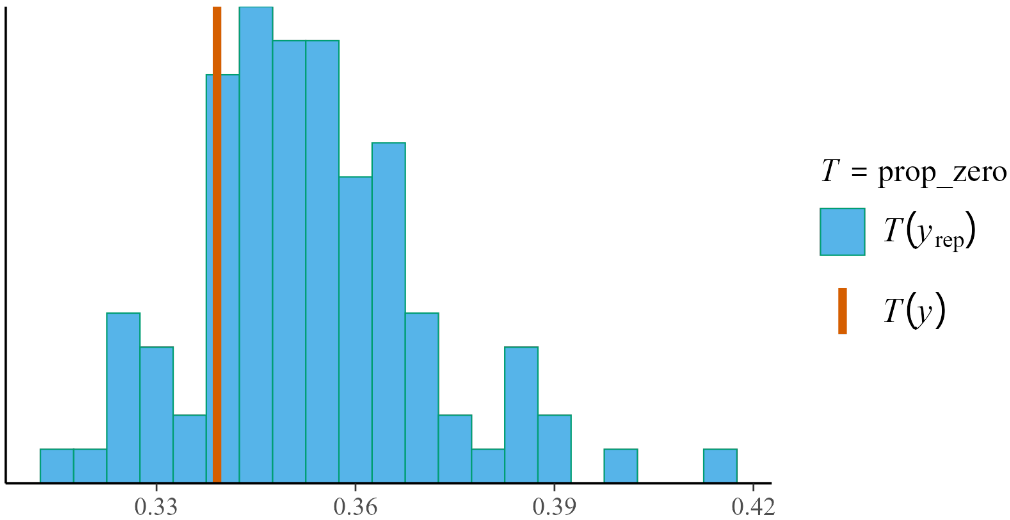

Proportion zeros age-group 6 Råneå

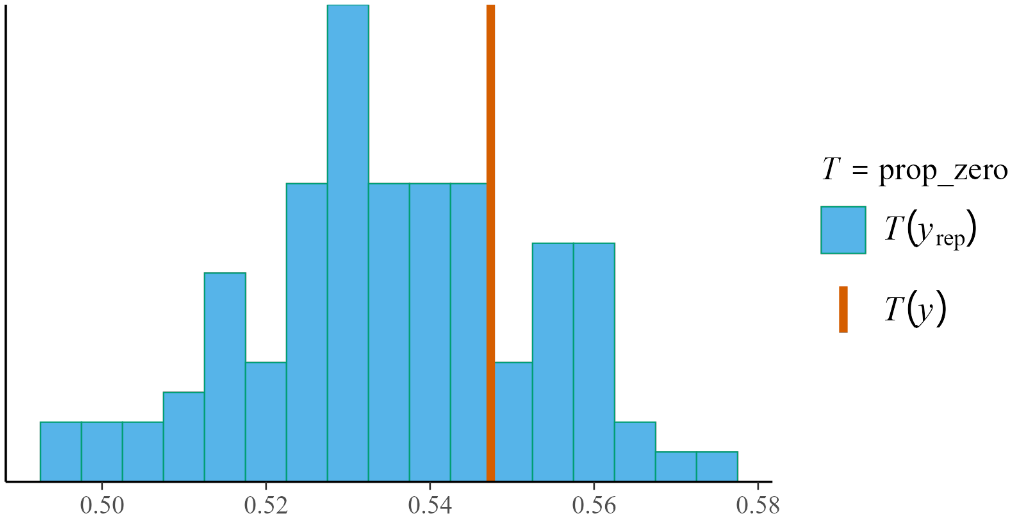

Proportion zeros age-group 7 Råneå

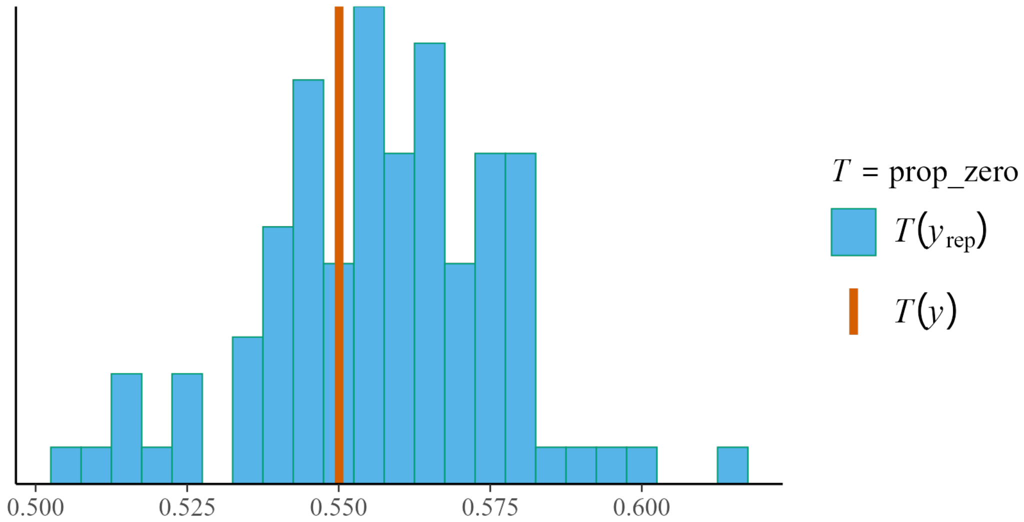

Proportion zeros age-group 1 Kinnbäcksfjärden

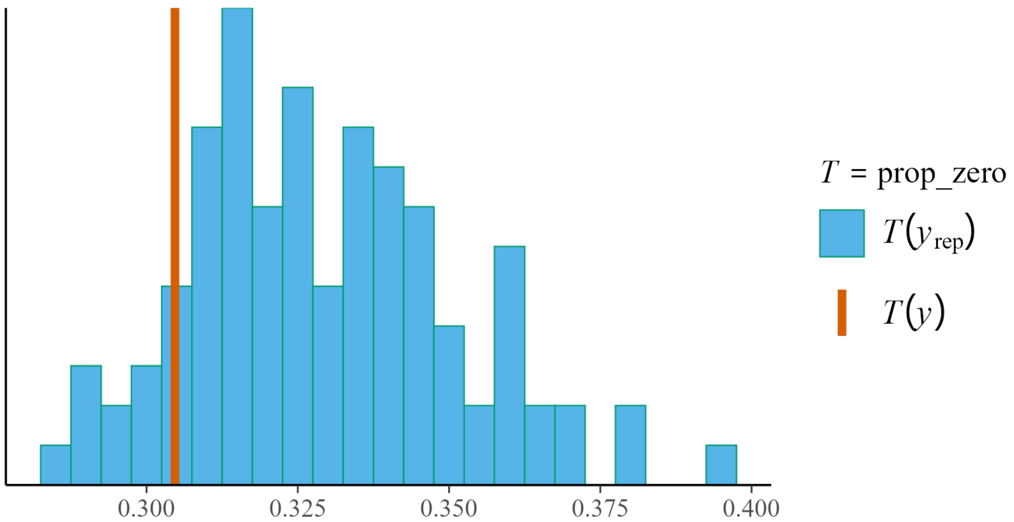

Proportion zeros age-group 2 Kinnbäcksfjärden

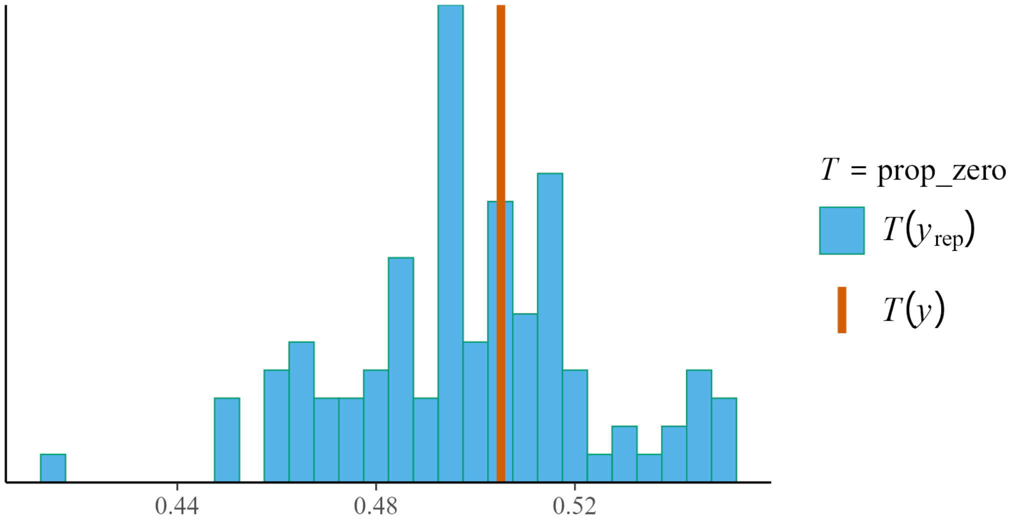

Proportion zeros age-group 3 Kinnbäcksfjärden

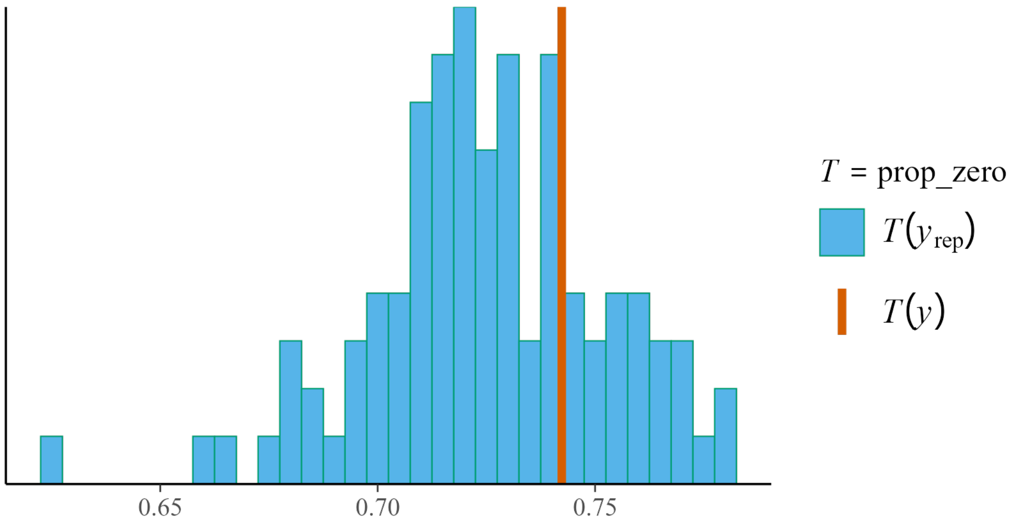

Proportion zeros age-group 1 Holmön

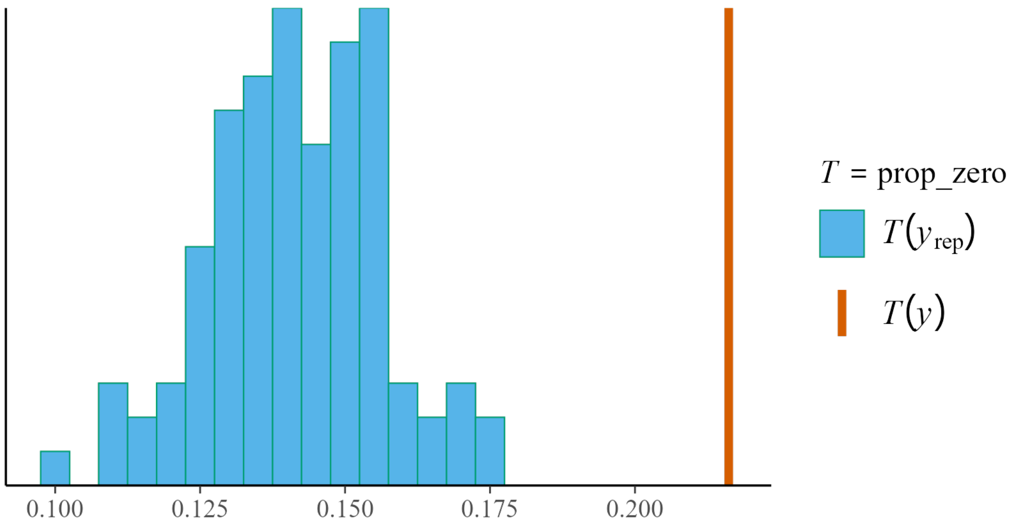

Proportion zeros age-group 2 Holmön

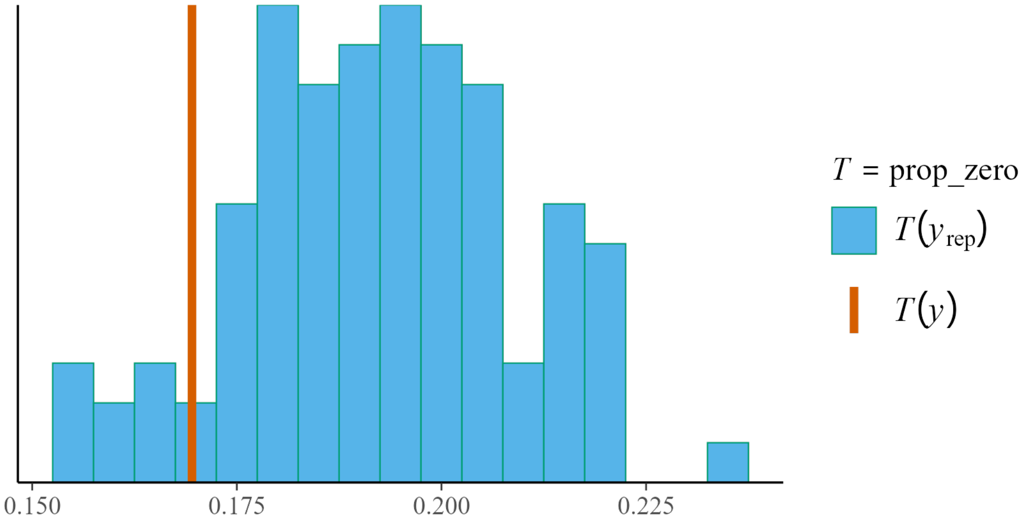

Proportion zeros age-group 3 Holmön

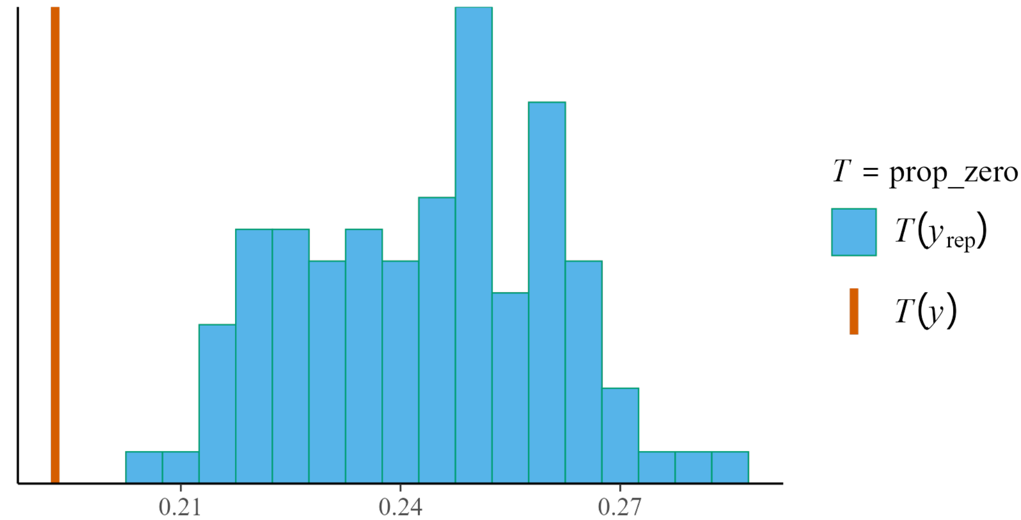

Proportion zeros age-group 4 Holmön

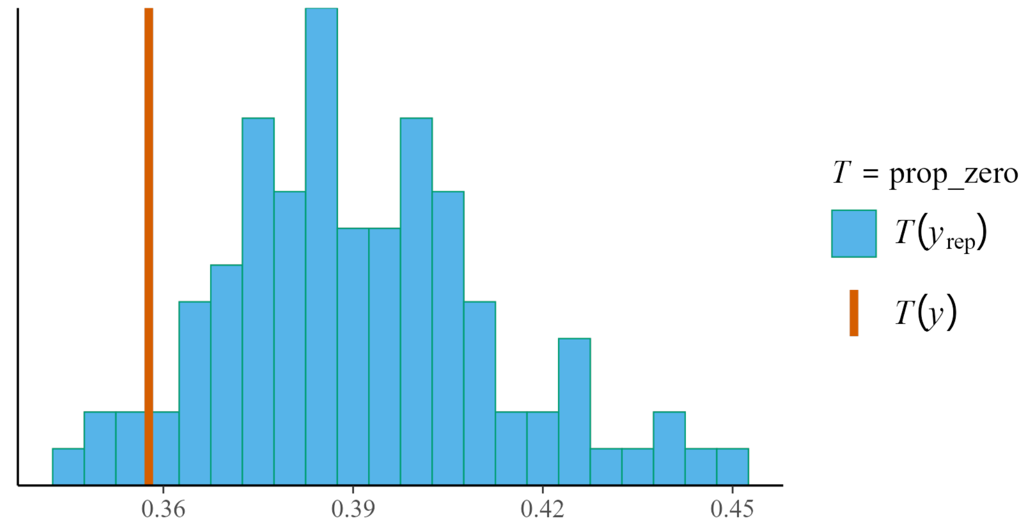

Proportion zeros age-group 5 Holmön

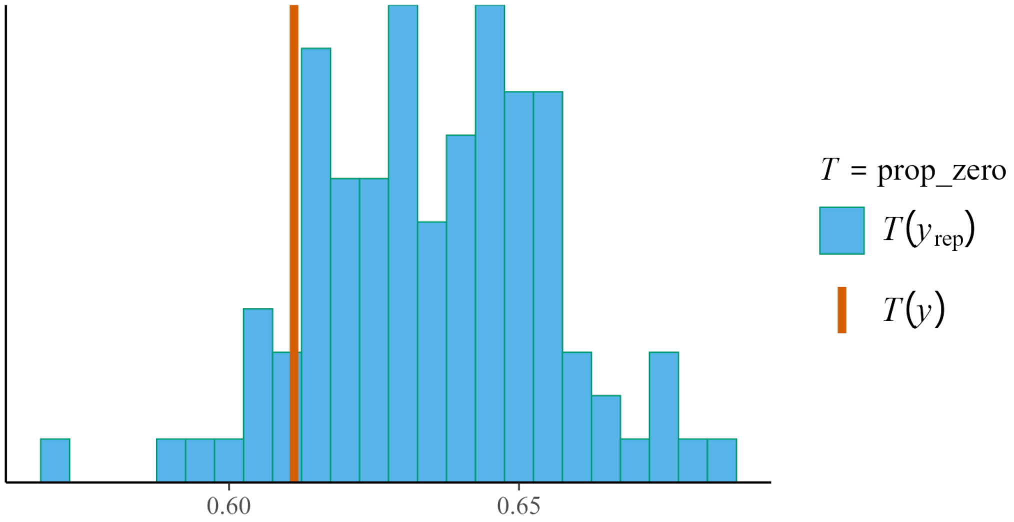

Proportion zeros age-group 6 Holmön

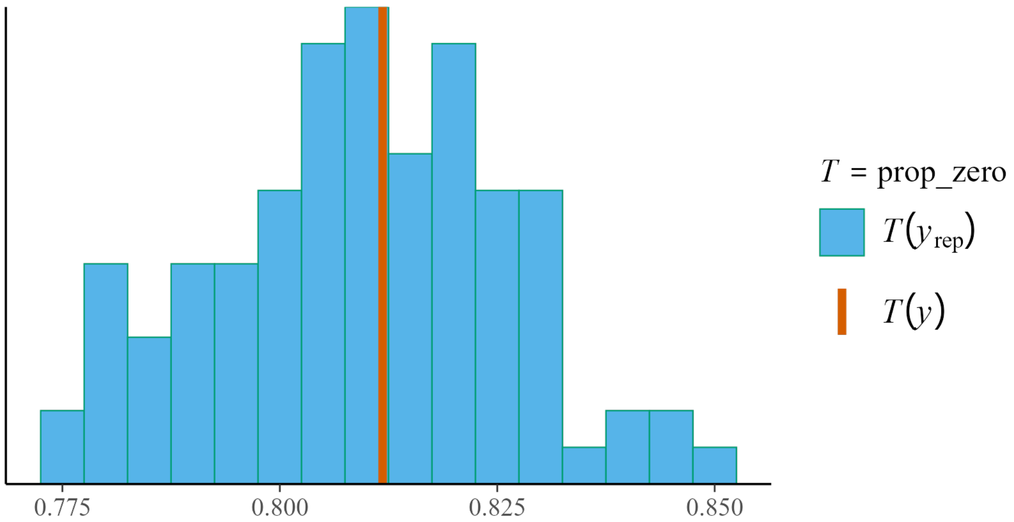

Proportion zeros age-group 1 Norrbyn

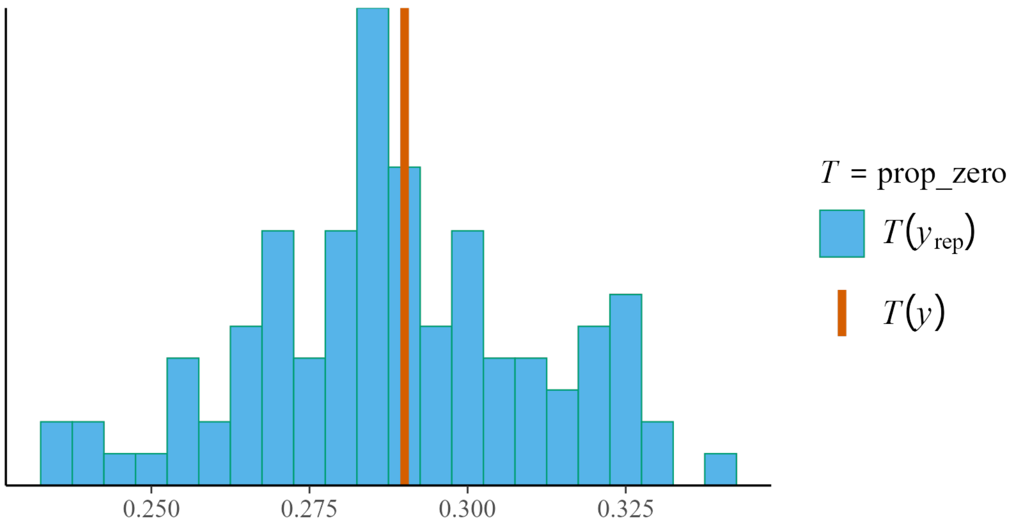

Proportion zeros age-group 2 Norrbyn

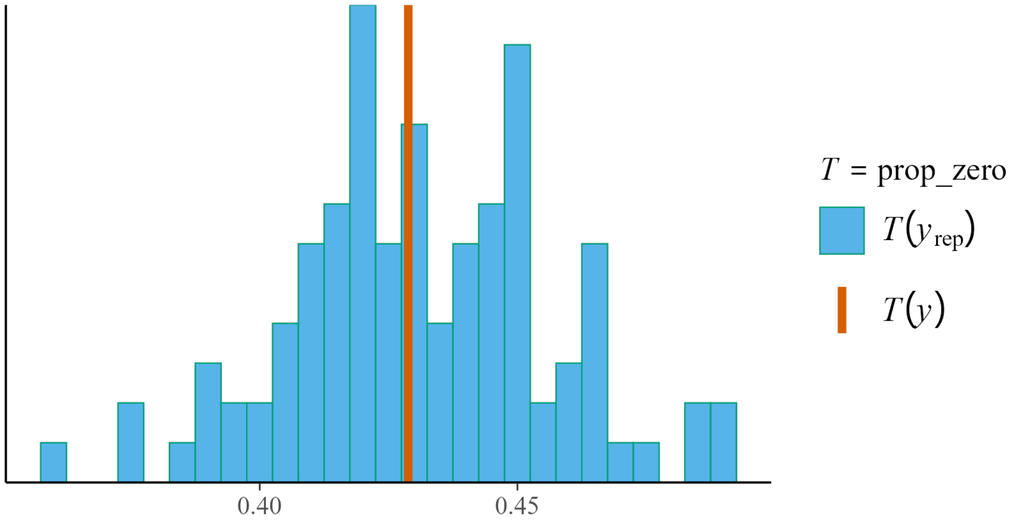

Proportion zeros age-group 3 Norrbyn

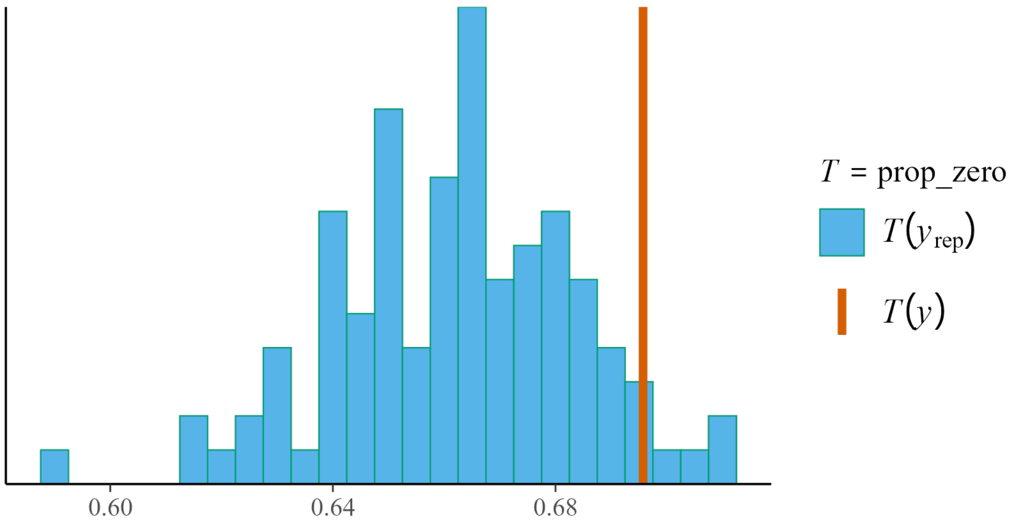

Proportion zeros age-group 1 Gaviksfjärden

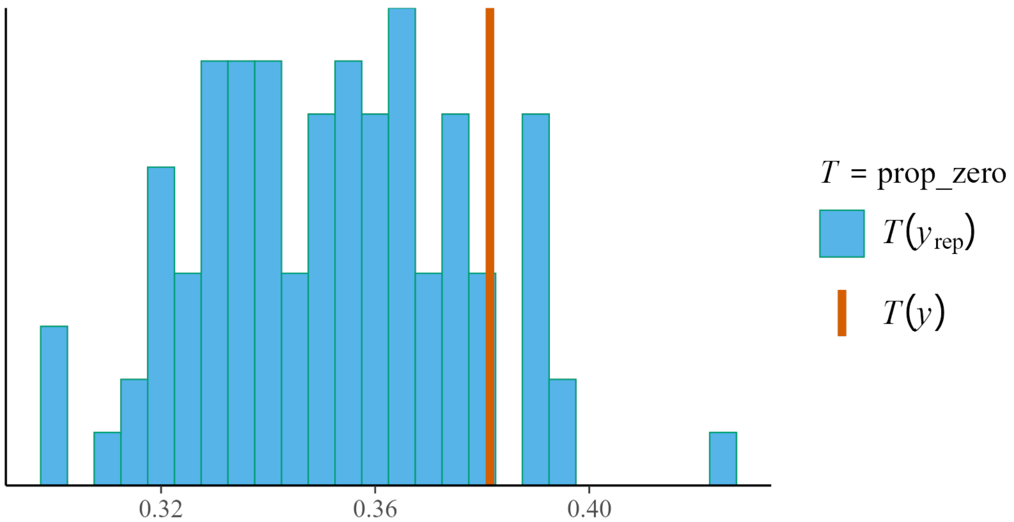

Proportion zeros age-group 2 Gaviksfjärden

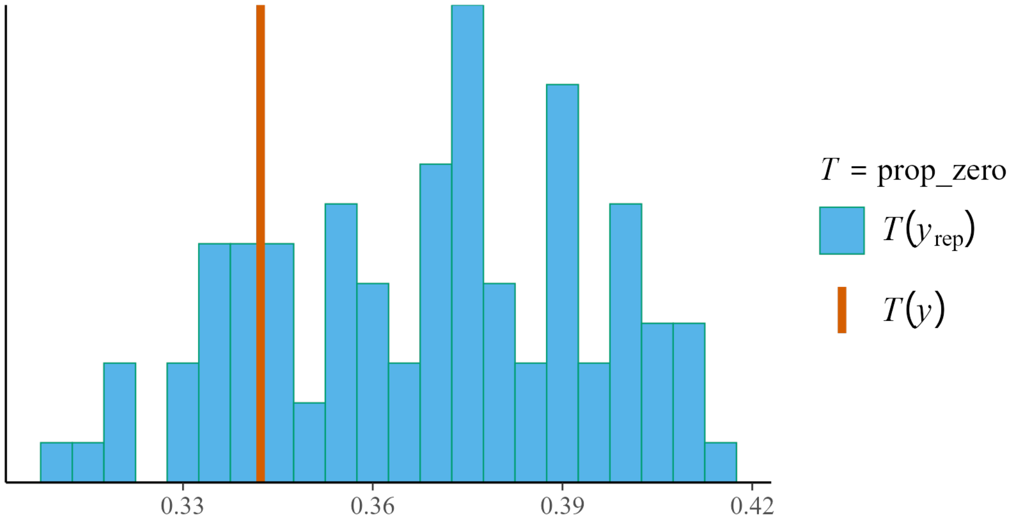

Proportion zeros age-group 3 Gaviksfjärden

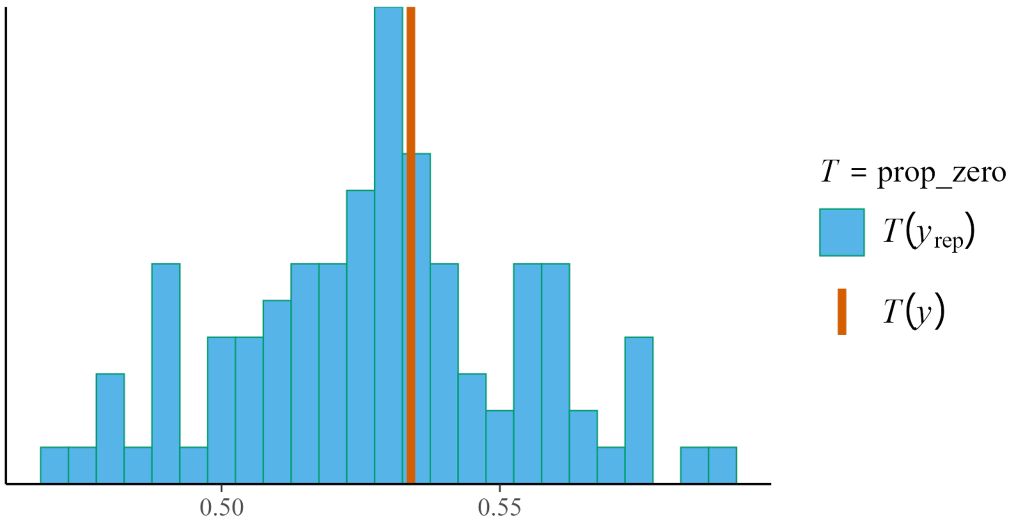

Proportion zeros age-group 4 Gaviksfjärden

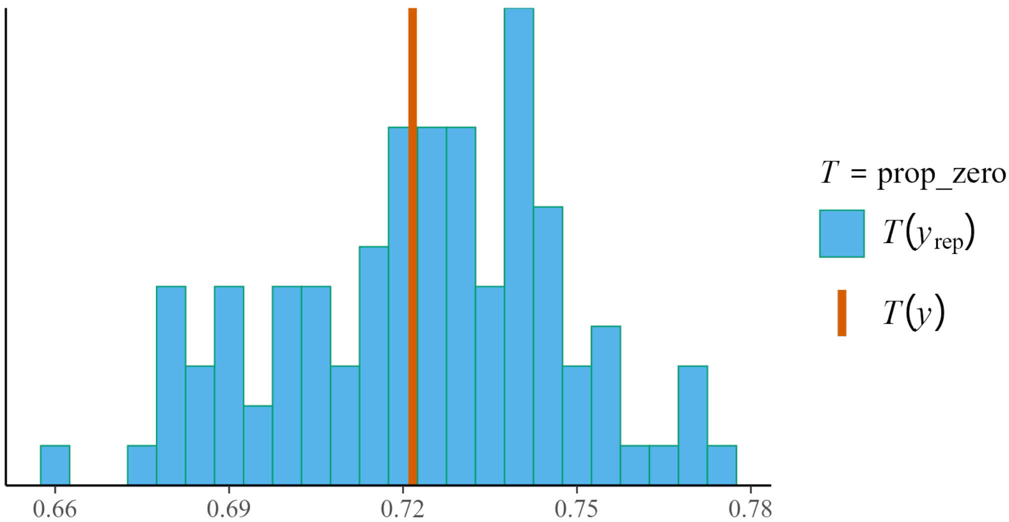

Proportion zeros age-group 1 Långvindsfjärden

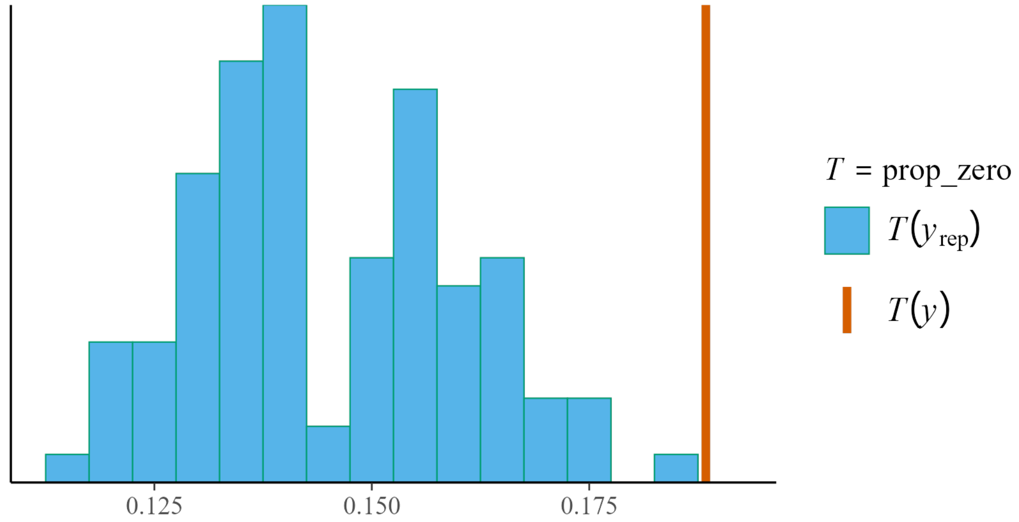

Proportion zeros age-group 2 Långvindsfjärden

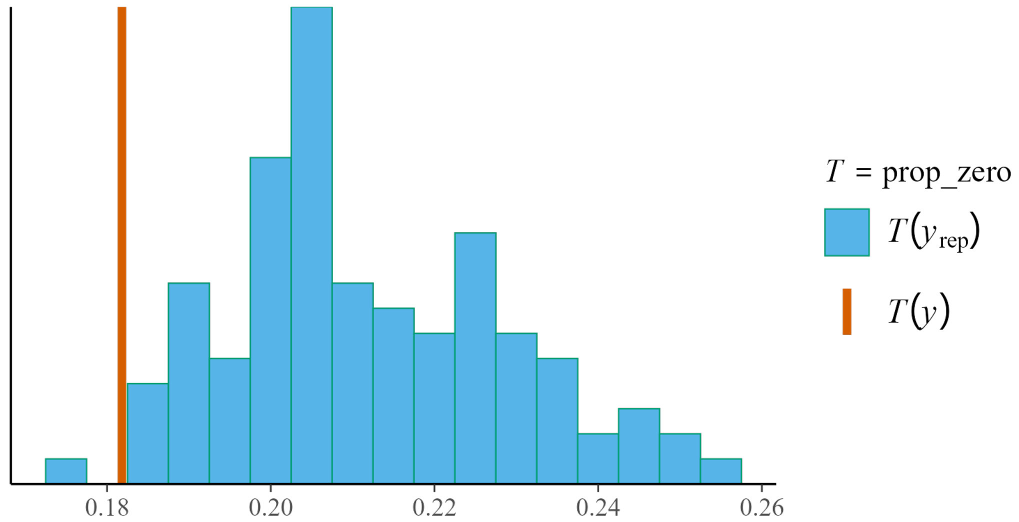

Proportion zeros age-group 3 Långvindsfjärden

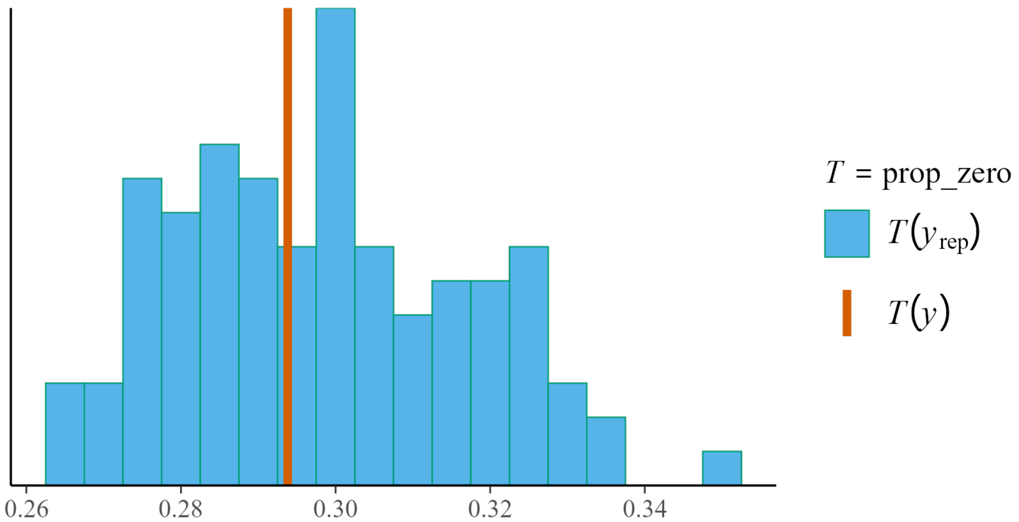

Proportion zeros age-group 4 Långvindsfjärden

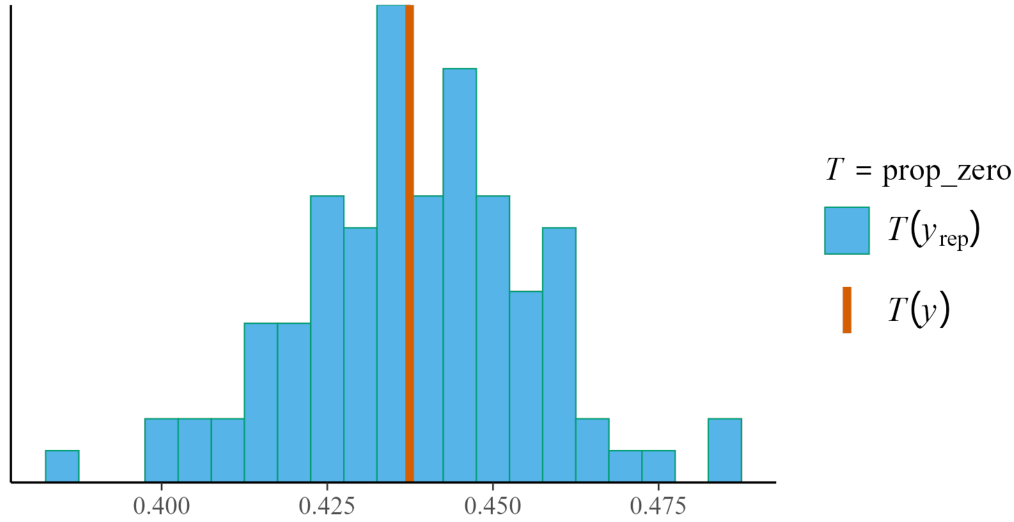

Proportion zeros age-group 5 Långvindsfjärden

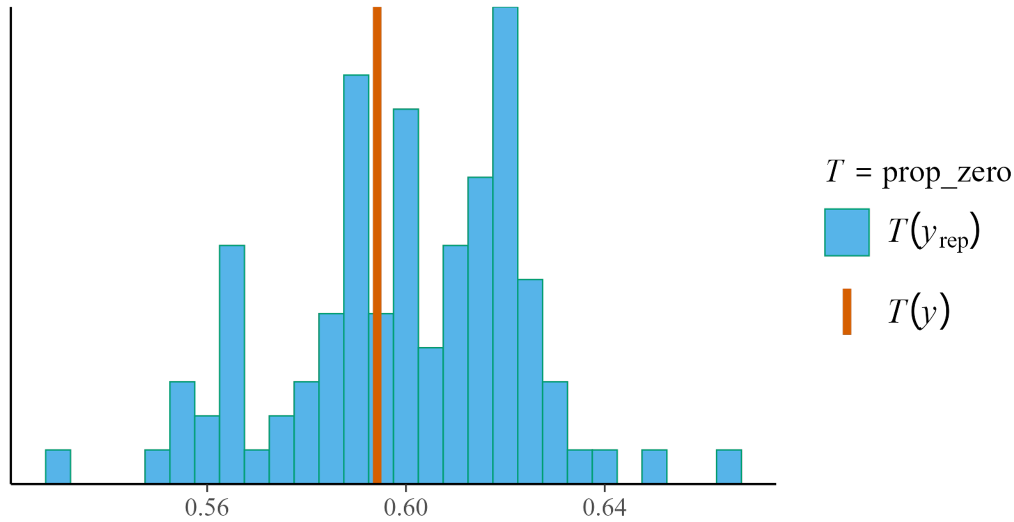

Proportion zeros age-group 6 Långvindsfjärden

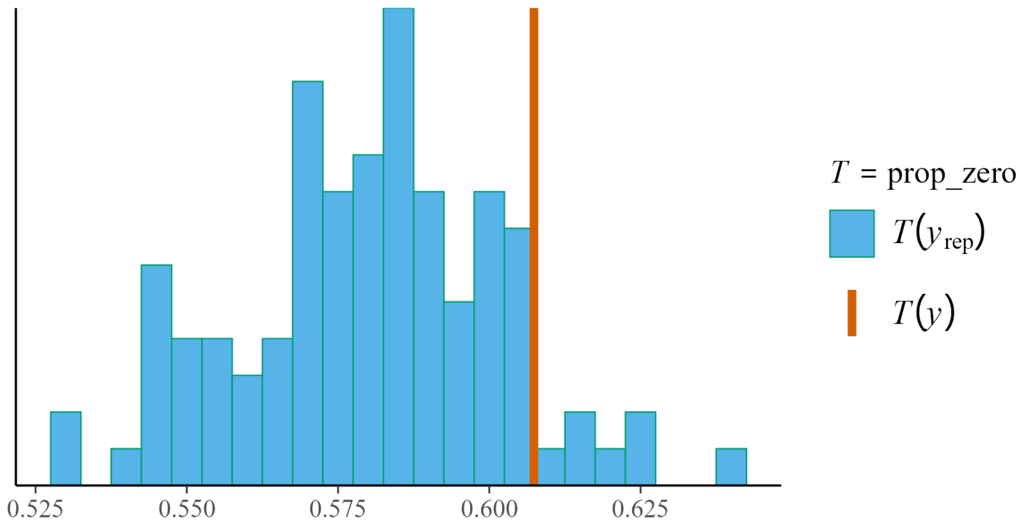

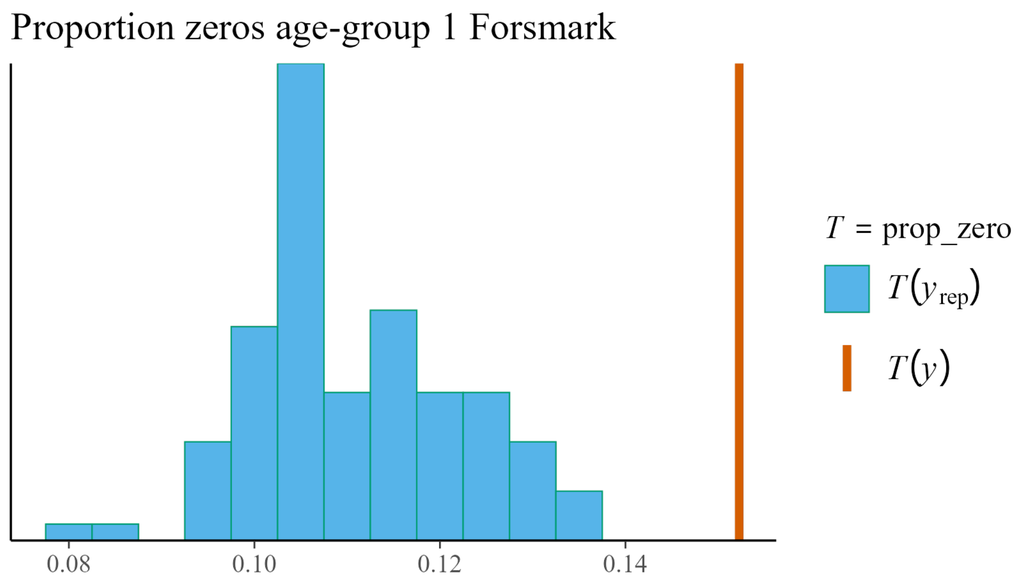
Proportion zeros age-group 1 Forsmark
0.08
0.10
0.12
0.14
T = prop_zero
T(y_rep)
T(y)

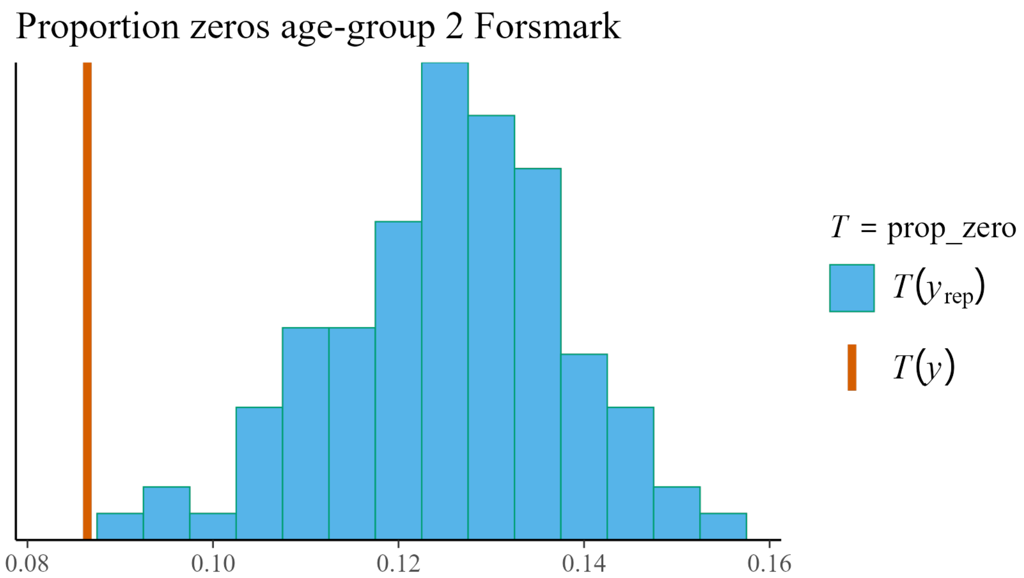
Proportion zeros age-group 2 Forsmark
0.08
0.10
0.12
0.14
0.16
T = prop_zero
T(y_rep)
T(y)

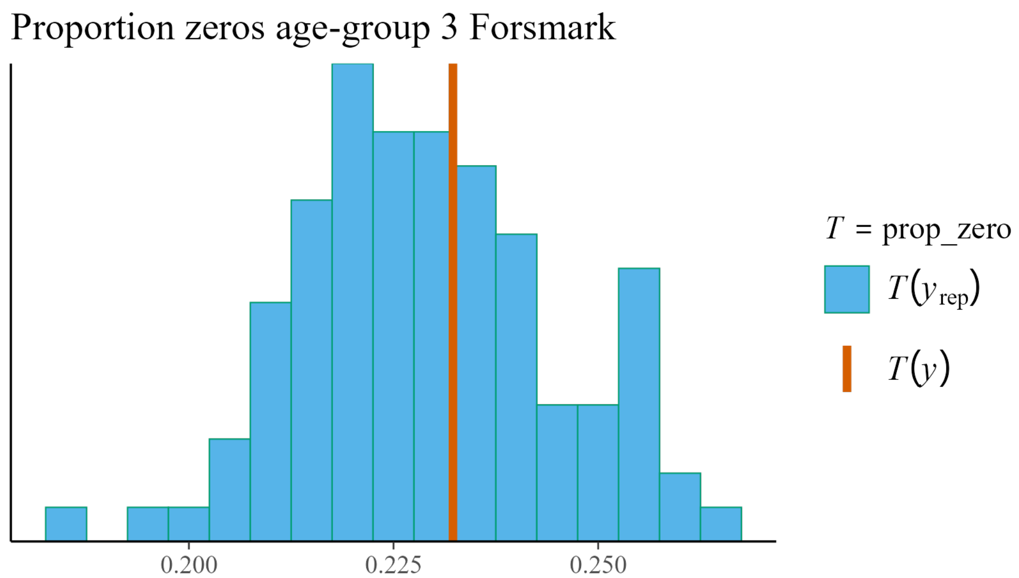
Proportion zeros age-group 3 Forsmark
0.200
0.225
0.250
T = prop_zero
T(y_rep)
T(y)

Proportion zeros age-group 4 Forsmark

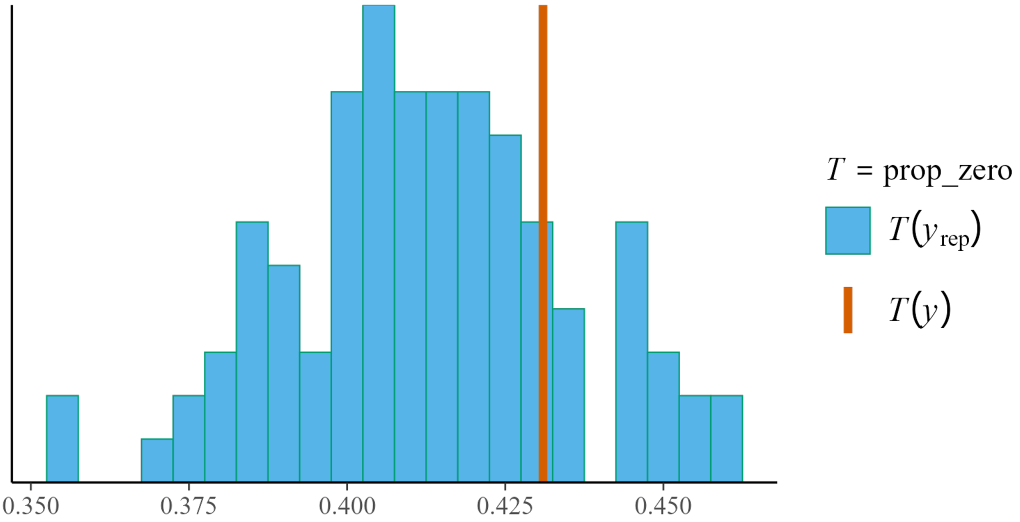

Proportion zeros age-group 5 Forsmark

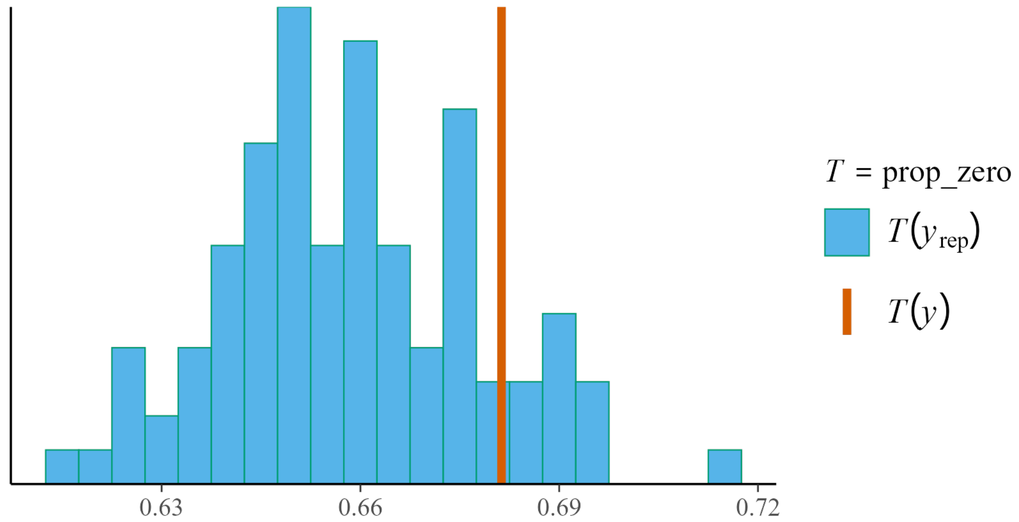

Proportion zeros age-group 6 Forsmark

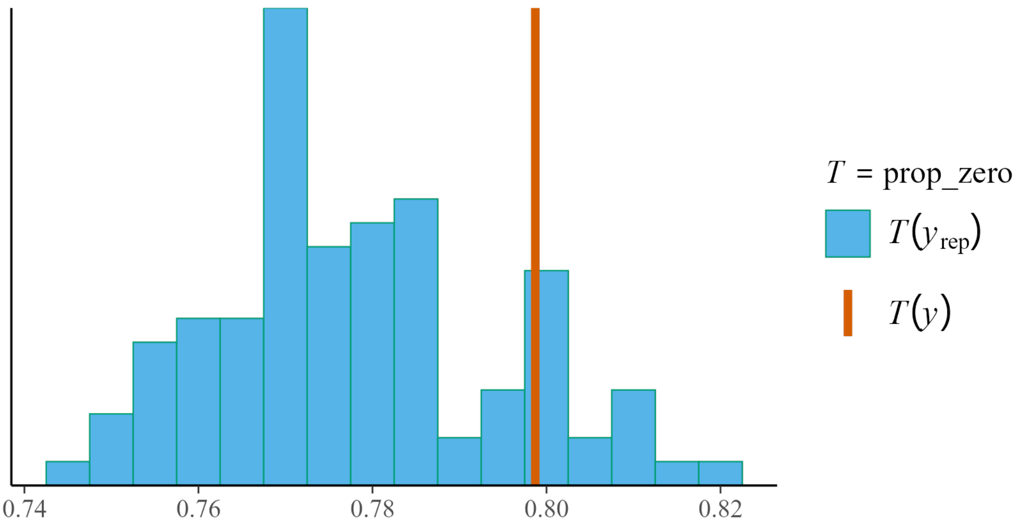

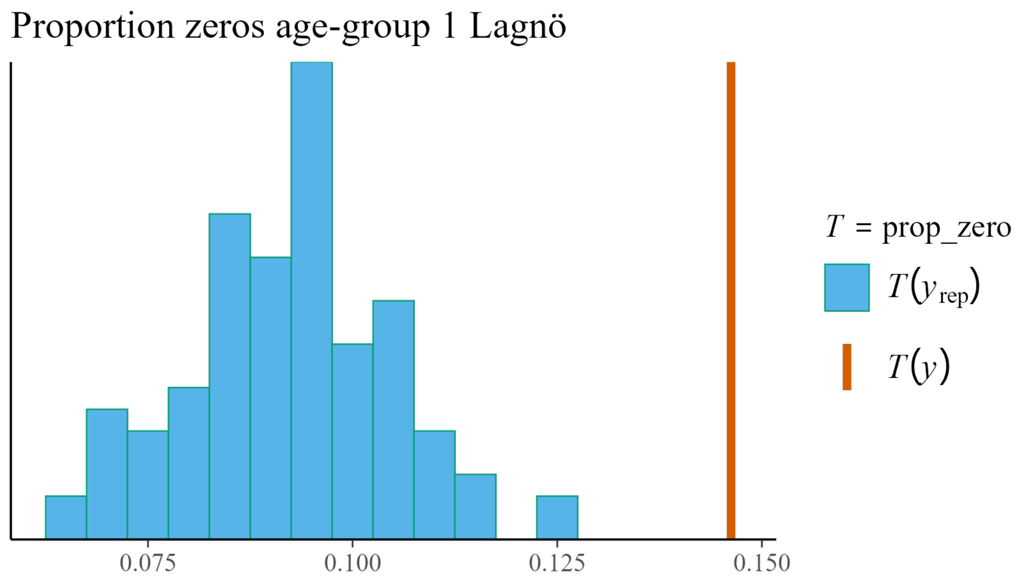
Proportion zeros age-group 1 Lagnö
0.075
0.100
0.125
0.150
T = prop_zero
T(y_rep)
T(y)

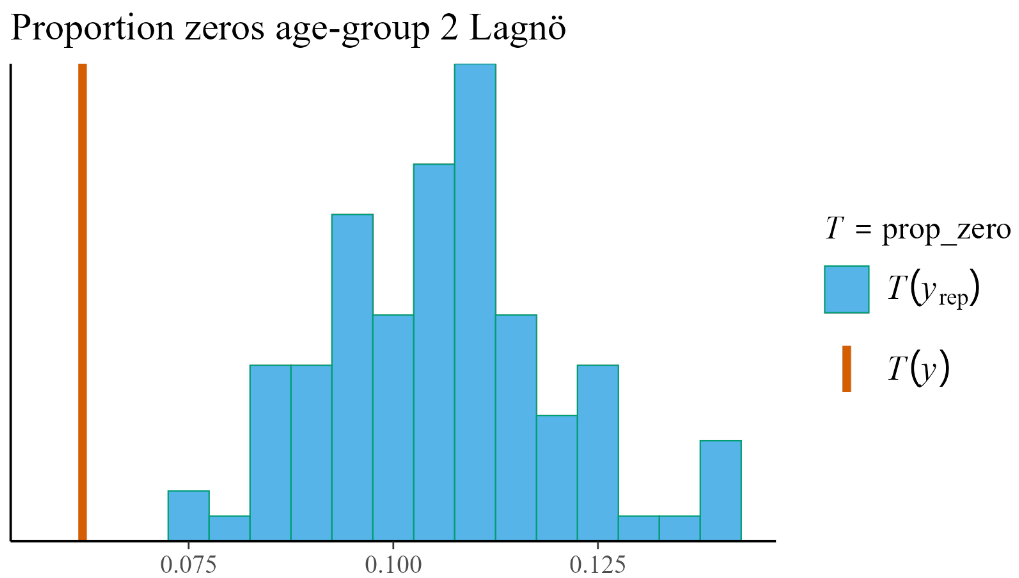
Proportion zeros age-group 2 Lagnö
0.075
0.100
0.125
T = prop_zero
T(y_rep)
T(y)

Proportion zeros age-group 3 Lagnö

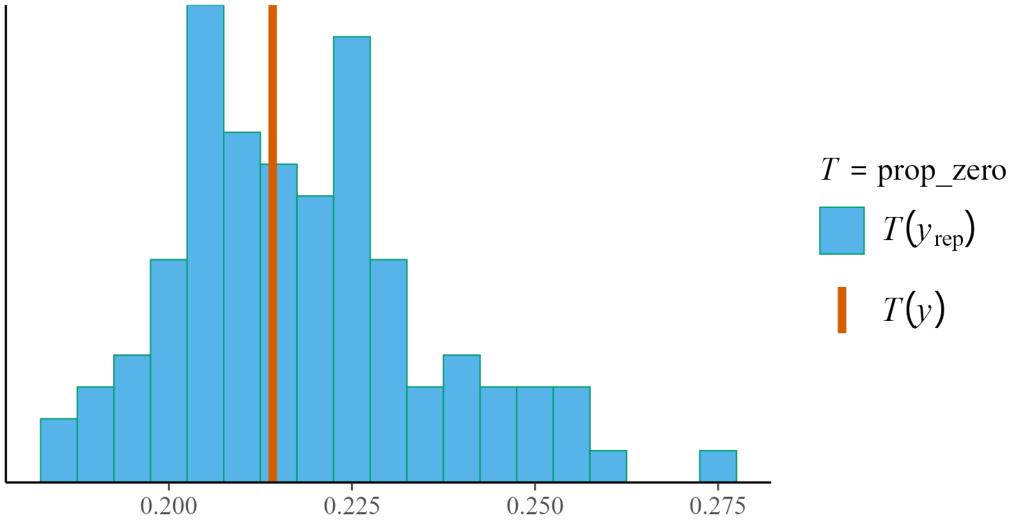

Proportion zeros age-group 4 Lagnö

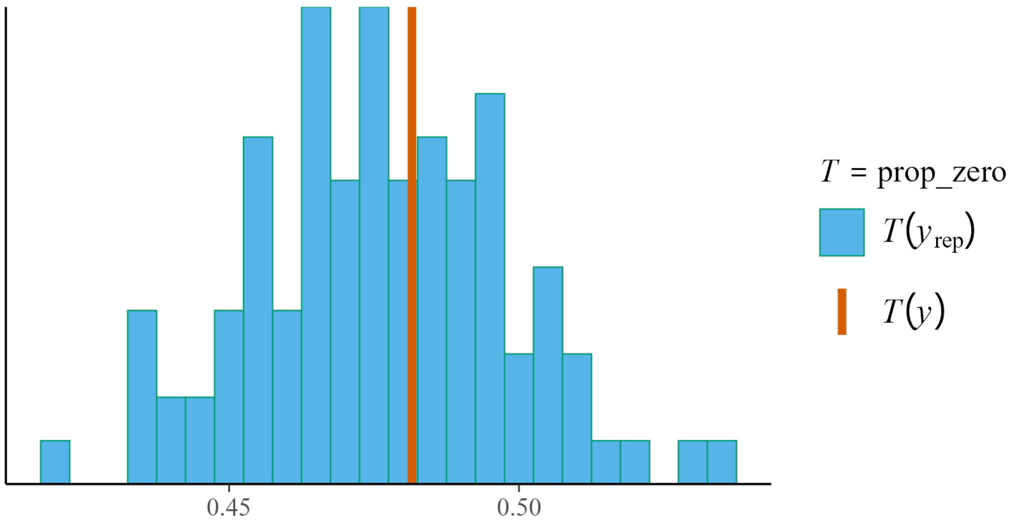

Proportion zeros age-group 5 Lagnö

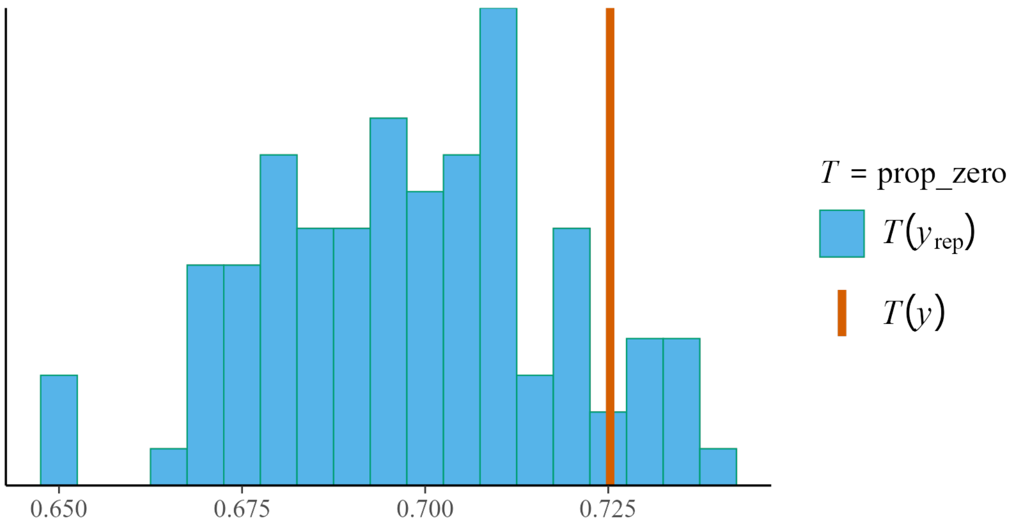

Proportion zeros age-group 1 Asköfjärden

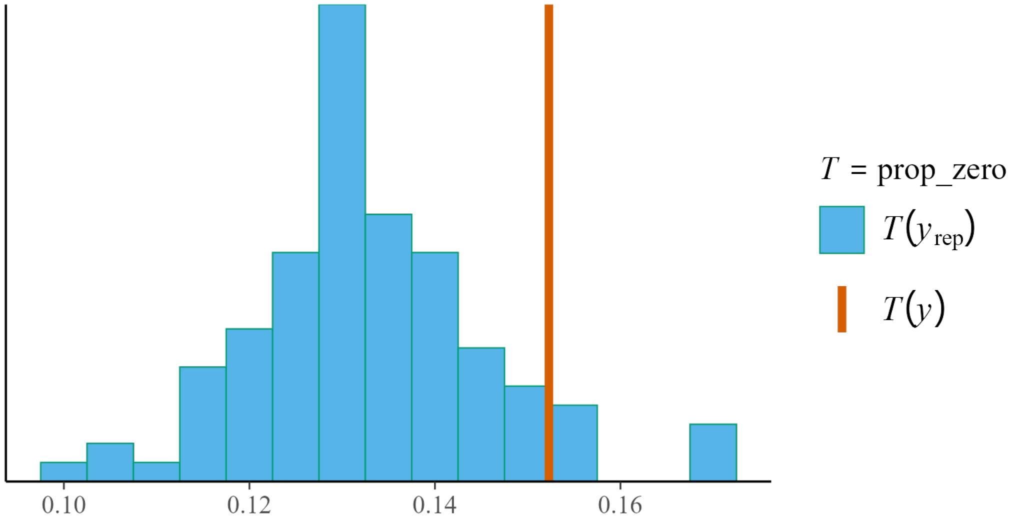

Proportion zeros age-group 2 Asköfjärden

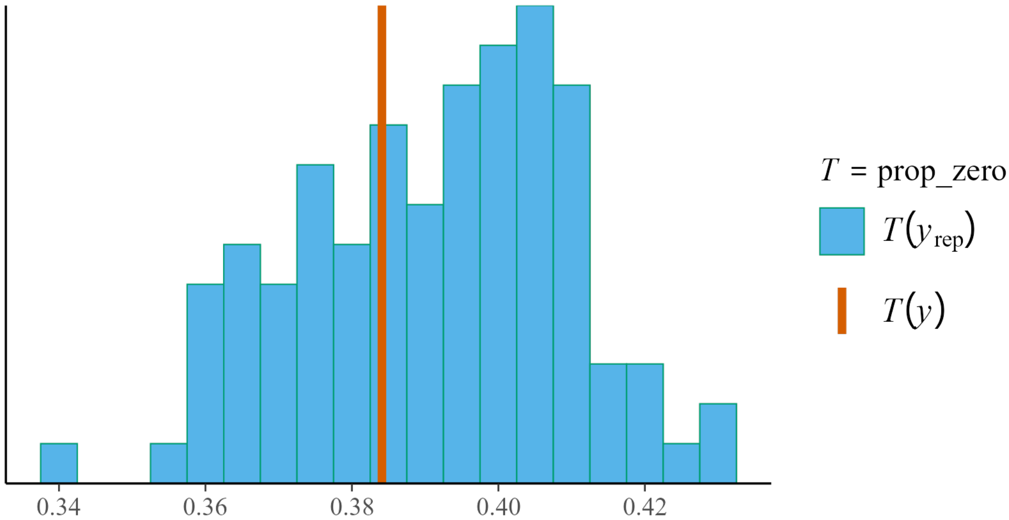

Proportion zeros age-group 3 Asköfjärden

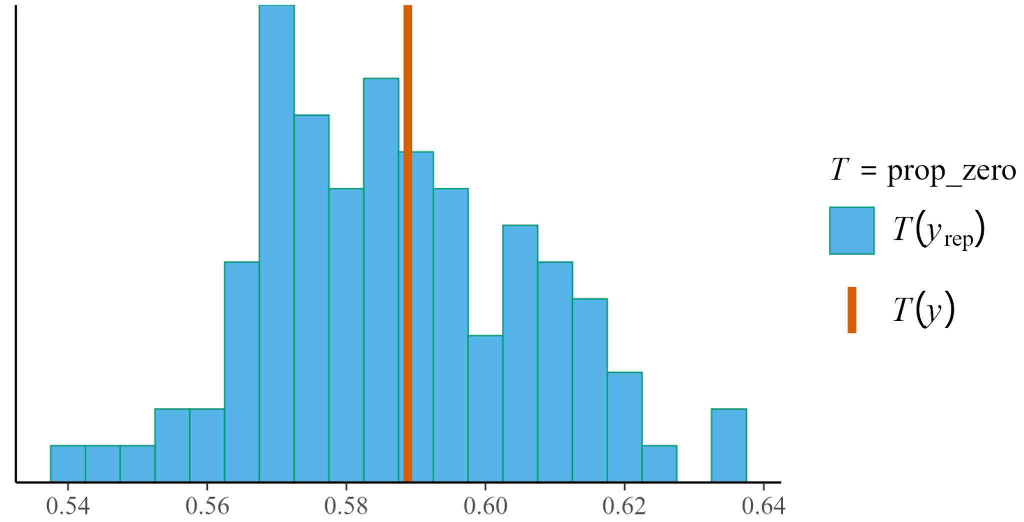

Proportion zeros age-group 4 Asköfjärden

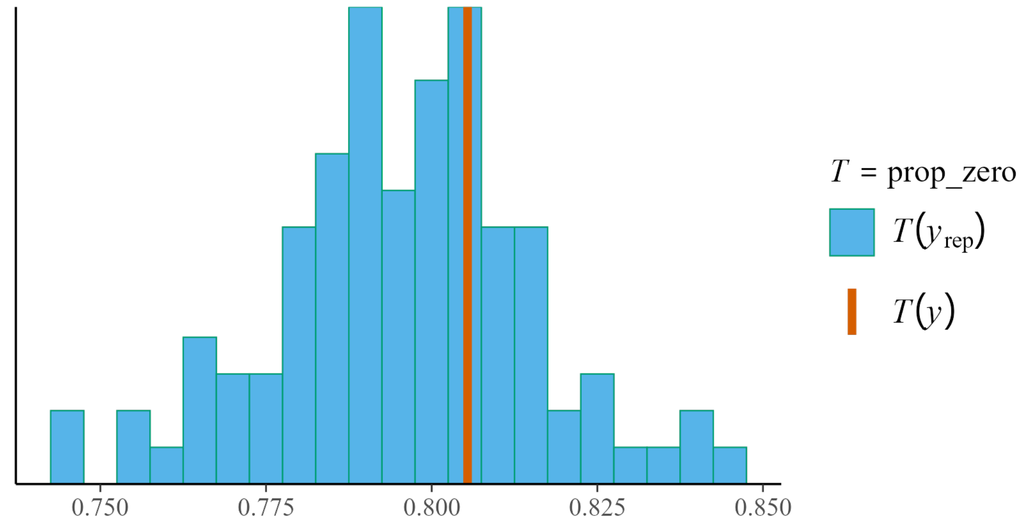

Proportion zeros age-group 1 Kvädöfjärden

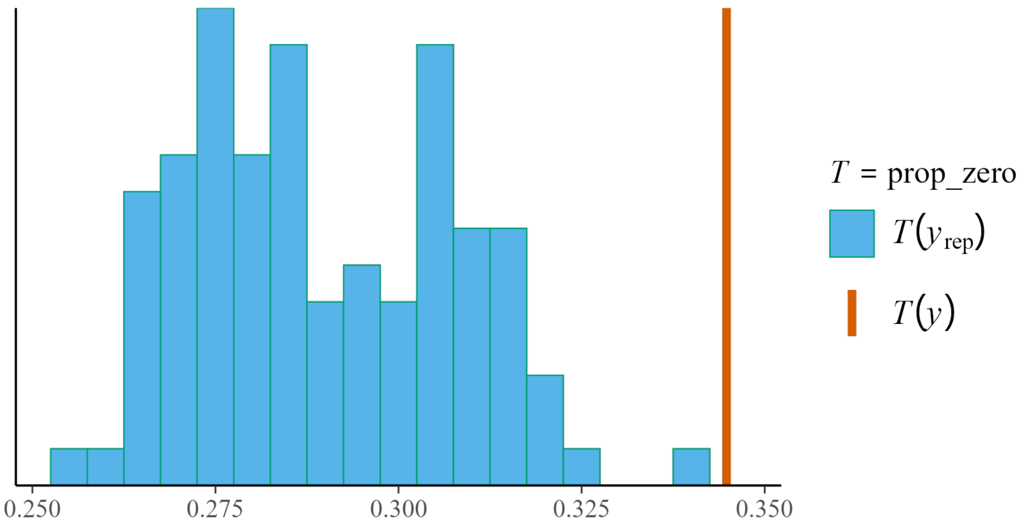

Proportion zeros age-group 2 Kvädöfjärden

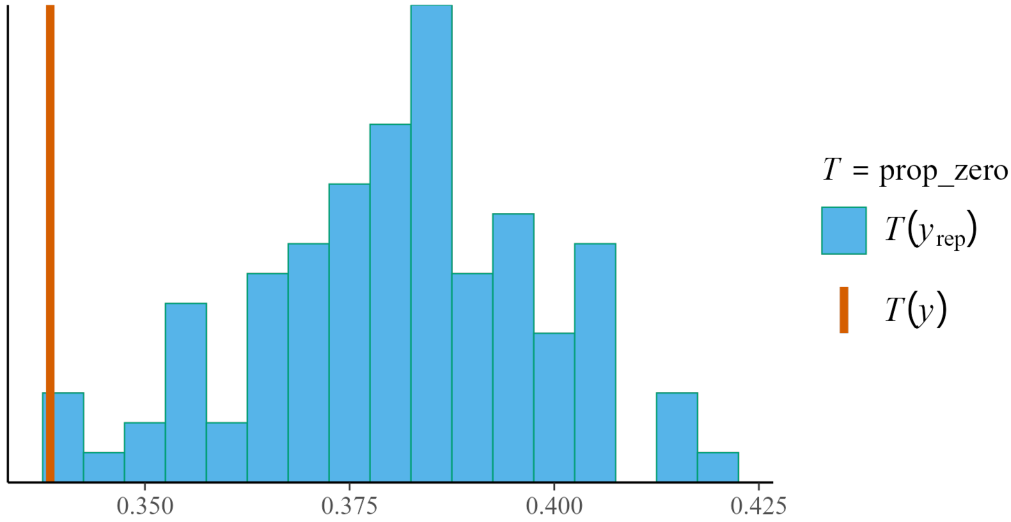

Proportion zeros age-group 3 Kvädöfjärden

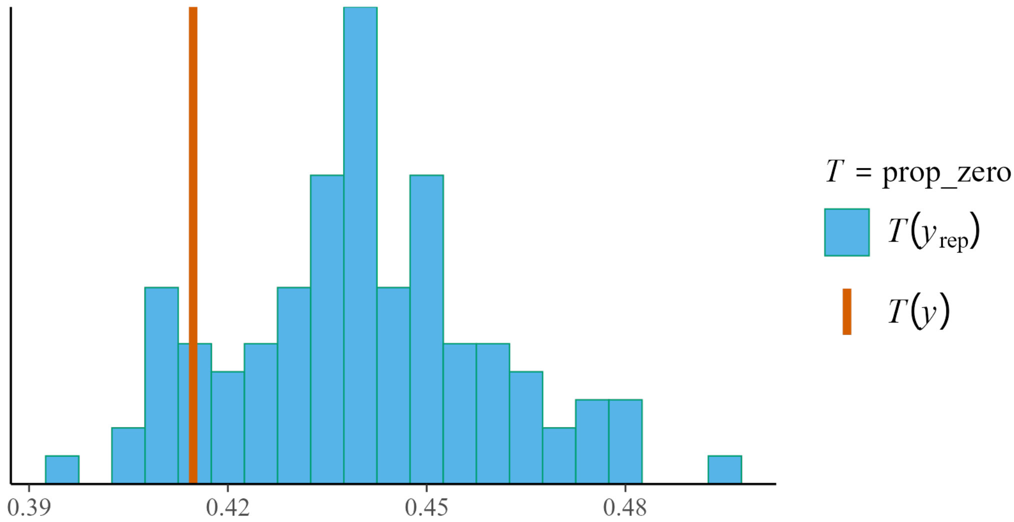

Proportion zeros age-group 4 Kvädöfjärden

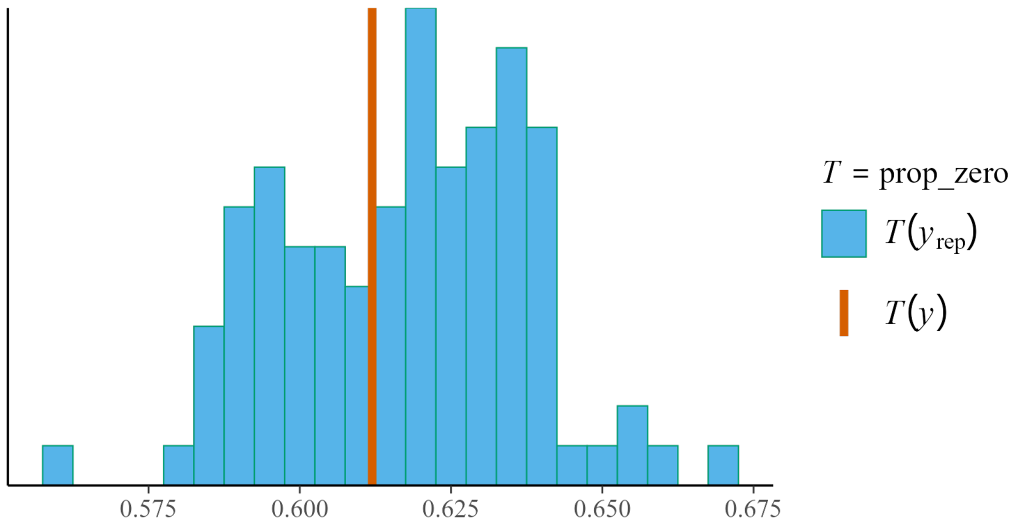

Proportion zeros age-group 5 Kvädöfjärden

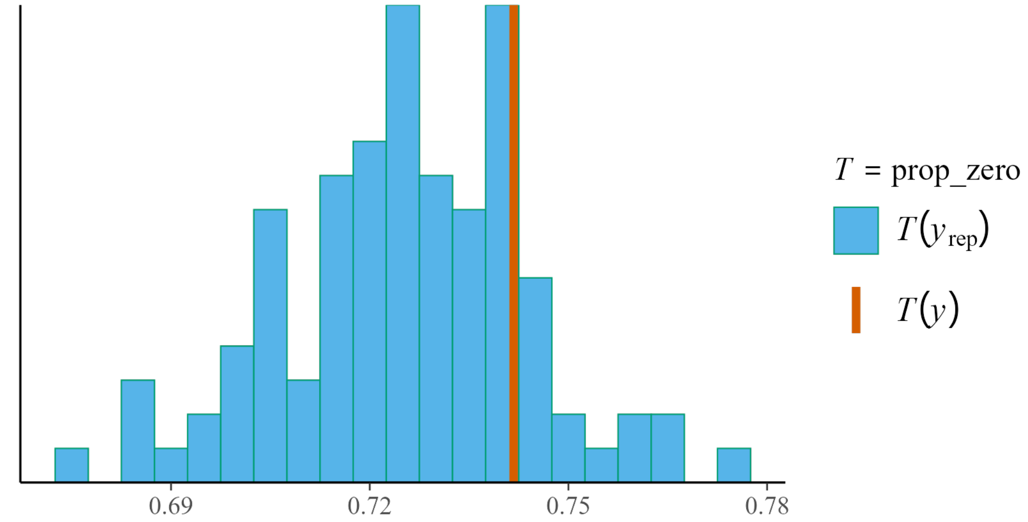

Proportion zeros age-group 6 Kvädöfjärden

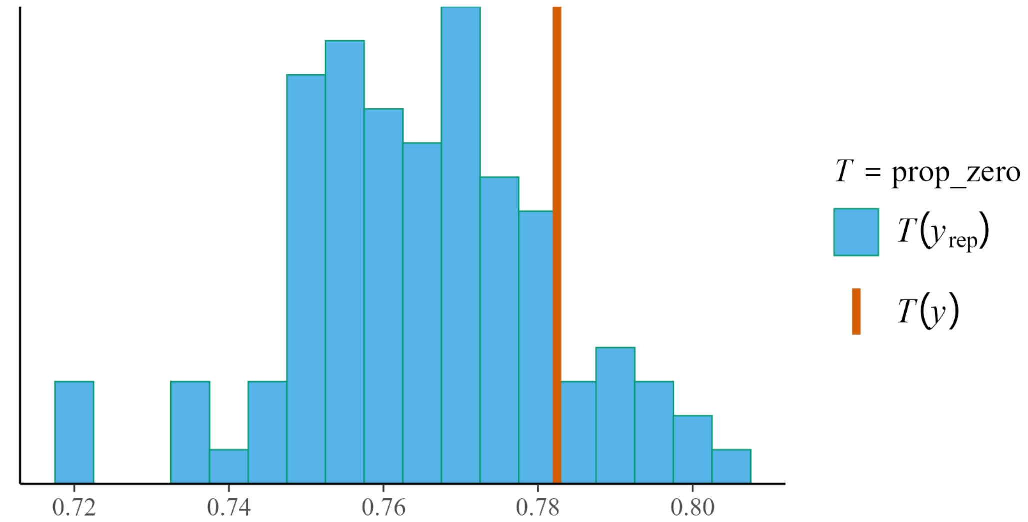

Proportion zeros age-group 1 Torhamn

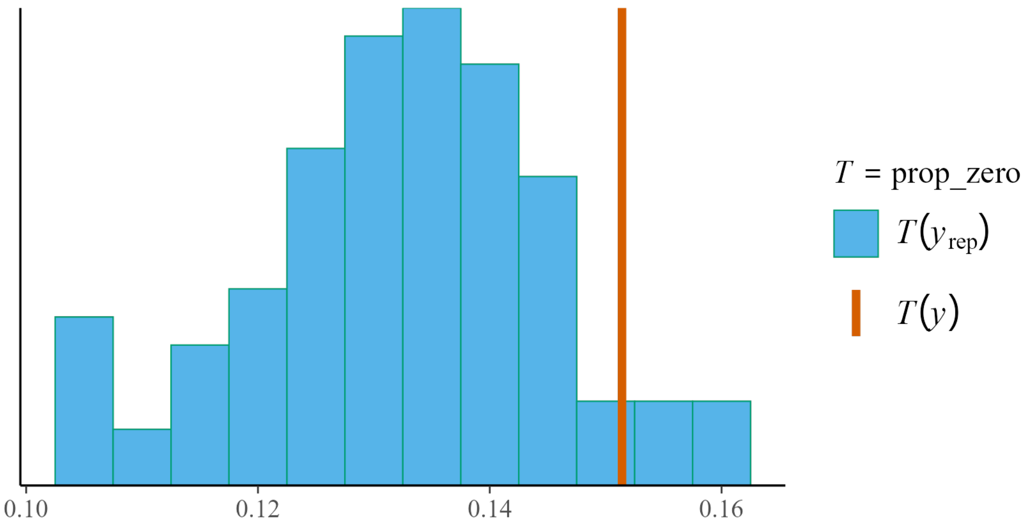

Proportion zeros age-group 2 Torhamn

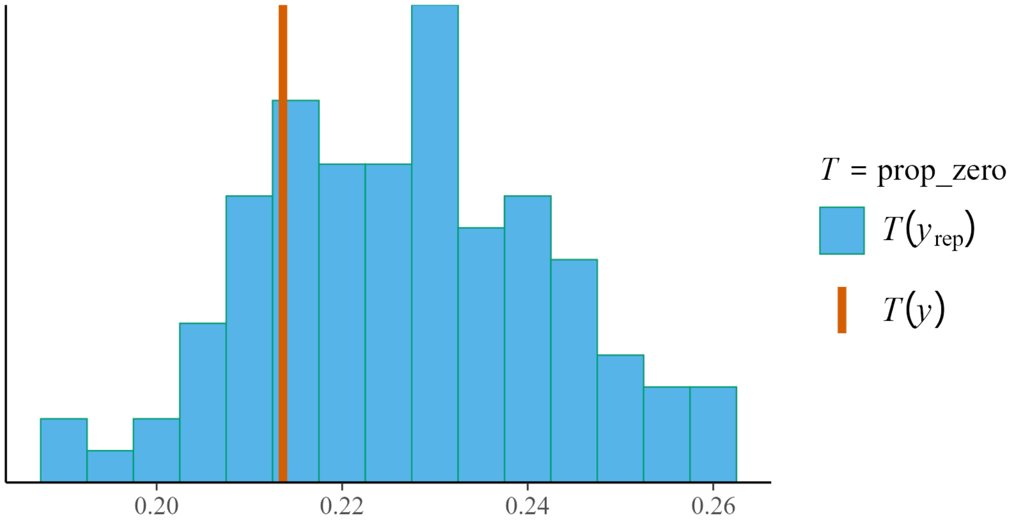

Proportion zeros age-group 3 Torhamn

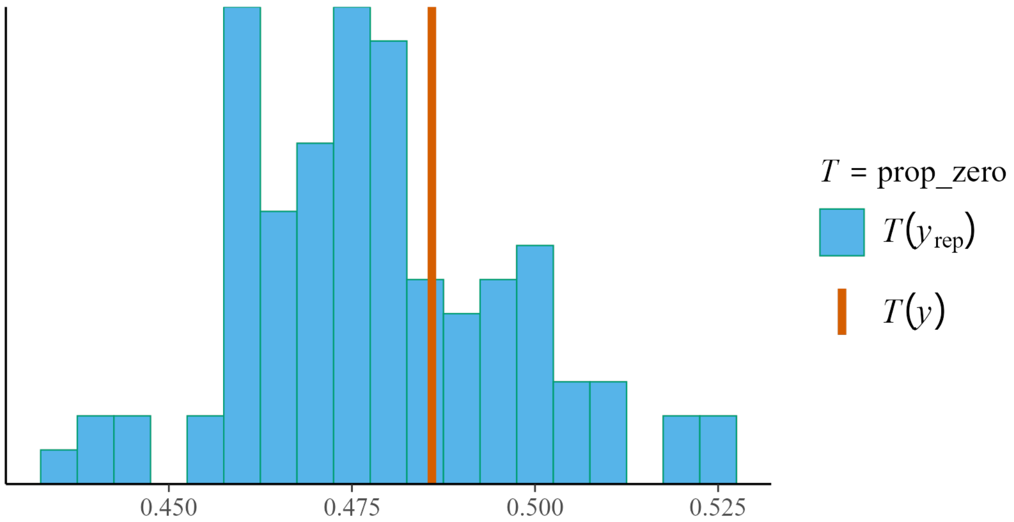

Appendix 4 – Age-class specific abundance

This appendix shows plots of the expected number of individuals, of age a year t, caught per gillnet-night ($\widehat{N}_{a,t}$). Light blue lines show posterior medians and ribbons display 90% credibility intervals. Black dots represent the mean number of individuals of age a caught per net night for a given year.

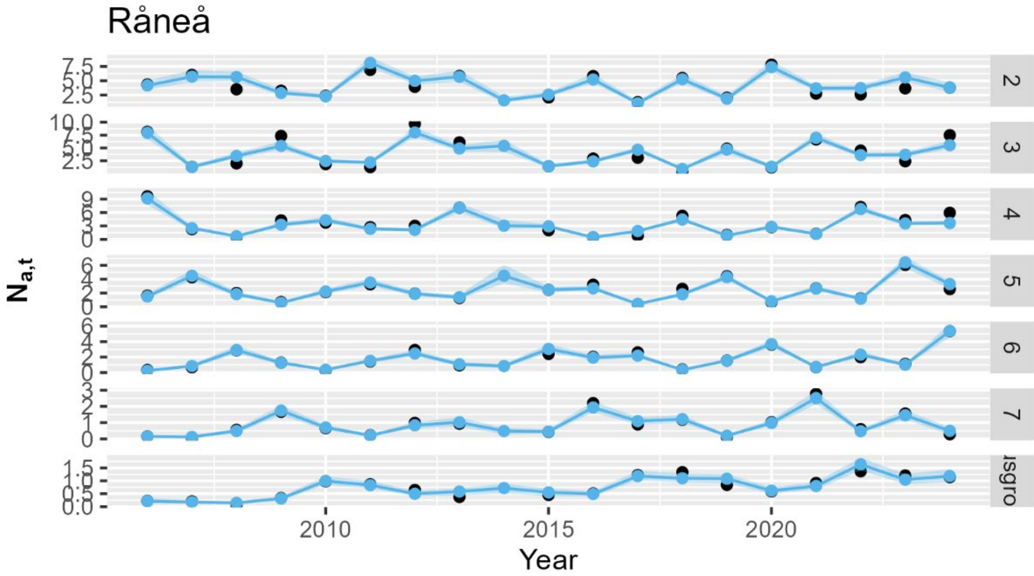
Råneå
$N_{a,t}$
Year
2010
2015
2020
2
3
4
5
6
7

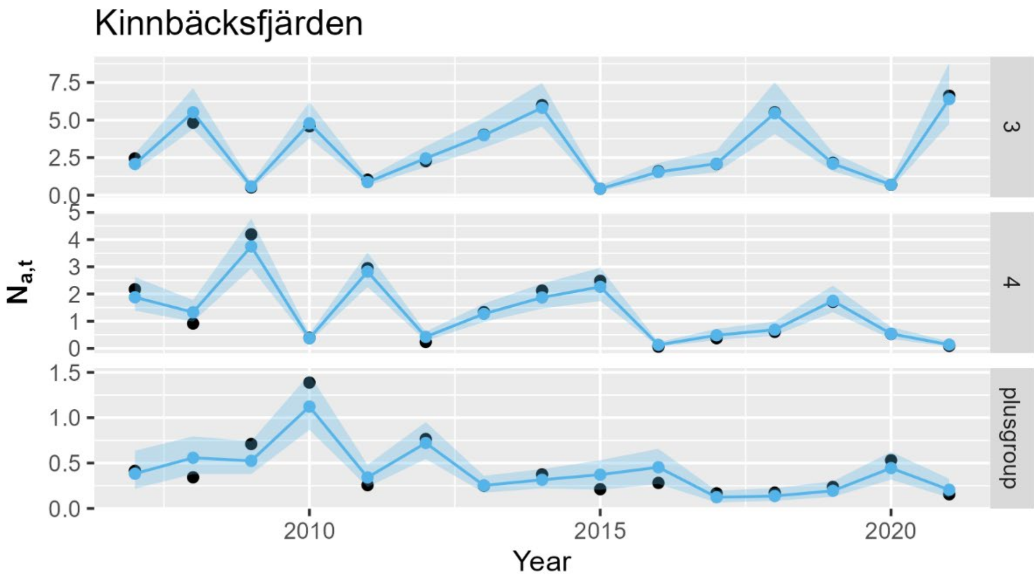
Kinnbäcksfjärden
$N_{a,t}$
Year
2010
2015
2020
3
4
plusgroup

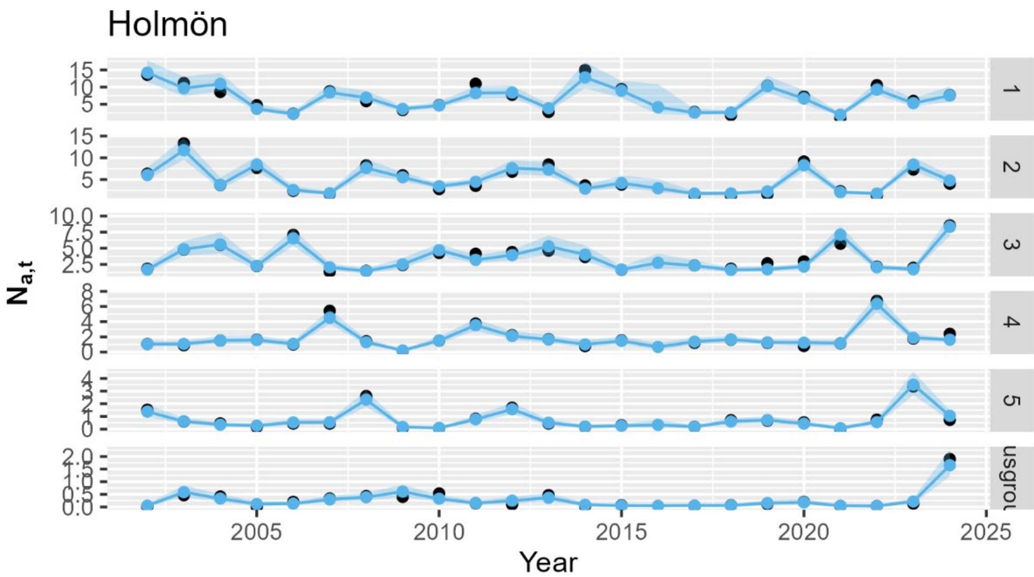
Holmön
$N_{a,t}$
Year
2005
2010
2015
2020
2025
1
2
3
4
5

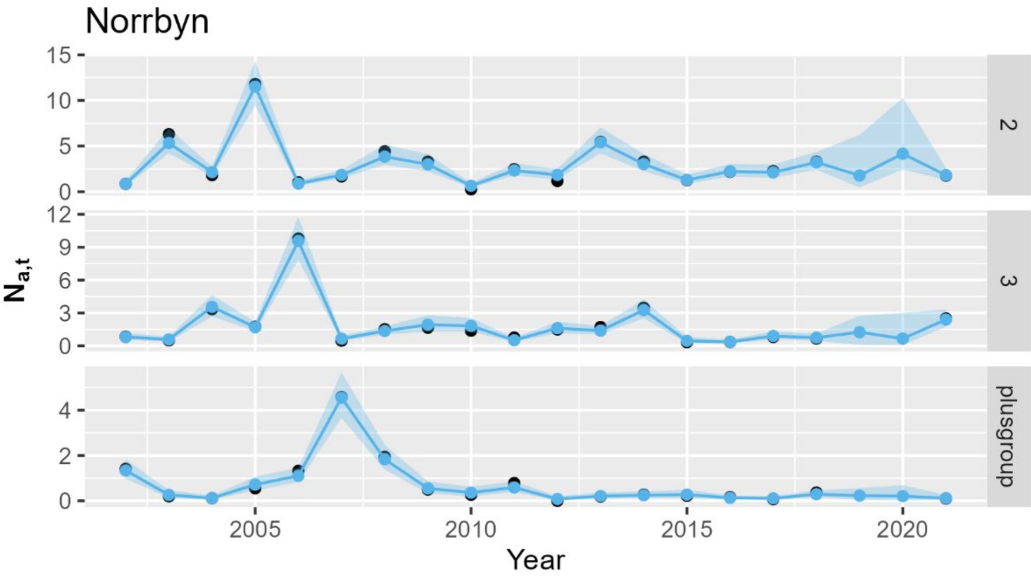
Norrbyn
$N_{a,t}$
2
3
plusgroup
2005
2010
2015
2020
Year

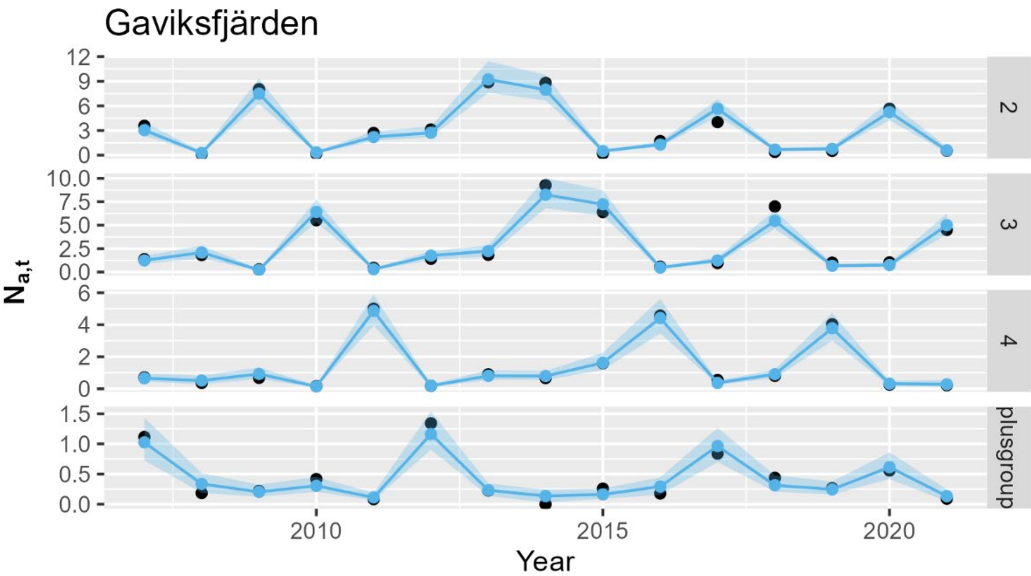
Gaviksfjärden
$N_{a,t}$
2
3
4
plusgroup
2010
2015
2020
Year

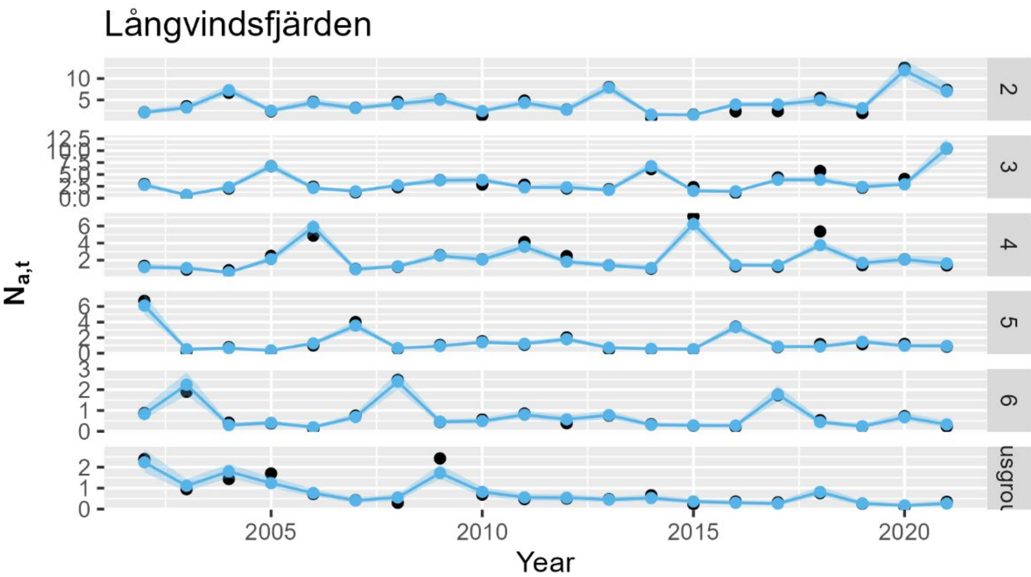
Långvindsfjärden
$N_{a,t}$
2
3
4
5
6
2005
2010
2015
2020
Year

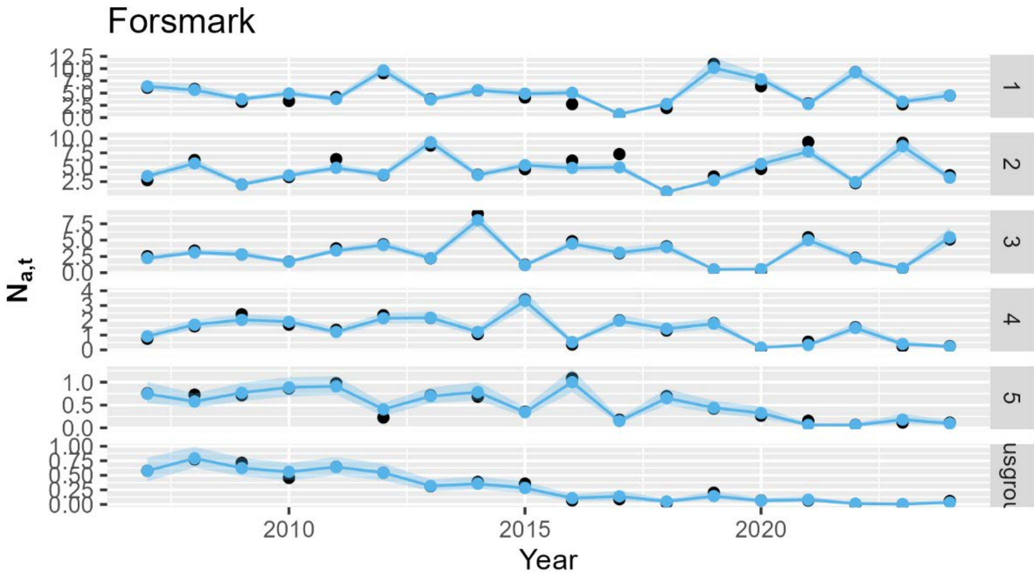
Forsmark
$N_{a,t}$
Year
2010
2015
2020
1
2
3
4
5

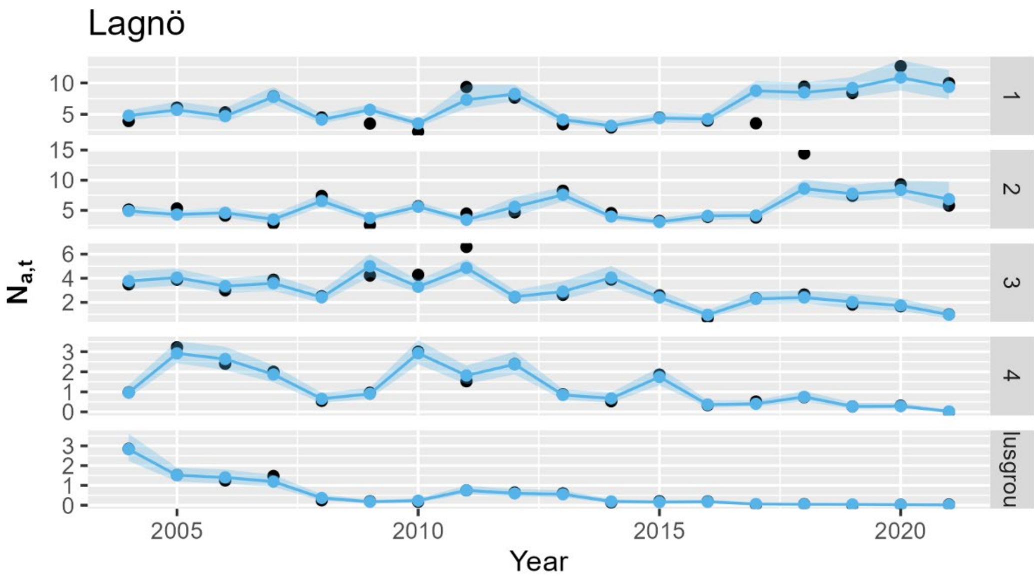
Lagnö
$N_{a,t}$
Year
2005
2010
2015
2020
1
2
3
4

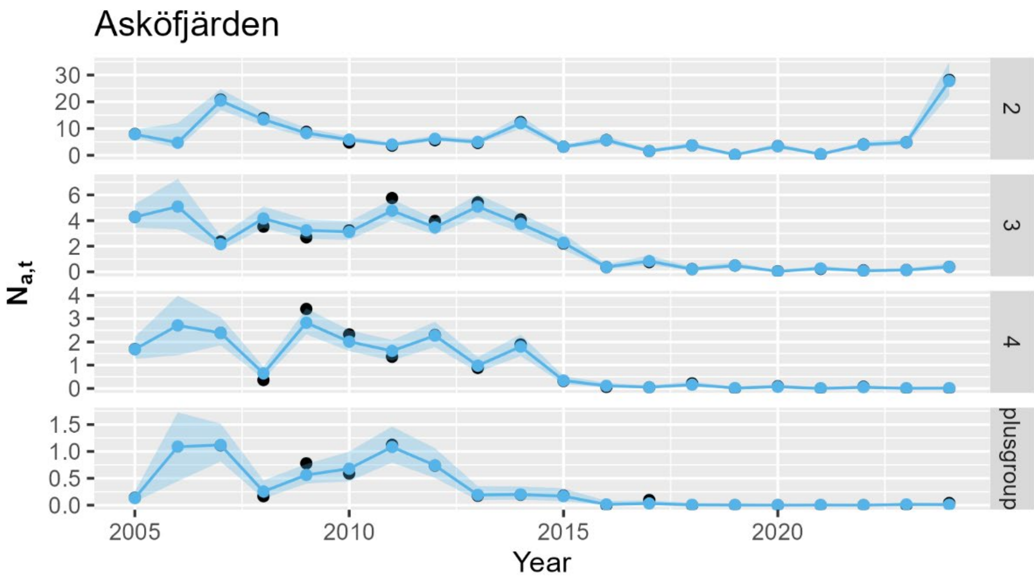
Asköfjärden
$N_{a,t}$
Year
2005
2010
2015
2020
2
3
4
plusgroup

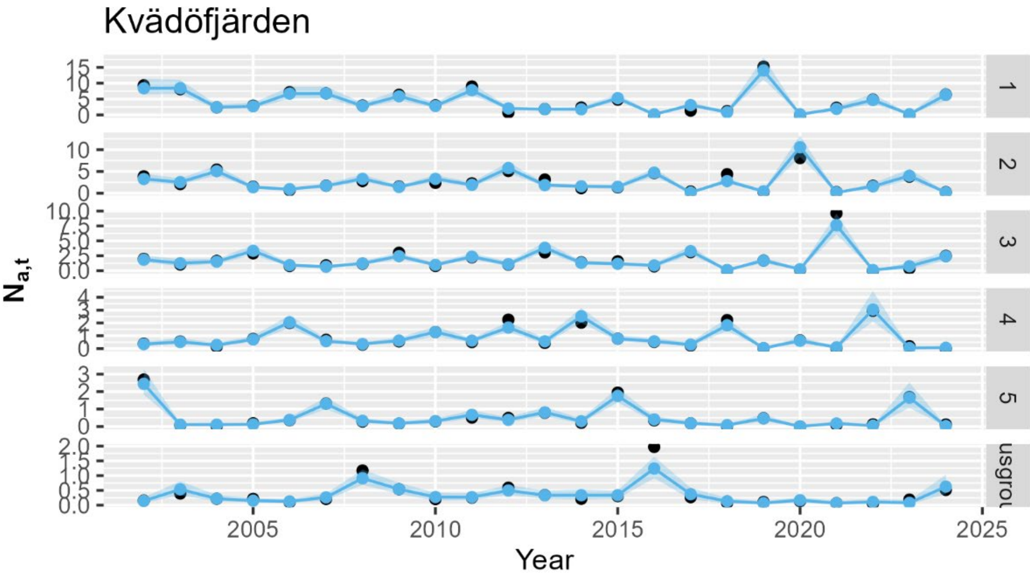
Kvädöfjärden
$N_{a,t}$
1
2
3
4
5
Year
2005
2010
2015
2020
2025

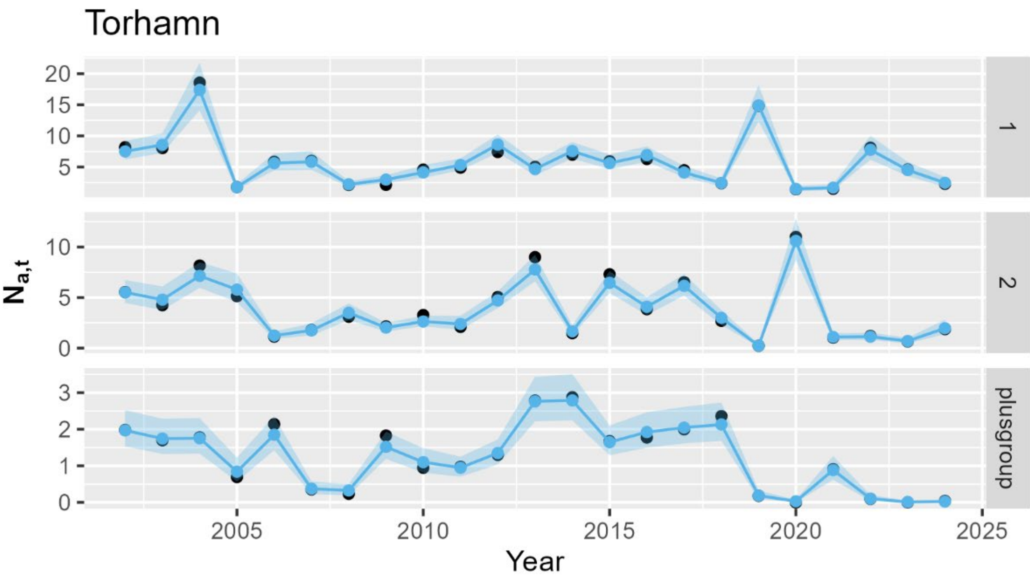
Torhamn
$N_{a,t}$
1
2
plusgroup
Year
2005
2010
2015
2020
2025

Appendix 5 – Retrospective pattern in estimates of age-class specific total mortality ($Z_{a,t}$)

This appendix shows visual retrospective analyses of age-class specific mortality rates (Eq. 4). Peels refer to the number of data points removed from the full data set (Peel0). The titel of each subpanel is the index of the age-class.

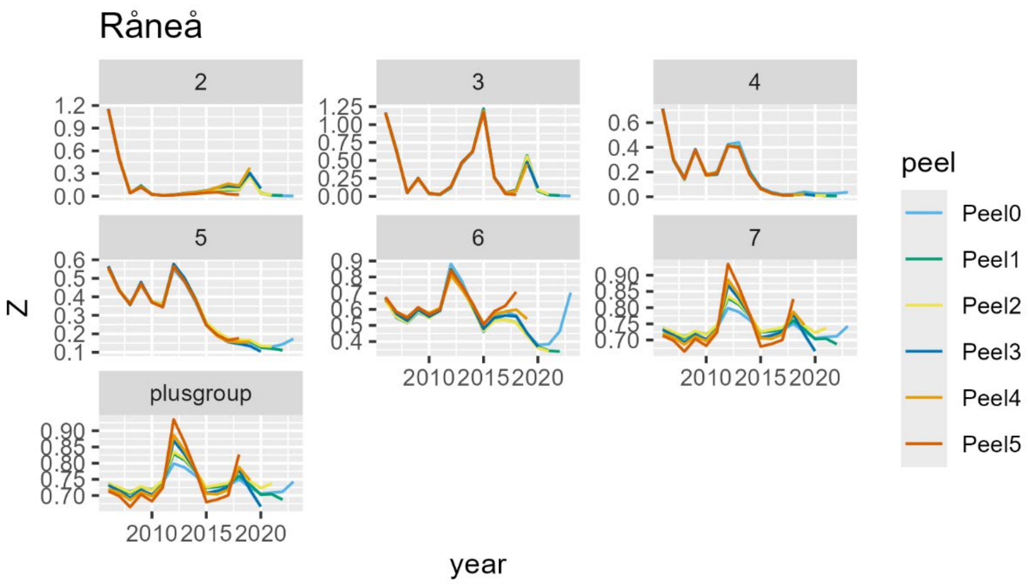
Råneå
2
3
4
5
6
7
plusgroup
Z
year
peel
Peel0
Peel1
Peel2
Peel3
Peel4
Peel5

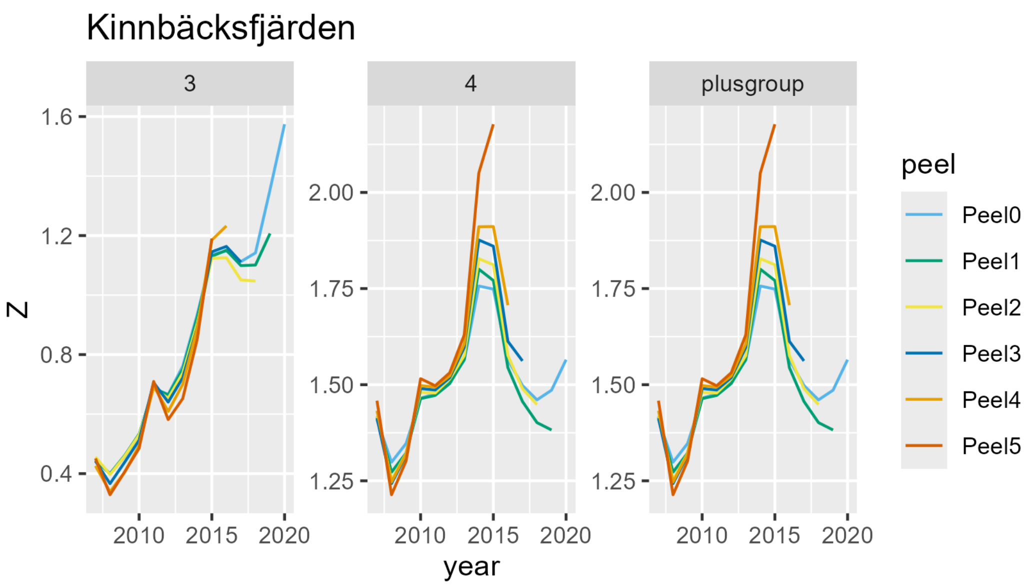
Kinnbäcksfjärden
3
4
plusgroup
Z
year
peel
Peel0
Peel1
Peel2
Peel3
Peel4
Peel5

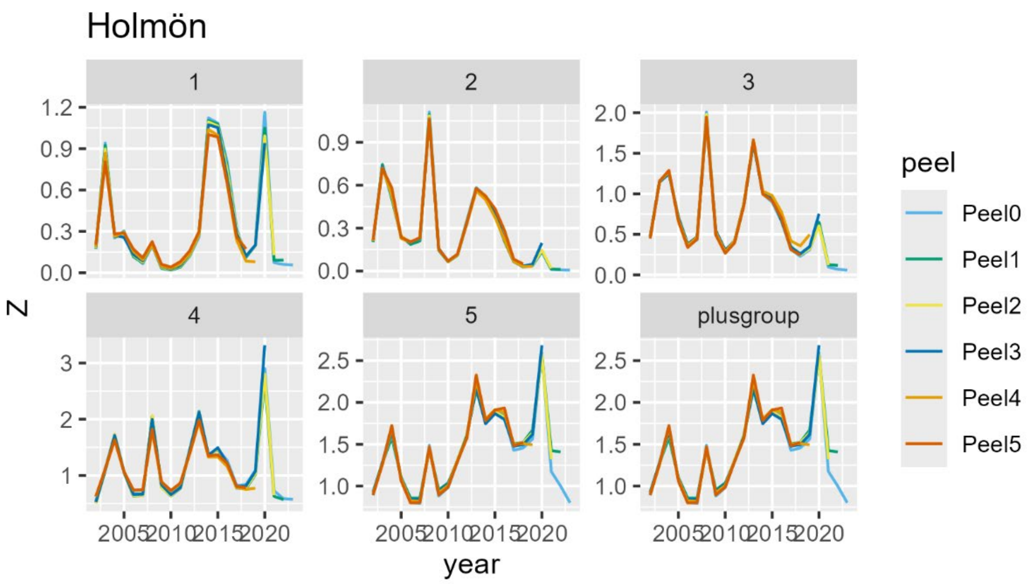
Holmön
1
2
3
4
5
plusgroup
Z
year
2005
2010
2015
2020
peel
Peel0
Peel1
Peel2
Peel3
Peel4
Peel5

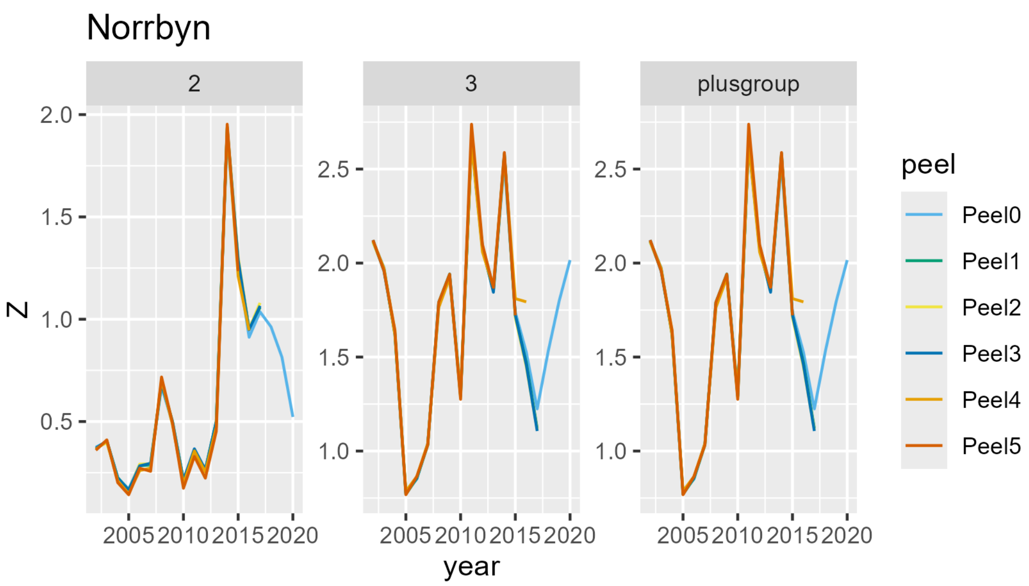
Norrbyn
2
3
plusgroup
Z
year
2005
2010
2015
2020
peel
Peel0
Peel1
Peel2
Peel3
Peel4
Peel5

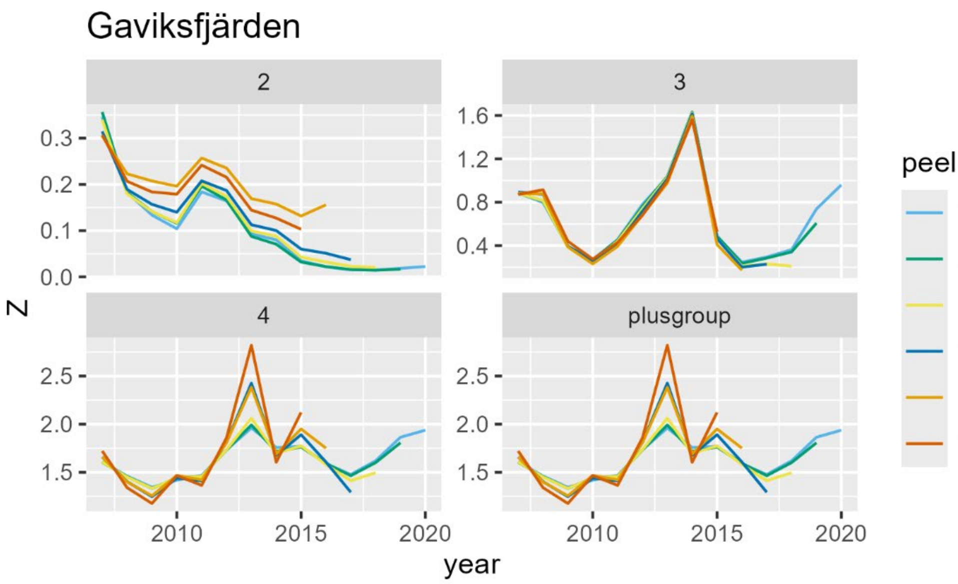
Gaviksfjärden
2
3
4
plusgroup
Z
year
peel
Peel0
Peel1
Peel2
Peel3
Peel4
Peel5

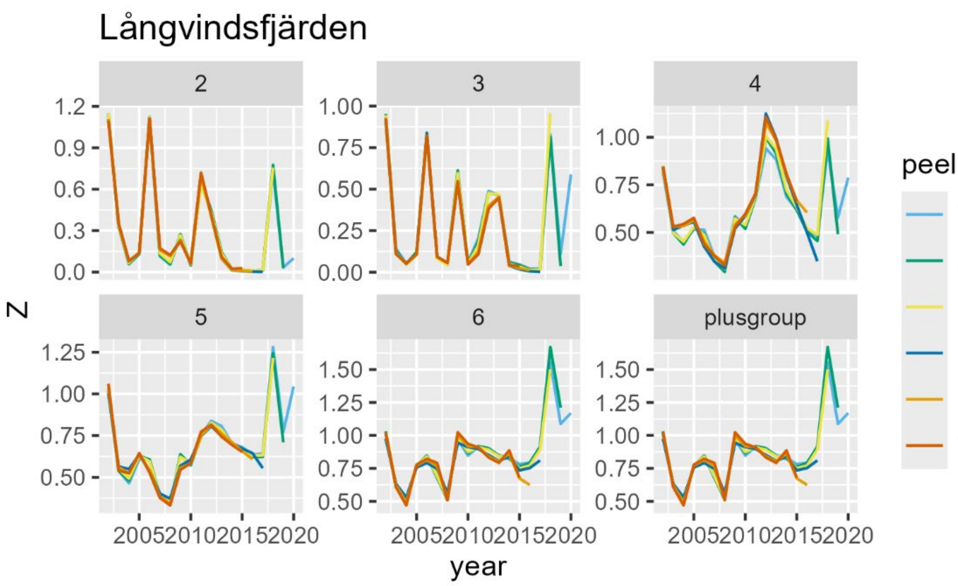
Långvindsfjärden
2
3
4
5
6
plusgroup
Z
year
peel
Peel0
Peel1
Peel2
Peel3
Peel4
Peel5

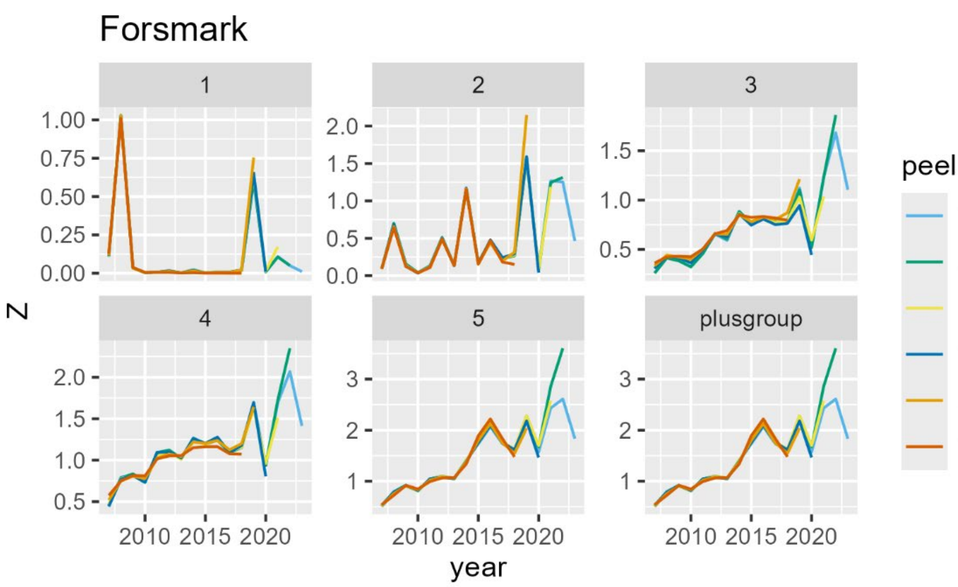
Forsmark
1
2
3
4
5
plusgroup
Z
year
peel
Peel0
Peel1
Peel2
Peel3
Peel4
Peel5

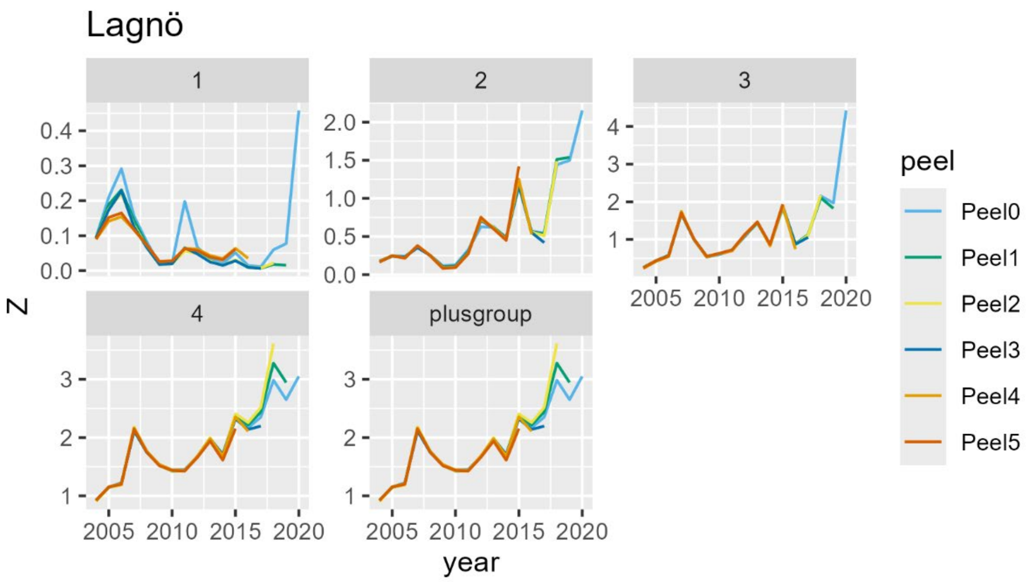
Lagnö
1
2
3
4
plusgroup
Z
year
peel
Peel0
Peel1
Peel2
Peel3
Peel4
Peel5

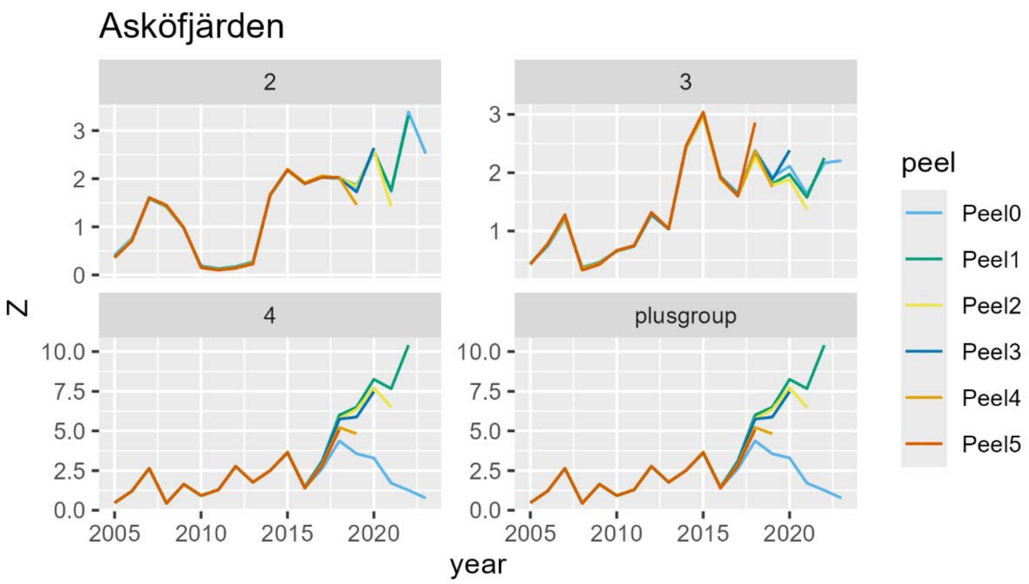
Asköfjärden
2
3
4
plusgroup
Z
year
peel
Peel0
Peel1
Peel2
Peel3
Peel4
Peel5

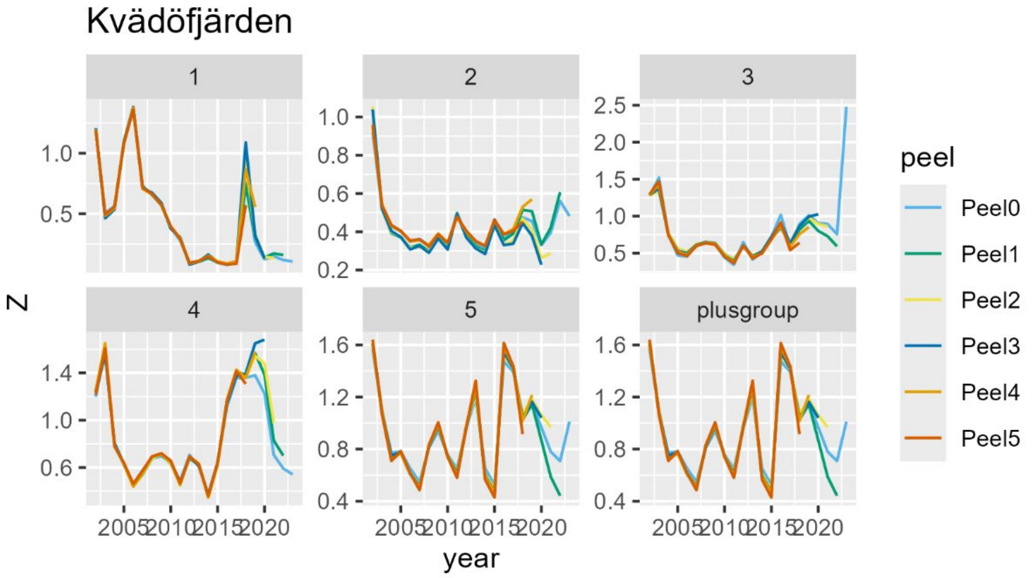
Kvädöfjärden
1
2
3
4
5
plusgroup
Z
year
2005
2010
2015
2020
peel
Peel0
Peel1
Peel2
Peel3
Peel4
Peel5

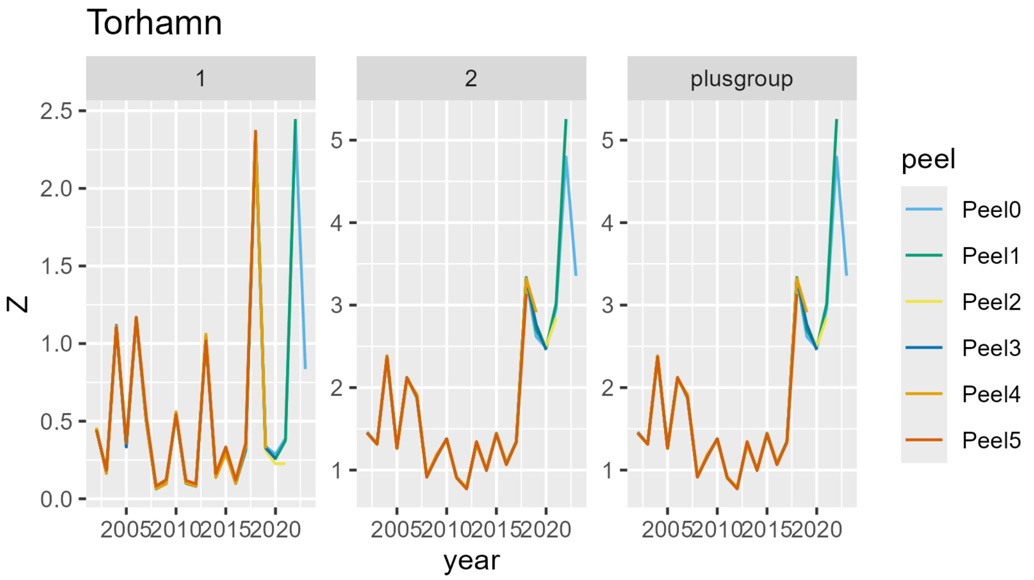
Torhamn
1
2
plusgroup
Z
year
2005
2010
2015
2020
peel
Peel0
Peel1
Peel2
Peel3
Peel4
Peel5

Appendix 6 – Retrospective pattern in estimates of age-class specific abundance ($N_{a,t}$)

This appendix shows retrospective patterns in estimates of age-class specific female abundance (Eq. 2). Peels refer to the number of data points removed from the full data set (Peel0). The title of each subpanel is the index of the age-class.

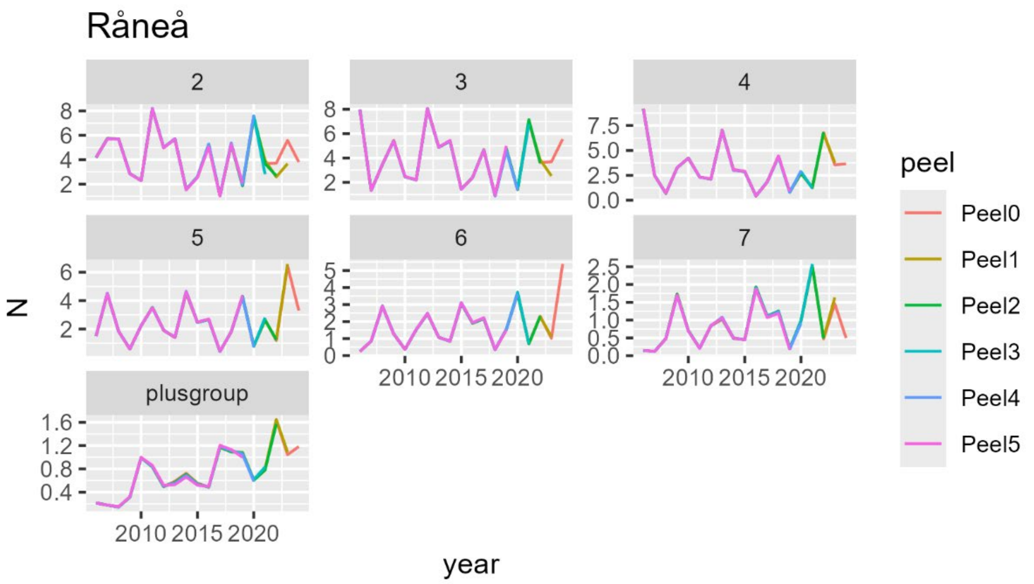
Råneå
2
3
4
5
6
7
plusgroup
N
year
peel
Peel0
Peel1
Peel2
Peel3
Peel4
Peel5

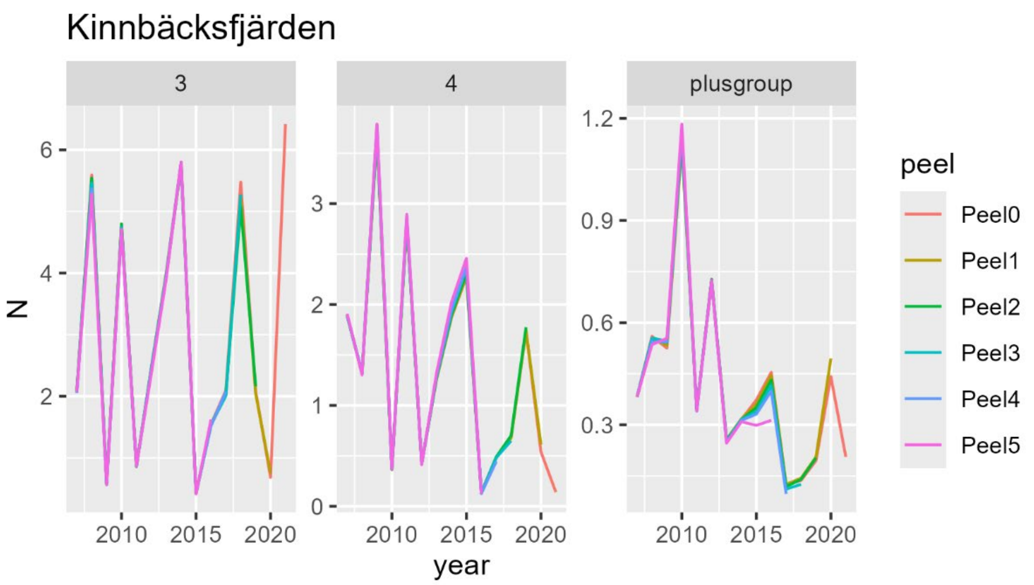
Kinnbäcksfjärden
3
4
plusgroup
N
year
peel
Peel0
Peel1
Peel2
Peel3
Peel4
Peel5

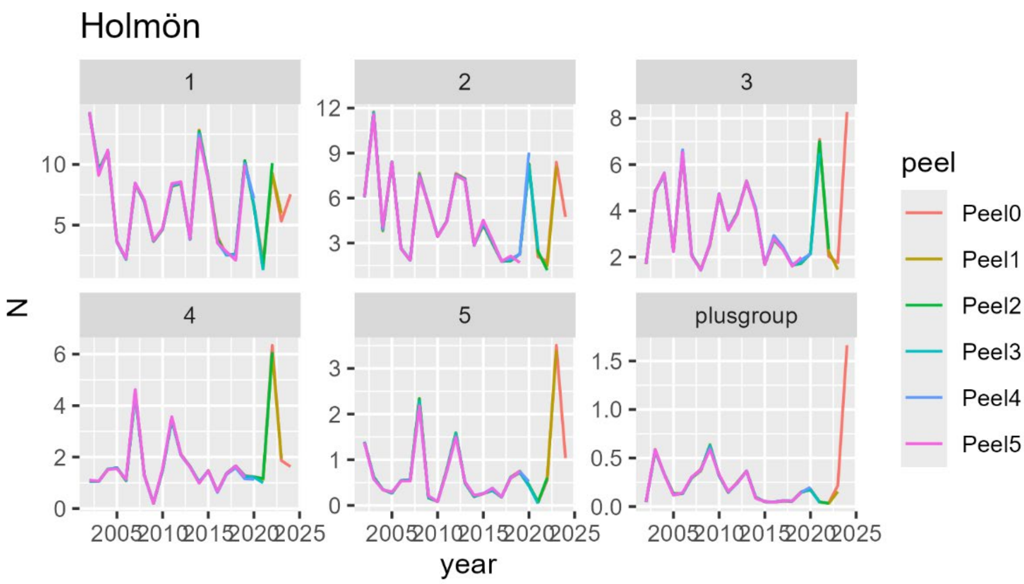
Holmön
1
2
3
4
5
plusgroup
N
year
peel
Peel0
Peel1
Peel2
Peel3
Peel4
Peel5

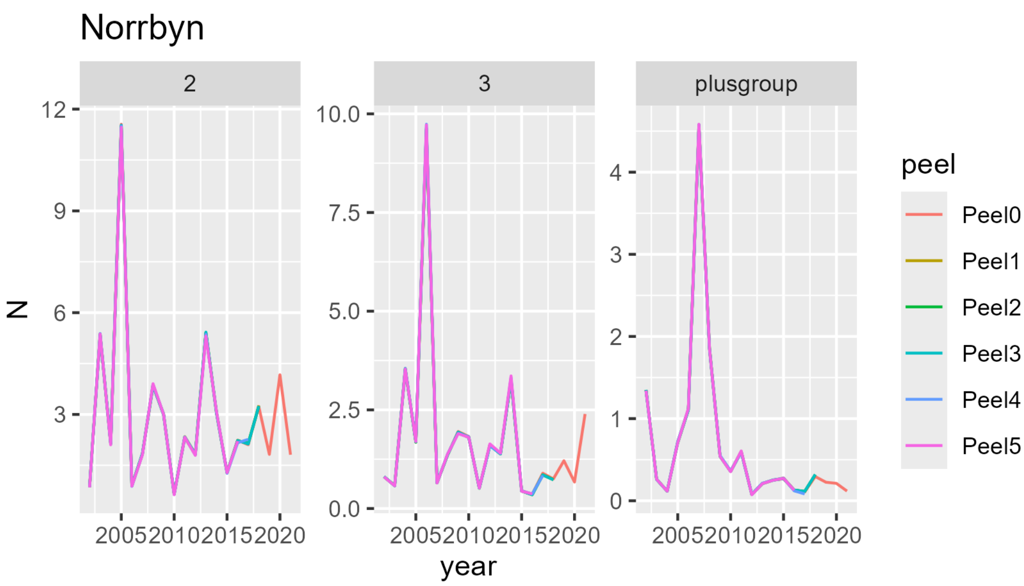
Norrbyn
2
3
plusgroup
N
year
peel
Peel0
Peel1
Peel2
Peel3
Peel4
Peel5

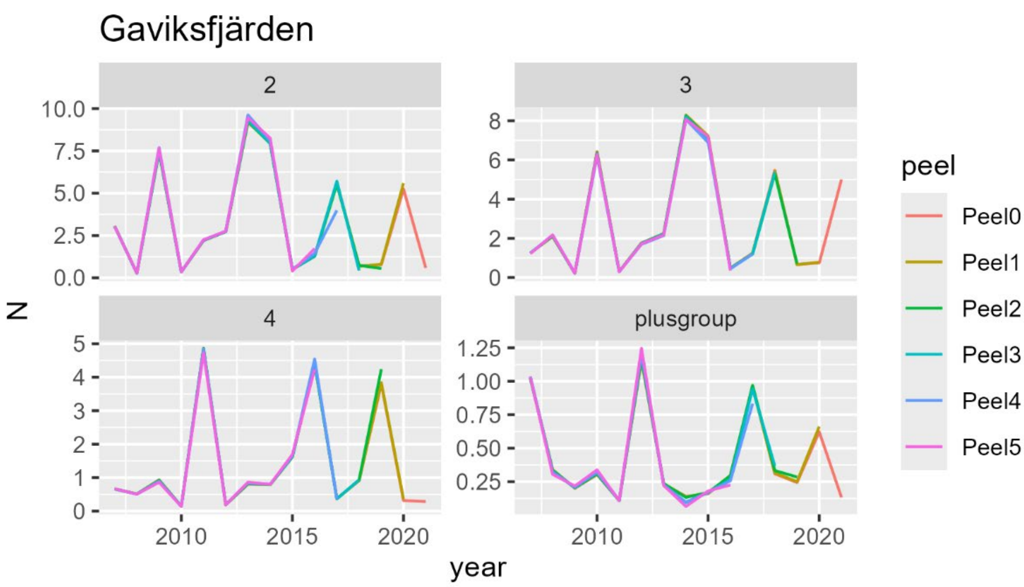
Gaviksfjärden
2
3
4
plusgroup
N
year
peel
Peel0
Peel1
Peel2
Peel3
Peel4
Peel5

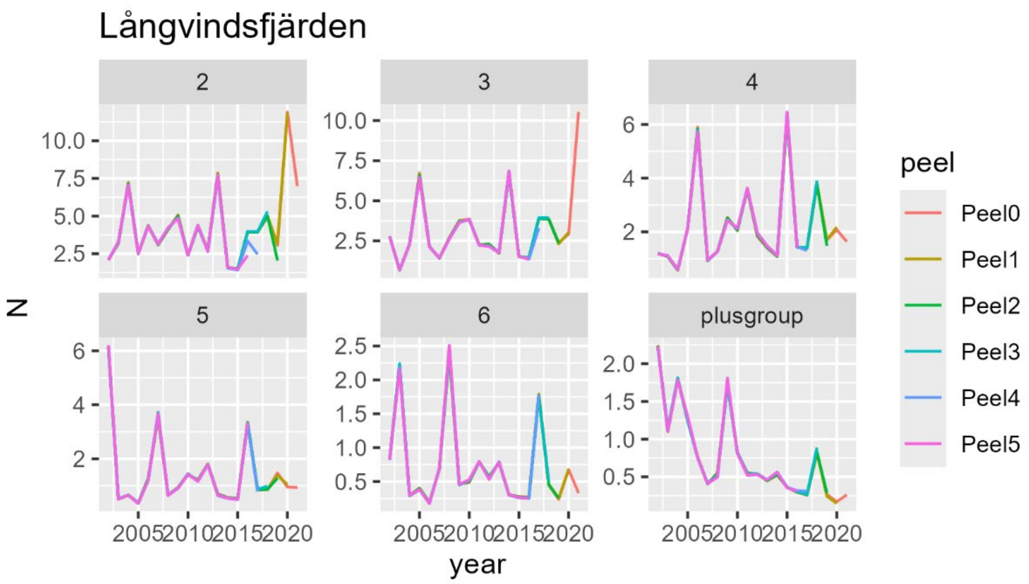
Långvindsfjärden
2
3
4
5
6
plusgroup
N
year
10.0
7.5
5.0
2.5
6
4
2
2.5
2.0
1.5
1.0
0.5
2005
2010
2015
2020
peel
Peel0
Peel1
Peel2
Peel3
Peel4
Peel5

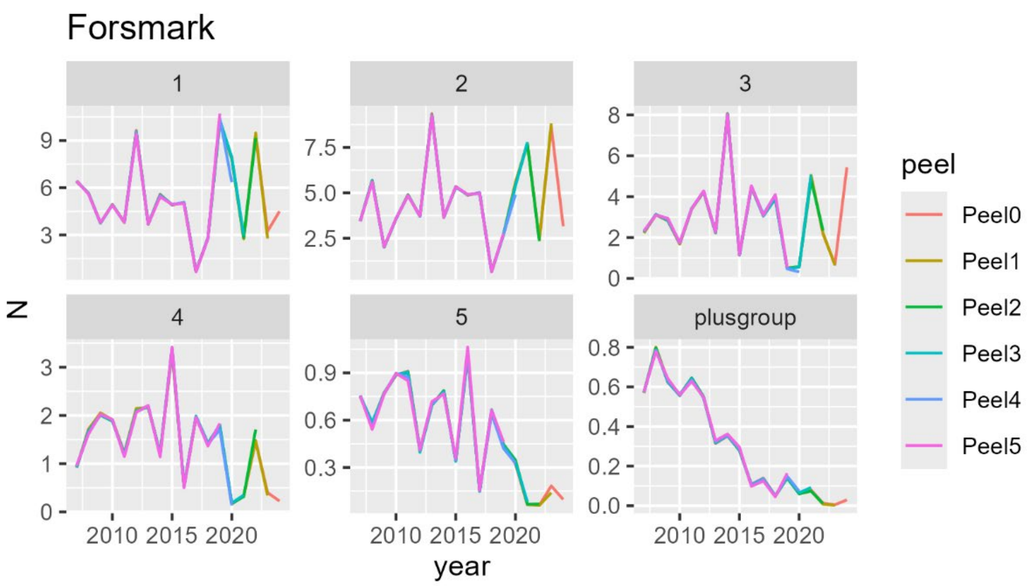
Forsmark
1
2
3
4
5
plusgroup
N
year
9
6
3
7.5
5.0
2.5
8
6
4
2
0
1
0.9
0.6
0.3
0.8
0.4
0.2
0.0
2010
2015
2020
peel
Peel0
Peel1
Peel2
Peel3
Peel4
Peel5

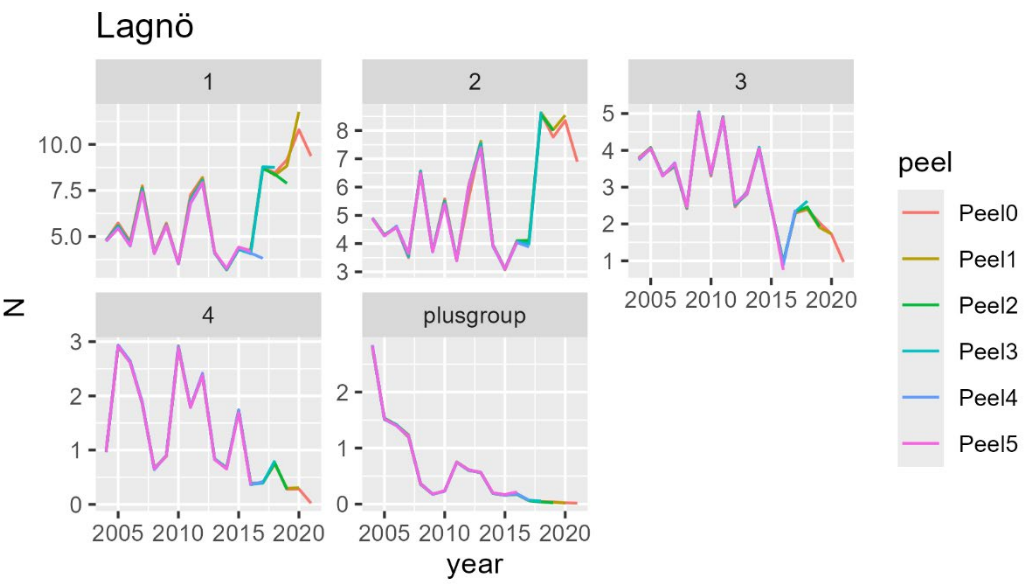
Lagnö
1
2
3
4
plusgroup
N
year
peel
Peel0
Peel1
Peel2
Peel3
Peel4
Peel5

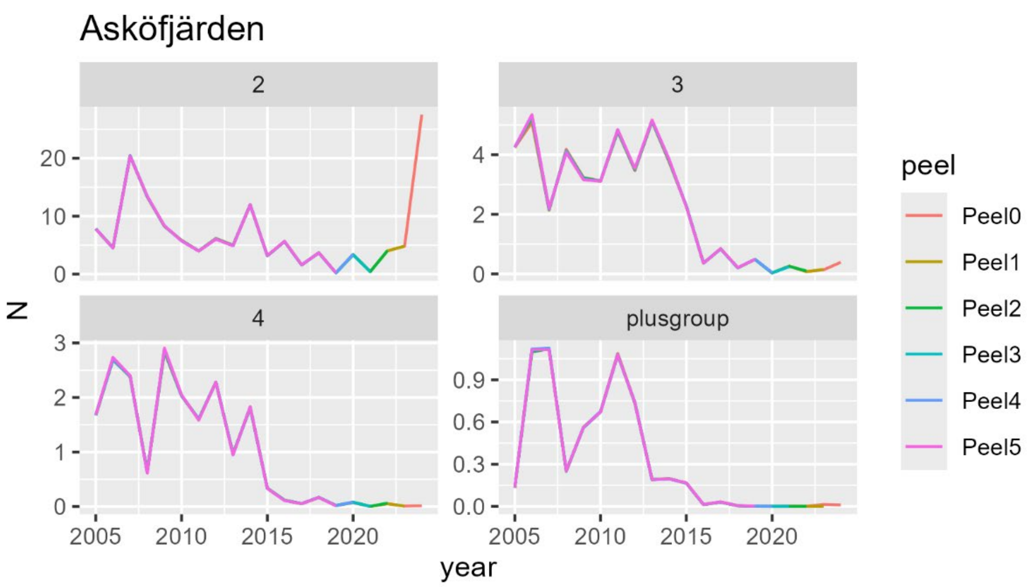
Asköfjärden
2
3
4
plusgroup
N
year
peel
Peel0
Peel1
Peel2
Peel3
Peel4
Peel5

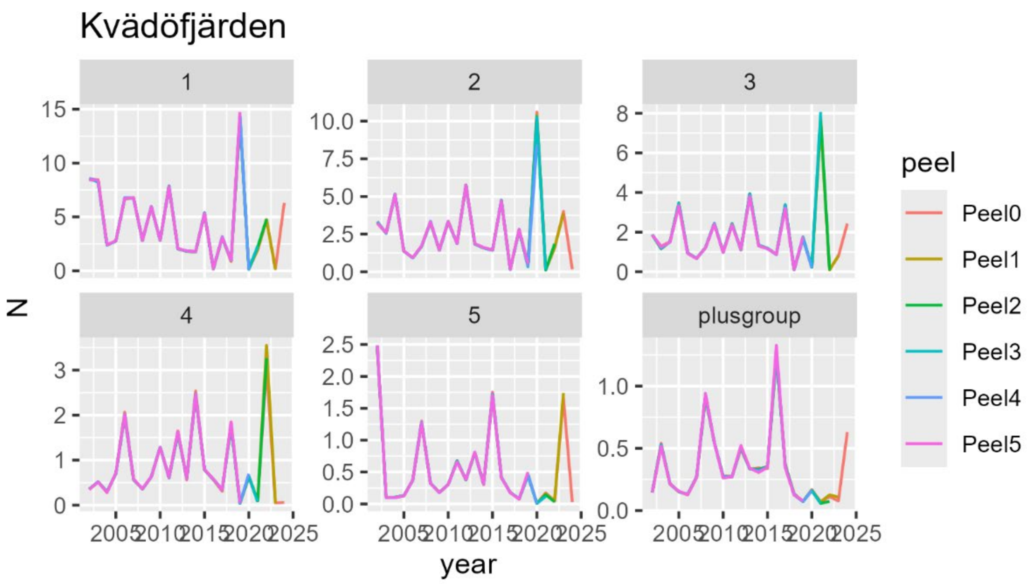
Kvädöfjärden
1
2
3
4
5
plusgroup
N
year
peel
Peel0
Peel1
Peel2
Peel3
Peel4
Peel5

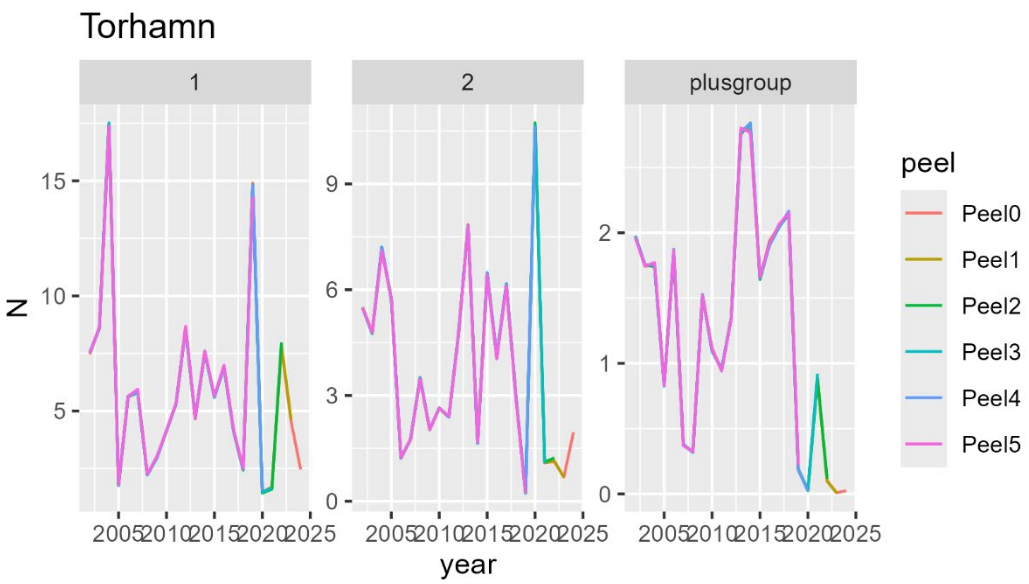
Torhamn
1
2
plusgroup
N
year
peel
Peel0
Peel1
Peel2
Peel3
Peel4
Peel5

Appendix 7 – Age-class specific total mortality rates

This appendix shows the development of age-class specific total mortality rates for all survey areas (Eq. 4). The title of each subpanel is the index of the age-class. Blue lines with dots show posterior medians and ribbons display 90% credibility bounds.

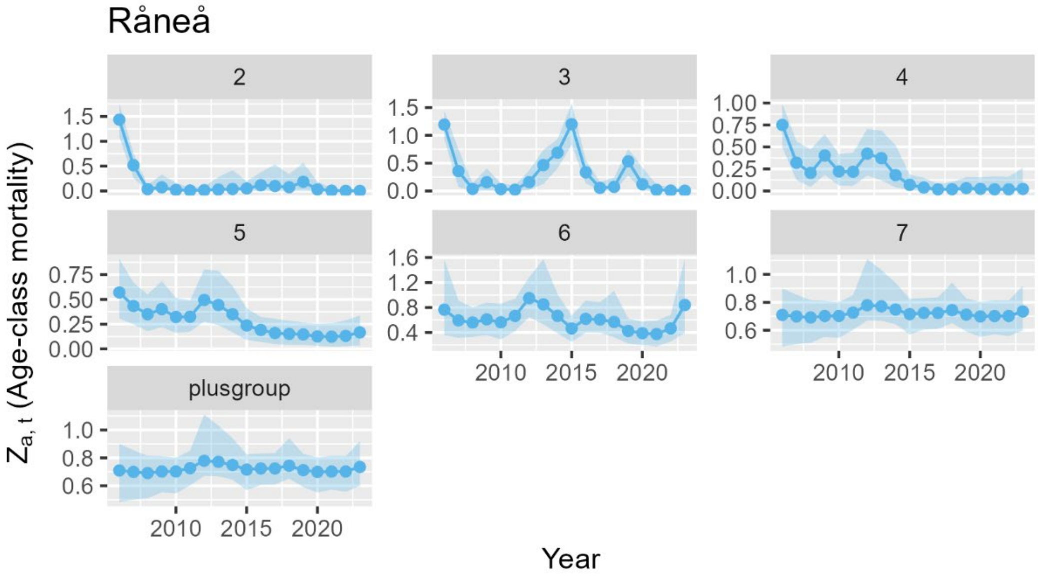
Råneå
2
3
4
5
6
7
plusgroup
$Z_{a,t}$ (Age-class mortality)
Year

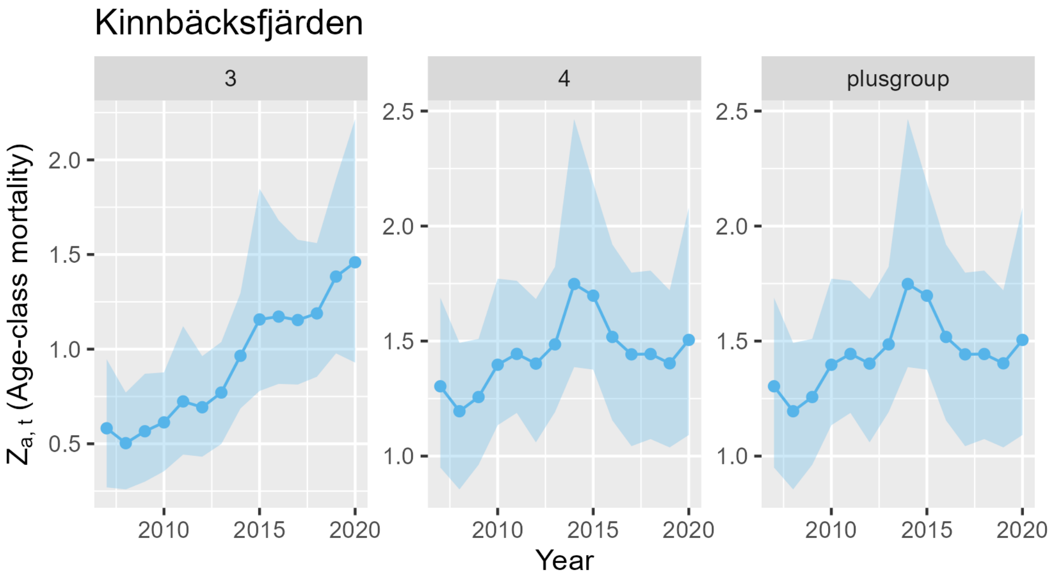
Kinnbäcksfjärden
3
4
plusgroup
$Z_{a,t}$ (Age-class mortality)
Year

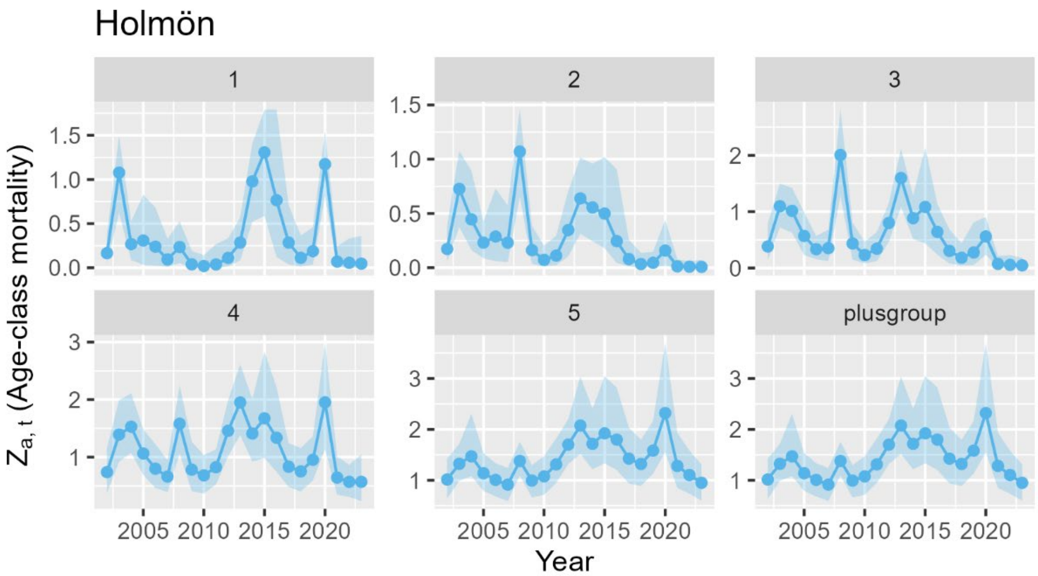
Holmön
1
2
3
4
5
plusgroup
$Z_{a,t}$ (Age-class mortality)
Year

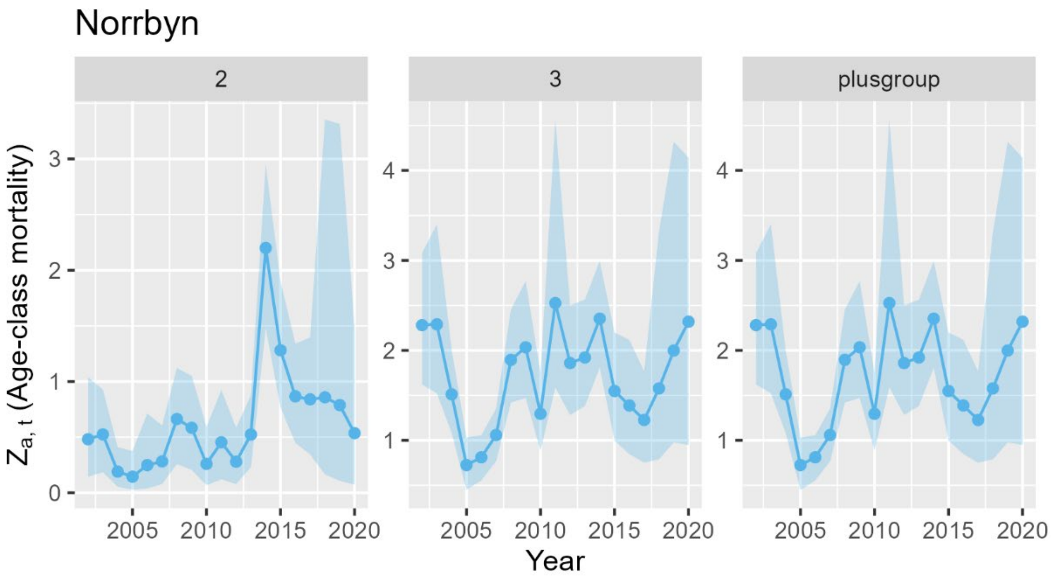
Norrbyn
2
3
plusgroup
$Z_{a,t}$ (Age-class mortality)
Year

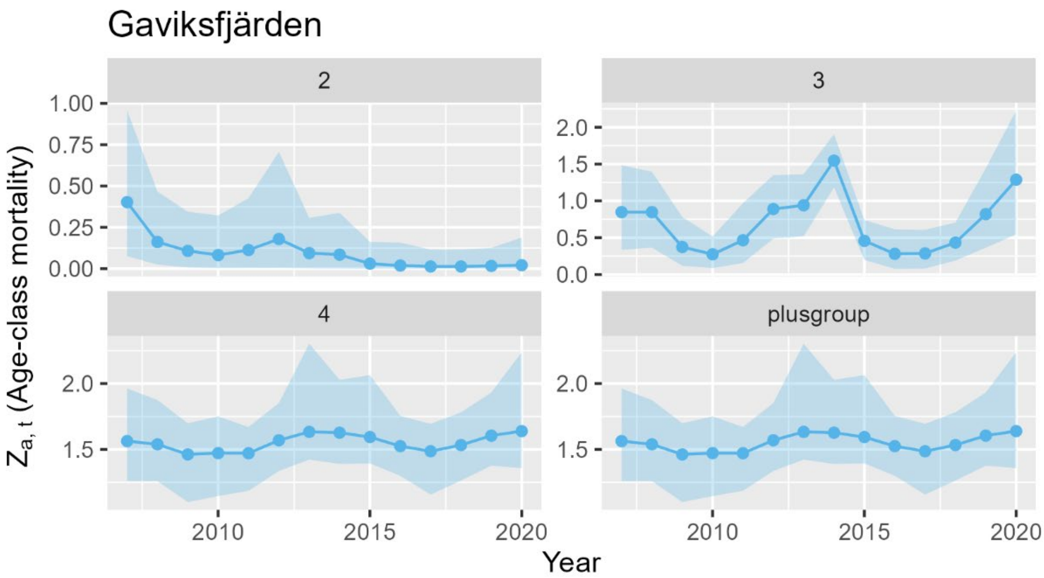
Gaviksfjärden
2
3
4
plusgroup
$Z_{a,t}$ (Age-class mortality)
Year

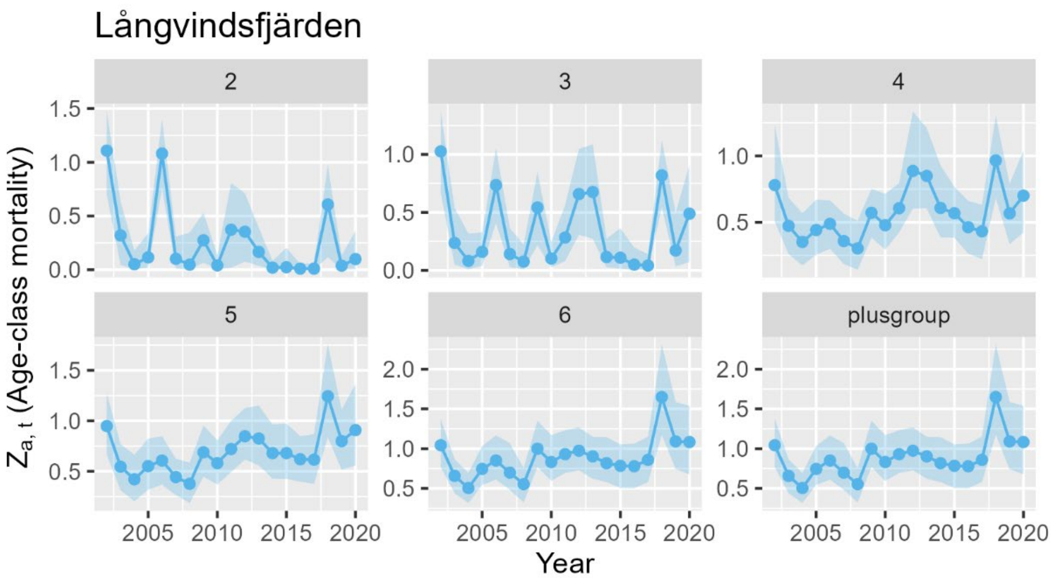
Långvindsfjärden
2
3
4
5
6
plusgroup
$Z_{a,t}$ (Age-class mortality)
Year

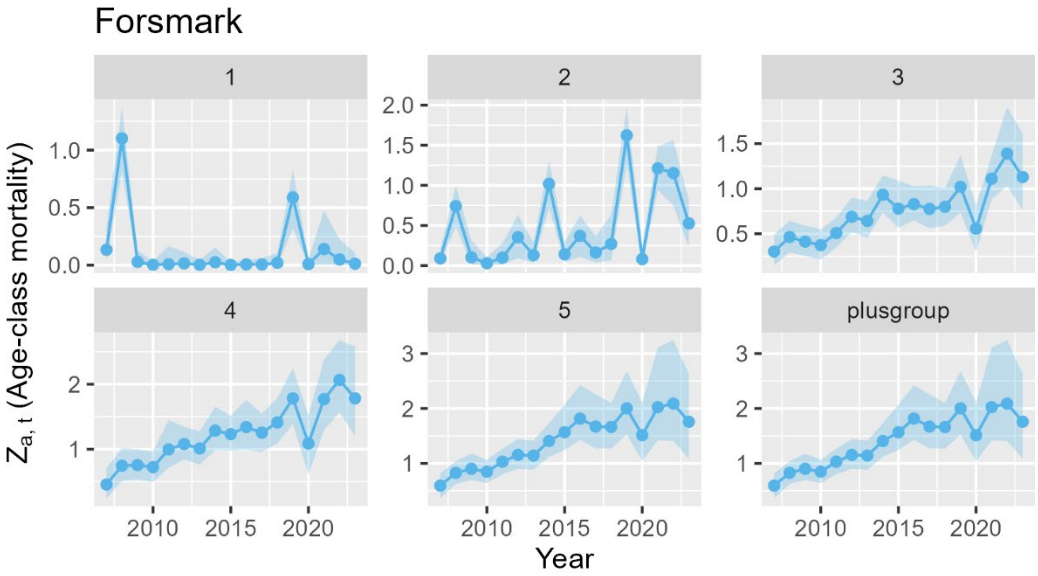
Forsmark
1
2
3
4
5
plusgroup
Za, t (Age-class mortality)
Year

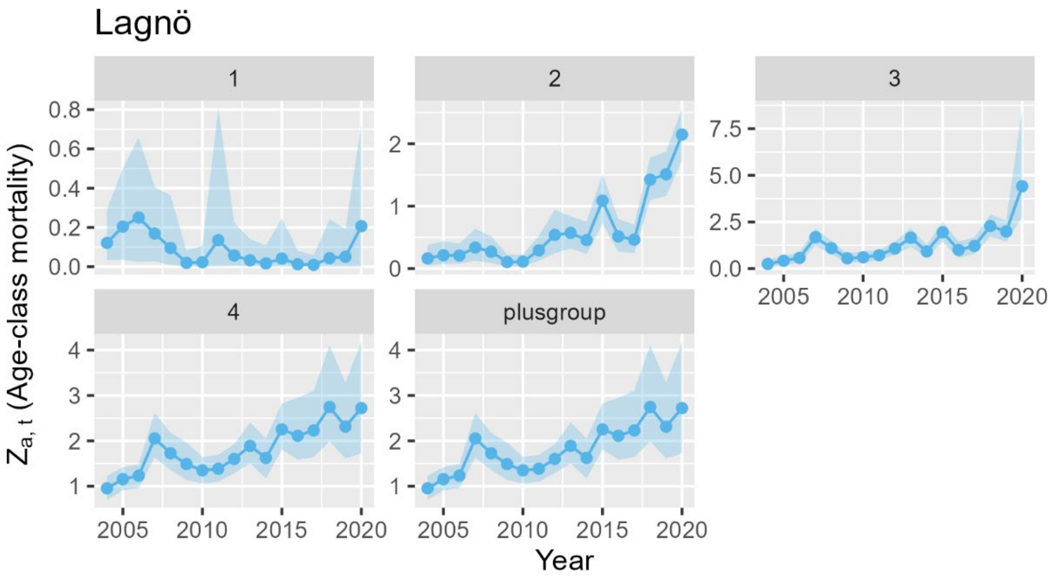
Lagnö
1
2
3
4
plusgroup
Za, t (Age-class mortality)
Year

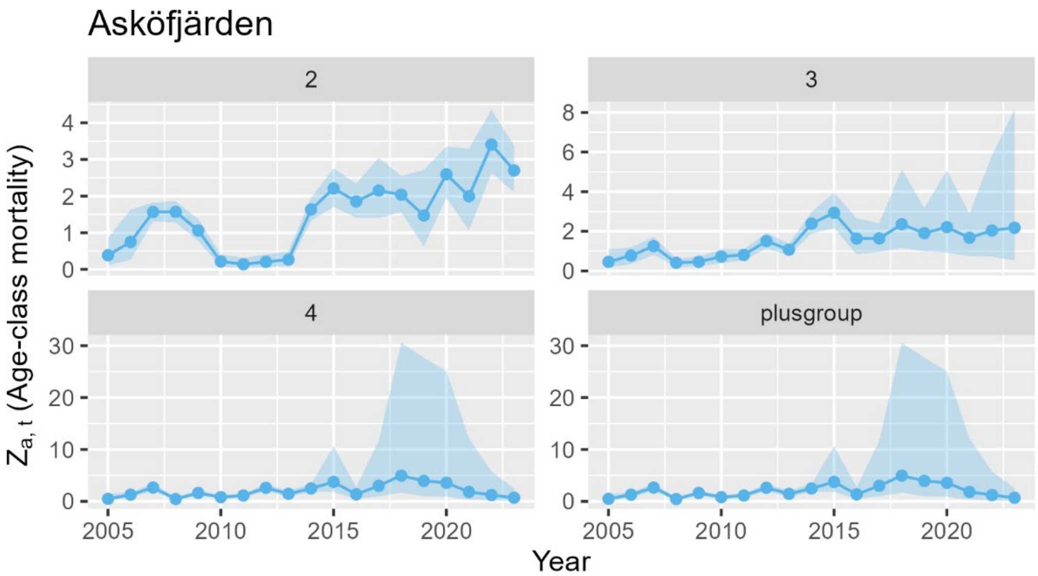
Asköfjärden
2
3
4
plusgroup
Za, t (Age-class mortality)
Year

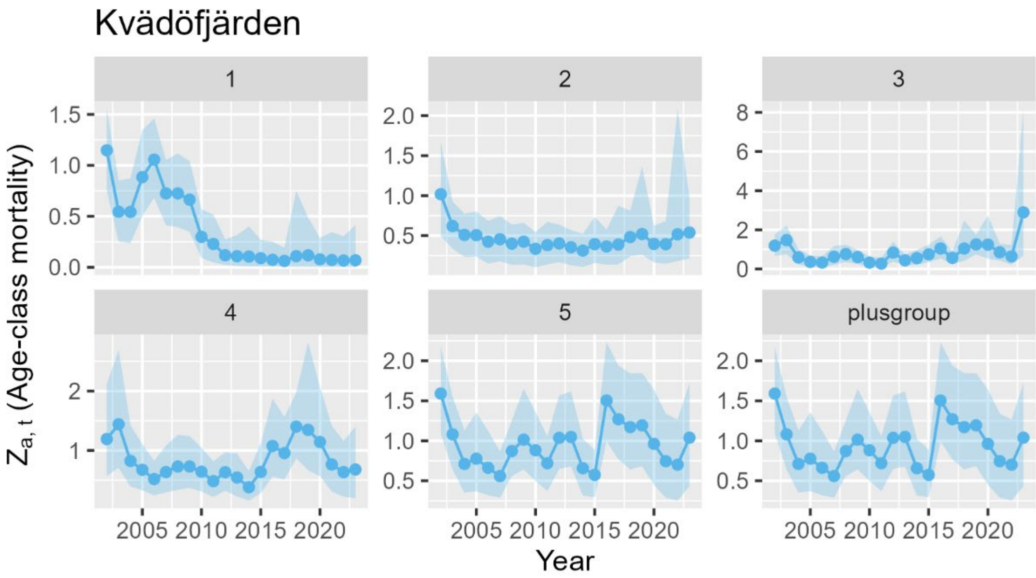
Kvädöfjärden
1
2
3
4
5
plusgroup
$Z_{a,t}$ (Age-class mortality)
Year
2005 2010 2015 2020

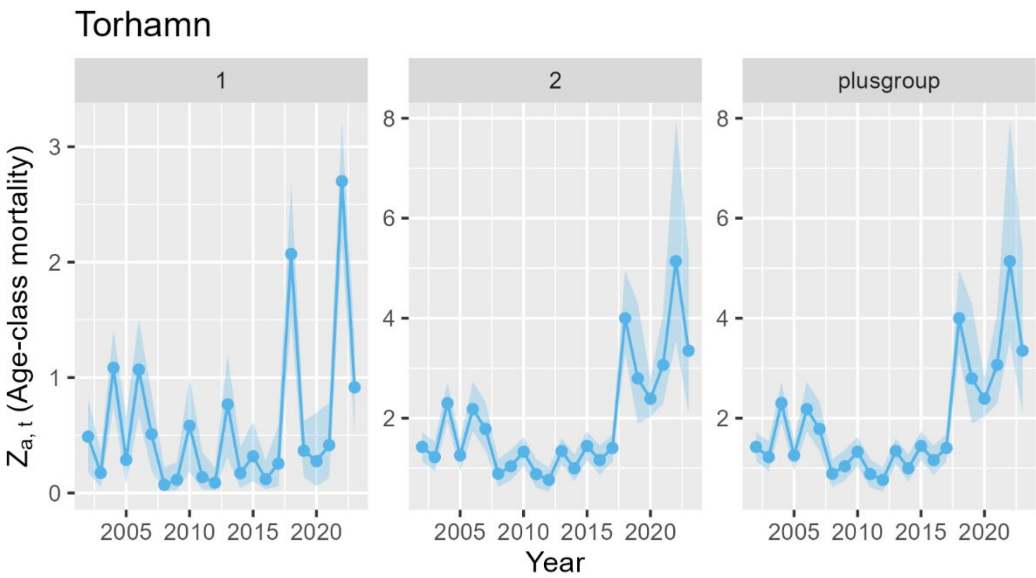
Torhamn
1
2
plusgroup
$Z_{a,t}$ (Age-class mortality)
Year
2005 2010 2015 2020

Appendix 8 – Mean age-class mortality ($\bar{Z}_a$)

This appendix shows mean age-class specific mortality rates (Eq. 19) for all survey areas. Age-classes are displayed on the x-axis. Light blue bars show medians of the posterior distribution and black dots with vertical lines show uncertainty in parameter estimates (dots represent posterior medians and lines 90 % credibility intervals).

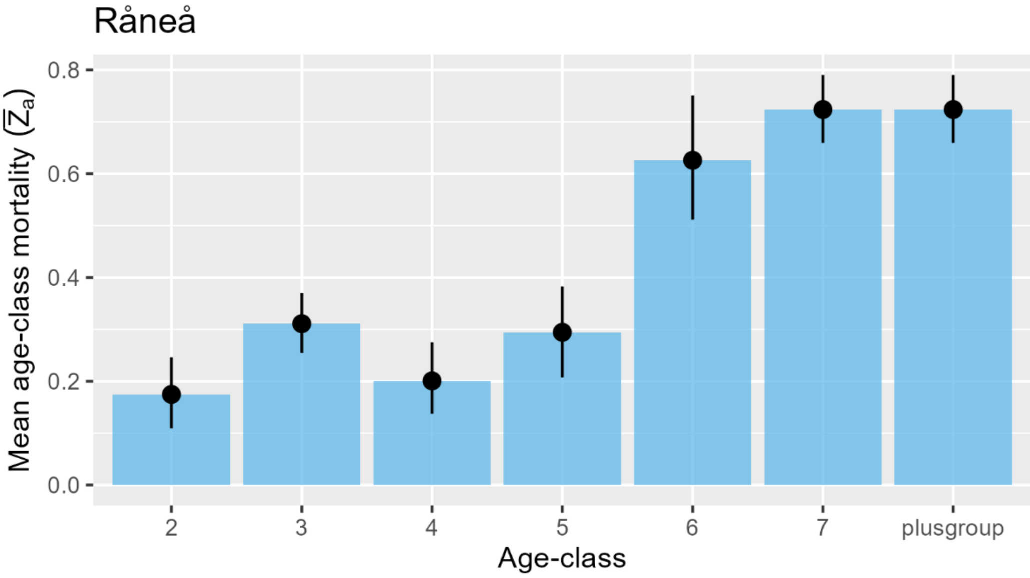
Råneå
Mean age-class mortality ($\overline{Z}_a$)
0.8
0.6
0.4
0.2
0.0
2
3
4
5
6
7
plusgroup
Age-class

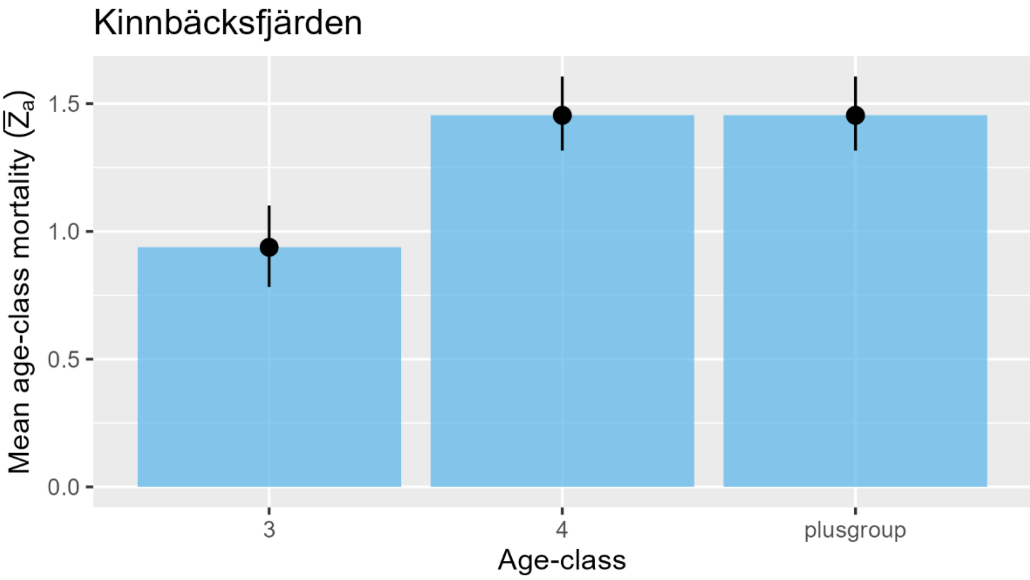
Kinnbäcksfjärden
Mean age-class mortality ($\overline{Z}_a$)
1.5
1.0
0.5
0.0
3
4
plusgroup
Age-class

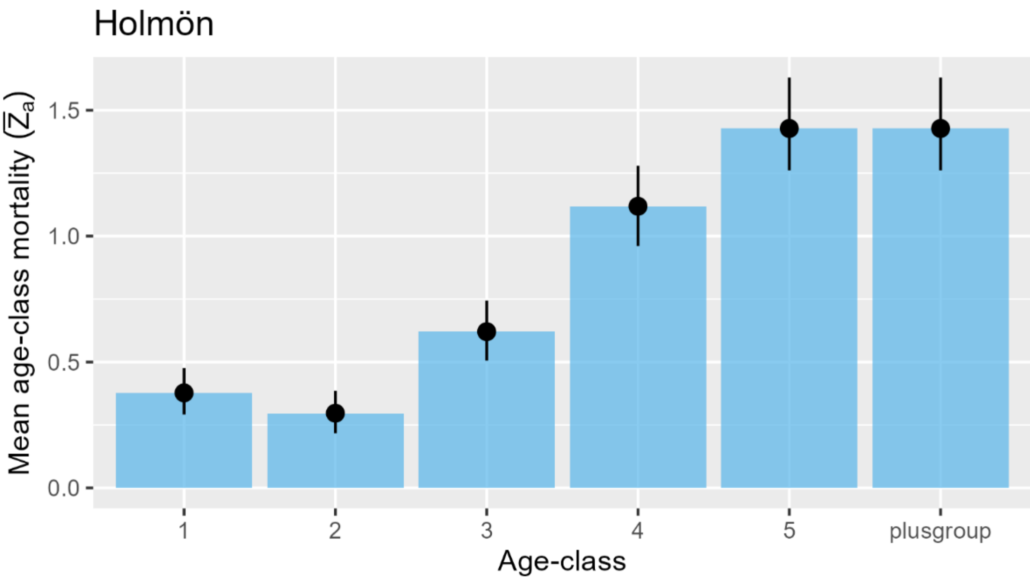
Holmön
Mean age-class mortality ($\overline{Z}_a$)
1.5
1.0
0.5
0.0
1
2
3
4
5
plusgroup
Age-class

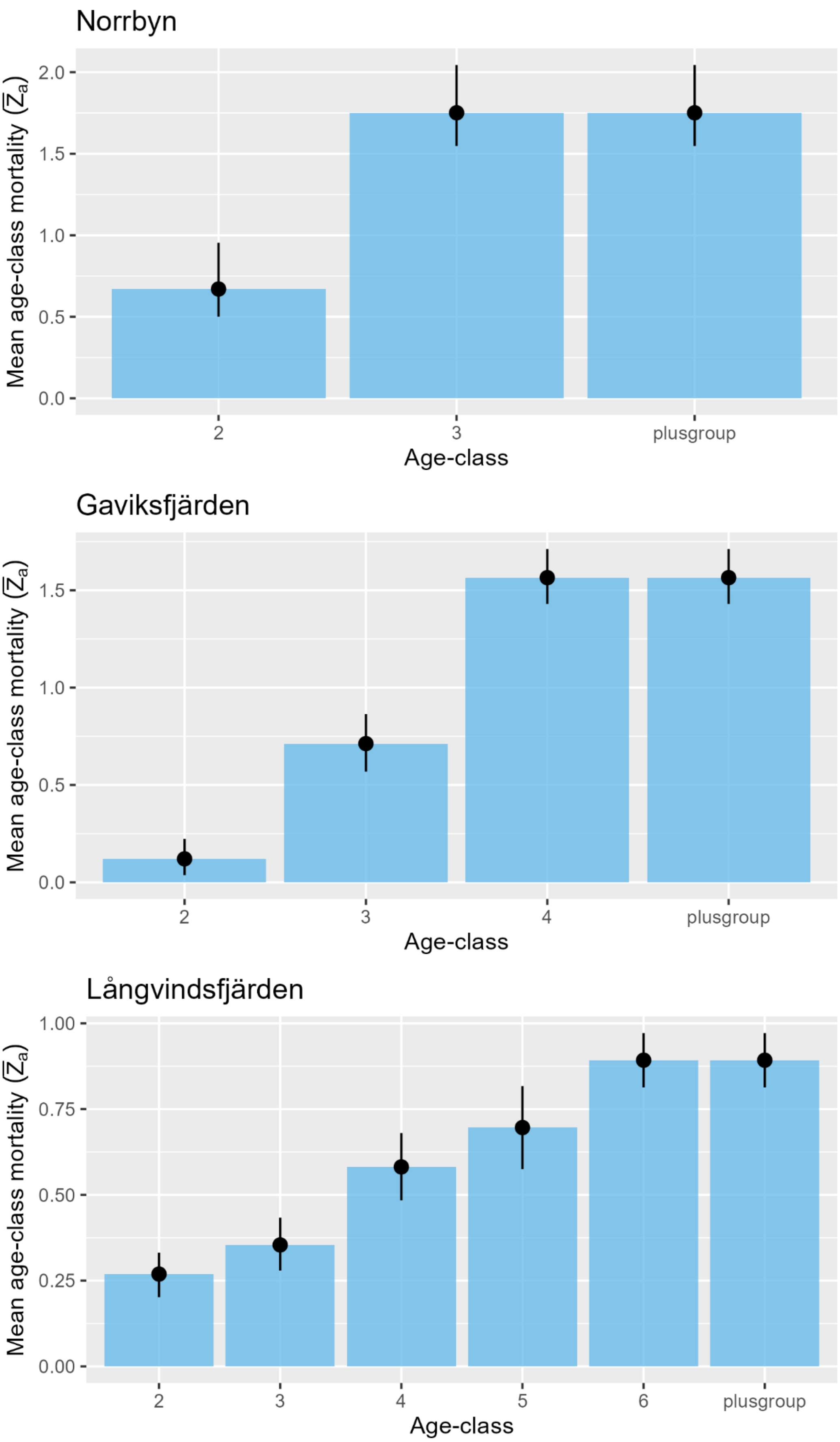

Norrbyn
Mean age-class mortality ($\overline{Z}_a$)
2.0
1.5
1.0
0.5
0.0
2
3
plusgroup
Age-class
Gaviksfjärden
Mean age-class mortality ($\overline{Z}_a$)
1.5
1.0
0.5
0.0
2
3
4
plusgroup
Age-class
Långvindsfjärden
Mean age-class mortality ($\overline{Z}_a$)
1.00
0.75
0.50
0.25
0.00
2
3
4
5
6
plusgroup
Age-class

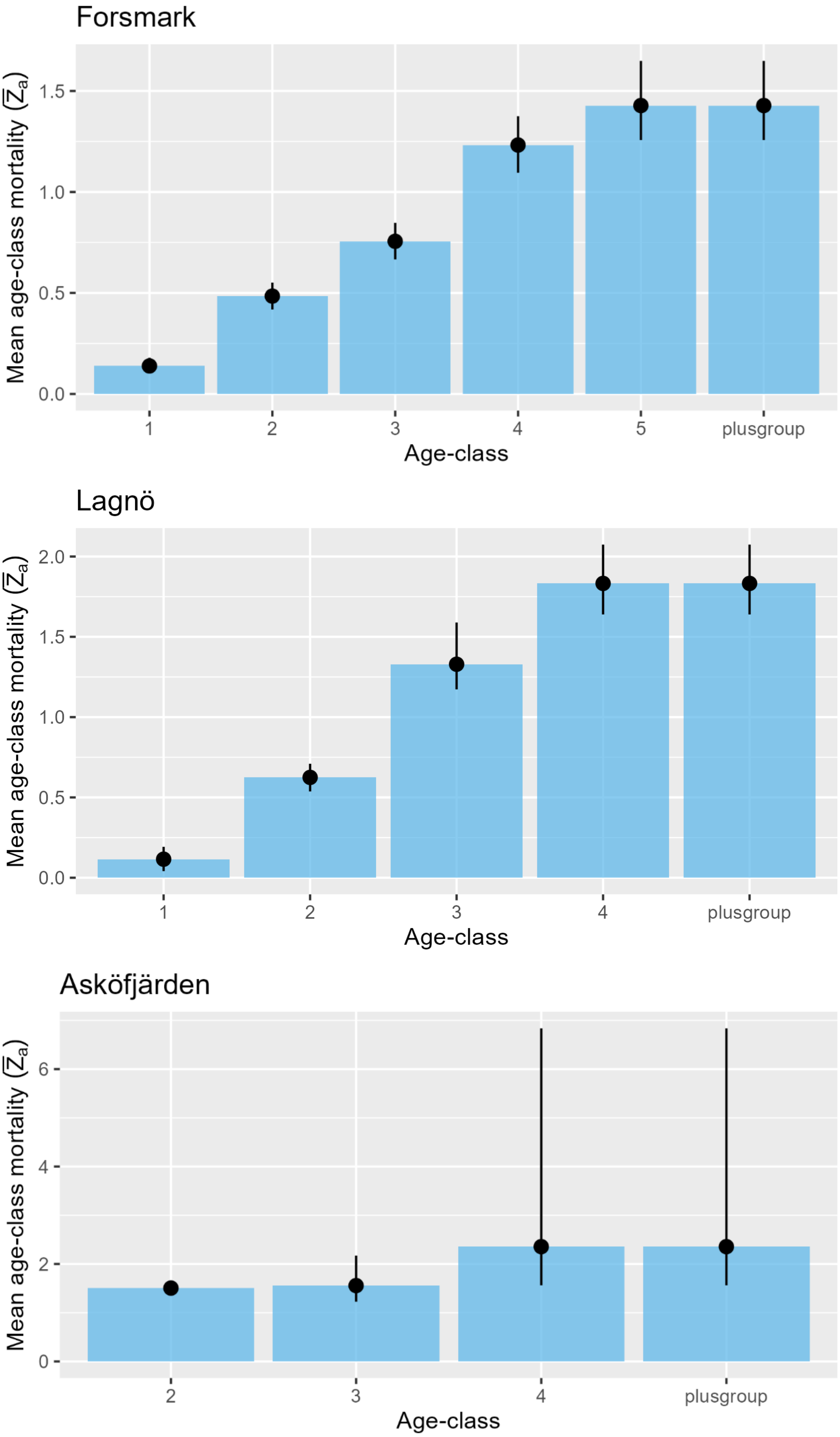
Forsmark
Mean age-class mortality ($\bar{Z}_a$)
0.0
0.5
1.0
1.5
1
2
3
4
5
plusgroup
Age-class
Lagnö
Mean age-class mortality ($\bar{Z}_a$)
0.0
0.5
1.0
1.5
2.0
1
2
3
4
plusgroup
Age-class
Asköfjärden
Mean age-class mortality ($\bar{Z}_a$)
0
2
4
6
2
3
4
plusgroup
Age-class

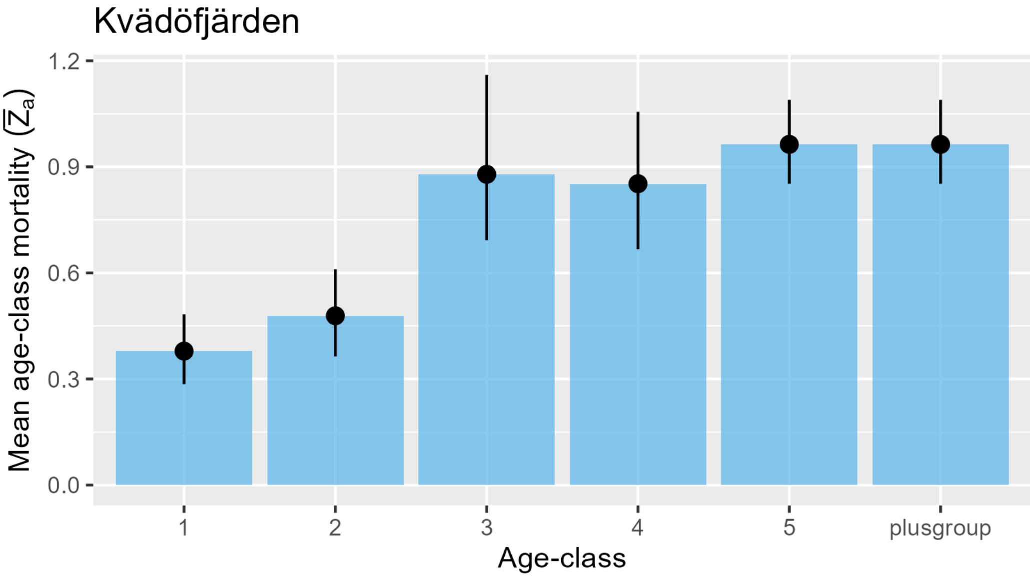
Kvädöfjärden
Mean age-class mortality ($\overline{Z}_a$)
1.2
0.9
0.6
0.3
0.0
1
2
3
4
5
plusgroup
Age-class

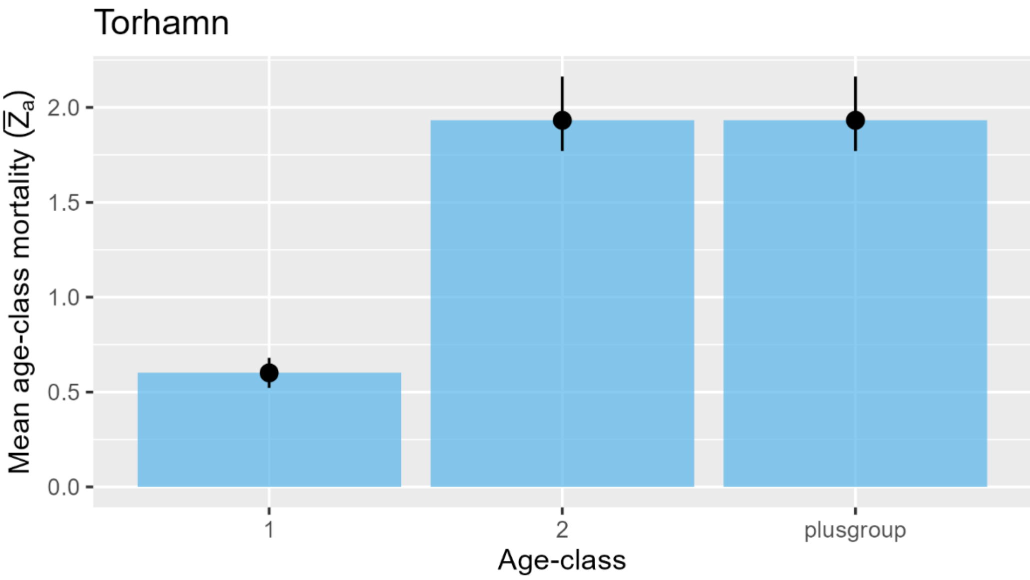
Torhamn
Mean age-class mortality ($\overline{Z}_a$)
2.0
1.5
1.0
0.5
0.0
1
2
plusgroup
Age-class